UNIVERSITY OF NAPOLI FEDERICO II

Doctorate School in Molecular Medicine

Doctorate Program in
Genetics and Molecular Medicine
Coordinator: Prof. Lucio Nitsch
XXVI Cycle

"The *Drosophila* H/ACA snoRNP pseudouridine synthase and its interplay with key developmental pathways"

CANDIDATE: Dr. Rosario Vicidomini
MENTOR: Prof. Maria Furia

Napoli 2014

Table of contents

LIST OF PUBLICATIONS RELATED TO THE THESIS

Vicidomini R, Tortoriello G, Furia M, Polese G. Laser microdissection applied to gene expression profiling of subset of cells from the Drosophila wing disc. J Vis Exp. 2010 Apr 30;(38).

Alberto Angrisani[1], Rosario Vicidomini[1], Mimmo Turano and Maria Furia. The human *DKC1* gene: beyond telomeres. Biol Chem. 2014 Jan 28. pii: /j/bchm.just-accepted/hsz-2013-0287/hsz-2013-0287.xml. doi: 10.1515/hsz-2013-0287.

[1]These authors contributed equally to this work

ABSTRACT

Loss of function of the DKC1 human gene causes the X-linked Dyskeratosis Congenital (X-DC) disease, whose main symptoms are abnormal skin pigmentation, nail dystrophy, mucosal leukoplakia, bone marrow failure and increased tumour susceptibility. DKC1 encodes a nucleolar protein, named dyskerin, whose sequence is characterized by a high degree of phylogenetic conservation. Eukaryal dyskerins represent one of the four proteic core components of the H/ACA small nucleolar RNA-associated ribonucleoprotein (snoRNP) complexes that are involved in rRNA processing, pseusourydilation of cellular RNAs, modulation of the efficiency of IRES-dependent translation, and stabilization of H/ACA snoRNAs. Besides participating in the formation of H/ACA snoRNPs, mammalian dyskerin also associates with telomeric RNA, which contains an H/ACA domain, being one of the essential components of the telomerase active complex.

One of the main challenges posed by X-DC pathogenesis is distinguishing between the effects caused by telomere shortening from those caused by altered snoRNPs functioning. Given that Drosophila lacks telomerase, and Drosophila dyskerin, encoded by the *Nop60b*/*minifly* (*mfl*) gene, is highly related to its human counterpart, this organism can serve as an useful model to investigate the telomerase-independent effects caused by depletion of snoRNP pseudouridine synthases.

In this thesis I evaluated the effects of in vivo localized *mfl* gene silencing on the development of the wing imaginal disc, which represents an excellent model to study the morphogenetic regulation of organ growth and patterning. I found that *mfl* silencing triggers a process of "apoptosis-induced proliferation" that is typical of regenerative phenomena. This process correlates with epithelial reorganization, that is marked by cytoskeletal remodeling, activation of the JNK pathway activity and transition of patches of cells from the epithelial to the mesenchimal state. Moreover, I observed that *mfl* silencing causes dysregulation of Notch signaling at the D/V boundary of the wing disc; this dysregulation cannot be attributed to apoptosis or to defective IRES-dependent translation of the Notch antagonist Hairless protein.

Altogheter, the results obtained reveal for the first time a close link that connects eukaryotic dyskerins with Notch signaling and JNK pathway. On the basis of their evolutionary conservation, I speculate that these events could be responsible for at least some of the symptoms shown by X-DC patients.

1 BACKGROUND

1.1 Dyskeratosis Congenita (DC)

Dyskeratosis Congenita (DC) is a disease characterized by a classic triad, made up of abnormal pigmentation of the skin, nail dystrophy and oral leukoplakia. Other symptoms include chronic bone marrow failure (which represent the main cause of death), stem cell deficiency, testicular atrophy, premature loss of teeth, premature graying and/or loss of hair, pulmonary fibrosis, increased susceptibility to cancer (which is the second leading cause of death), and a series of other defects. Indeed, DC is suspected in patients who have the features shown in Table 1 (data from Vulliamy et al. 2006; Savage and Bertuch 2010).

Table 1. Features of patients suspected to be affected by X-DC

Physical abnormalities	At least two features of the classic DC clinical triad (alteration of normal pigmentation of skin, nail dystrophy, oral leukoplakia), or one feature of the classic triad plus two or more of the following: Epiphora; Blepharitis; Abnormal eyelashes; Prematurely gray hair; Alopecia; Periodontal disease; Taurodontism (enlarged tooth pulp chambers) or decreased tooth root/crown ratio; Developmental delay; Short stature; Microcephaly; Hypogonadism; Esophageal stenosis; Urethral stenosis; Liver disease; Osteoporosis; Avascular necrosis of the hips or shoulders; Patients with DC may not present any of the above additional symptoms, which may appear or increase with age.
Progressive bone marrow failure (BMF)	May appear at any age and may be a presenting sign.
Myelodysplastic syndrome (MDS) or acute myelogenous leukemia (AML).	May be the presenting sign.
Cancer	Solid tumors, usually head/neck or anogenital cancer, in patients younger than 50 years old and without other risk factors. Solid tumors may be the first manifestation of DC in individuals who do not have BMF.

Figure 1 shows some symptoms presented by DC patients.

DC is a disease that presents locus heterogeneity. In fact, *DKC1*, *TERC*, *TERT*, *TINF2*, *NHP2*, *NOP10* and *WRAP53* are the genes in which mutations are known to cause DC. *TERC* (TElomerase RNA Component) is a ncRNA gene, while *DKC1*, *NHP2*, *NOP10*, *WRPAP53*, *TERT* and *TINF2* encode proteins called dyskerin, NHP2, NOP10, WRAP53, TERT (TElomerase Retro Transcriptase) and TINF2 (TRF1 Interacting Nuclear Factor 2) respectively.

Figure 1. Symptoms shown by DC patients. (A) Abnormal pigmentation of the skin. **(B)** Nail dystrophy. **(C)** Leukoplakia of the mucous. **(D)** Loss of teeth. **(E)** Testicular atrophy. **(F)** Horseshoe kidney. **(G)** Pulmonary fibrosis. **(H)** Chronic bone marrow failure (first cause of death). **(I)** Cerebellar hypoplasia. **(L-O)** Increased risk of malignancy (second cause of death); squamous carcinoma of the mouth **(L)**, squamous carcinoma of the skin **(M)**, pancreatic carcinoma **(N)** and Acute Myeloid Leukemia **(O)**.

The products of all seven genes associated with DC are components of the active telomerase complex responsible for telomeres maintenance. In addition, *DKC1, NHP2* and *NOP10* encoded proteins are also components of H/ACA snoRNP and H/ACA scaRNPs complexes known to be involved in several important cellular functions. Table 2 reports the proportion of DC attributed to mutations in the different genes and the respective mode of inheritance.

Although the different forms of

Table 2. Summary of the different forms of DC

Gene Symbol	Mode of Inheritance	Proportion of DC Attributed to Mutations in This Gene
DKC1	X-Linked	17%-36%
NHP2	Autosomal Recessive	< 1 %
NOP10	Autosomal Recessive	< 1%
WRAP53	Autosomal Recessive	3%
TERC	Autosomal Dominant	6-10%
TERT	Autosomal Dominant and Autosomal Recessive	1%-7%
TINF2	Autosomal Dominant	11%-24%

*** 1. Data from Vulliamy et al. 2006; Walne et al. 2007; Savage et al. 2008; Vulliamy et al. 2008; Walne et al. 2008**

dyskeratosis have very similar presentations, they differ for hematological, neoplastic and genitourinary symptoms (see Table 3).

Table 3. Genitourinary, hematological and neoplastic traits exhibited by patients affected by various forms of DC

	Genitourinary	Hematology	Neoplasia
DKC1	• External Genitalia (Male): Hypospadias; Phimosis • Internal Genitalia (Male): Testicular hypoplasia; Cryptorchidism • Kidneys: Horseshoe kidney • Bladder: Urethral stenosis	Bone marrow failure; Myelodysplasia; Pancytopenia; Thrombocytopenia; Leukopenia; Anemia	Squamous cell carcinoma (skin or mucosa); Acute myeloid leukemia; Hodgkin disease; Pancreatic carcinoma
NHP2	• External Genitalia (Male): Testicular atrophy	Bone marrow failure; Pancytopenia; Thrombocytopenia	–
NOP10	–	Bone marrow failure (classic feature); Aplastic anemia; Thrombocytopenia; Pancytopenia	Increased risk of malignancy (classic feature)
WRAP53	–	Bone marrow failure; Pancytopenia	Squamous cell carcinoma
TERC	–	Bone marrow failure; Aplastic anemia; Lymphopenia; Pancytopenia; Anemia; Thrombocytopenia; Elevated MCV; Hypoplastic myelodysplasia	Squamous cell carcinoma of the skin
TERT	–	Bone marrow failure; Pancytopenia; Aplastic anemia; Thrombocytopenia; Leukopenia	–
TINF2	• Internal Genitalia (Male): Cryptorchidism	Bone marrow failure; Pancytopenia; Aplastic anemia; Thrombocytopenia; Leukopenia; Increased fetal hemoglobin	Increased risk of malignancy

The data were obtained from the OMIM website (Online Mendelian Inheritance in Man), an Online Catalog of Human Genes and Genetic Disorders (http://www.omim.org). Entries: #305000, #613987, #224230, #613988, #127550, #613989 and #613990.

The X-linked Dyskeratosis Congenita (X-DC), caused by mutation in *DKC1* gene, is the most common and severe form of DC. In particular patients affected by X-DC are the only ones to show Acute Myeloid Leukemia, Hodgkin disease and pancreatic carcinoma. As expected, X-DC affects almost exclusively males, and development of clinical manifestation in female carriers is extremely rare. The *DKC1* gene deserves deep attention for the wide range of biological roles to whom it is connected and their potential impact on cell growth, proliferation and differentiation.

1.2 *DKC1* mutations cause X-DC

As mentioned above, X-DC is caused by mutations in the *DKC1* gene. The Pfam databank (http://pfam.sanger.ac.uk/ accession O60832) identifies within the encoded protein, called dyskerin, at least three well preserved functional domains: the dyskerin-like domain (DKLD; 48-106 aa) so far with unknown function, but typical of this protein family; the TruB_N pseudouridine synthase catalytic domain, that includes the active site (110-226 aa) directly involved in the pseudouridylation process, and the PUA RNA binding domain (297-370 aa), involved in recognition of snoRNAs of the H/ACA family (Figure 2). In addition, four low complexity regions (aa 11-20, 421-455, 467-480, 498-507), rich in lysine and arginine, are identified within the bipartite NLSs. More than 40 pathologic allelic variants are described for *DKC1*; the majority are missense mutations that change the amino acid residue (see Table 4). The Genebank accession numbers used are NM_001363 for cDNA sequence and NP_001354.1 for protein sequence. Mutations are organized by domain from the 5'-terminus/N-terminus to the 3'-terminus/C-terminus. Note that dyskerin mutations are mostly missense and are dispersed along the sequence, although mainly localized in the N-terminal region, in the PUA domain and in the C-terminal region. Sequence alignment of dyskerins from various organisms reveals presence of highly conserved regions that mirrors their functional conservation. This aspect was directly attested by swapping experiments, which showed that *Drosophila* and rat dyskerin were both able to rescue yeast Cbf5 mutations (Phillips et al. 1998; Yang et al. 2000). Their high level of evolutionary conservation further testifies the importance of proteins belonging

Figure 2. Structure of human dyskerin. In blue, low complexity regions corresponding to NLSs and Lysine Reach domains (LR); in green, DKLD domain; in red, TruB_N domain; in purple, aspartic 125 within the catalytic site; in yellow the PUA domain.

to the dyskerin family. For instance, the human dyskerin and its *Drosophila* homologue, the MFL protein, share 66% of identity and 79% of similarity (Giordano et al. 1999).

Table 3. *DKC1* Pathologic Allelic Variants

Domains	Mutation	AA substitution	Exon	References
URR	c.-141C>G	n/a	5' URR	Knight *et al*, 2001
	c.-142C>G	n/a	5' URR	Dokal *et al*, 2000
	c.5C>T	p.Ala2Val	1	Knight et al,1999.1
	c.16+592C>G r.16_17**ins**247, 16+343_589	p.Val6Ala**fs**X5	IVS1	Knight *et al*, 2001
	c.29C>T	p.Pro10Leu	2	Vulliamy *et al*, 2006
	c.85-5C>G	p.(?)	IVS2	Knight et al,1999.1
	c.91C>G	p.Gln31Glu	3	Wong *et al*, 2004
	c.106T>G	p.Phe36Val	3	Heiss *et al*, 1998
	c.109_111**del**CTT	p.Leu37**del**	3	Heiss *et al*, 1998
	c.113T>C	p.Ile38Thr	3	Cossu *et al*, 2002
	c.115A>G	p.Lys39Glu	3	Knight et al,1999.1
	c.119C>G	p.Pro40Arg	3	Heiss *et al*, 1998
	c.121G>A	p.Glu41Lys	3	Knight et al,1999.1
	c.127A>G	p.Lys43Glu	3	Heiss *et al*, 2001
	c.146C>T	p.Thr49Met	3	Knight et al,1999.2
	c.194G>C	p.Arg65Thr	4	Knight et al,1999.1
	c.196A>G	p.Thr66Ala	4	Knight et al,1999.1 Hassock *et al,* 1999
	c.200C>T	p.Thr67Ile	4	Vulliamy *et al*, 2006
	c.204C>A	p.His68Gln	4	Vulliamy *et al*, 2006
	c.214_215CT>TA	p.Leu72Tyr	4	Heiss *et al*, 1998
TruB	c.361A>G	p.Ser121Gly	5	Knight et al,1999.2
	c.472C>T	p.Arg158Trp	6	Knight *et al*, 2001
	c.838A>C	p.Ser280Arg	9	Knight *et al*, 2001
PUA	c.941A>G	p.Lys314Arg	10	Vulliamy *et al*, 2006
	c.949C>T	p.Leu317Phe	10	Marrone *et al,* 2003
	c.961C>G	p.Leu321Val	10	Knight et al,1999.1
	c.965G>A	p.Arg322Gln	10	Marrone *et al,* 2003
	c.1049T>C	p.Met350Thr	11	Knight et al,1999.1
	c.1050G>A	p.Met350Ile	11	Knight et al,1999.1
	c.1058C>T	p.Ala353Val	11	Knight et al,1999.1
	c.1075G>A	p.Asp359Asn	11	Vulliamy *et al*, 2006

	c.1150C>T	p.Pro384Ser	11	Marrone *et al,* 2003
	c.1151C>T	p.Pro384Leu	11	Knight *et al*, 2001
	c.1156G>A	p.Ala386Thr	12	Vulliamy *et al*, 2006
	c.1193T>C	p.Leu398Pro	12	Hiramatsu *et al*, 2002
	c.1204G>A	p.Gly402Arg	12	Knight et al,1999.1
	c.1205G>A	p.Gly402Glu	12	Heiss *et al*, 1998
	c.1223C>T	p.Thr408Ile	12	Vulliamy *et al*, 2006
	c.1226C>T	p.Pro409Leu	12	Ding *et al*, 2004
	c.1258_1259AG>TA	p.Ser420Tyr	12	Vulliamy *et al*, 2006
	c.1477-2A>G	p.(?)	IVS14	Vulliamy *et al*, 2006
	c.1476+51_oMPP1:c.(?)**del**	p.Asp493Val**fs**X12	15	Vulliamy *et al*, 1999

1.3 The *DKC1* gene and the molecular mechanisms underlining X-DC

The causative gene of the X-DC, *DKC1,* was identified on 1998, when a screening of candidate cDNAs from unrelated patients unrevealed that some of them shared mutations in its coding region (Heiss et al. 1998). *DKC1* encodes a 58 kDa nucleolar protein, named dyskerin, and its sequence is characterized by a high degree of phylogenetical conservation that testifies a great biological importance. Indeed, the *Cbf5* yeast gene, originally described to encode a centromere and microtubule binding protein (Jiang et al. 1993), was the first member of this gene family to be identified. Immediately after, a mammalian orthologue, named Nap57, was recognized in rats, and postulated to be involved in nucleo-cytoplasmic shuttling of pre-ribosomal structures (Meier and Blobel 1994). Later on, yeast *Cbf5* inactivation was shown to be lethal, and the lethality attributed to defective processing and pseudouridylation of rRNAs precursors (Cadwell et al. 1997; Zebarjadian et al. 1999). In the same period, a *Drosophila* orthologue, named *Nop60B/minifly*, was recognized (Phillips et al. 1998) and shown necessary for proper maturation and pseudouridylation of rRNA precursors (Giordano et al. 1999). Identification of *DKC1* as causative of X-DC attracted further attention on members of gene family, so that related orthologues were then rapidly described in plant, fungal, protist and even archaeabacterial genomes (Maceluch et al. 2001; Watanabe and Gray 2000; Lin and Momany 2003). In each species where genetic analysis has been performed, functionality of members of this gene family proved to be indispensable for survival, while hypomorphic mutations or gene silencing cause a plethora of disparate phenotypic abnormalities (see for example Giordano et al. 1999; Ruggero et al. 2003; Tortoriello et al. 2010; Zhang et al. 2012). All eukaryal dyskerins described so far have a prevalent nuclear localization. Within the nucleus, dyskerins participate to three essential complexes: the H/ACA small nucleolar ribonucleoparticles (snoRNPs; Kiss et al. 2006), the active telomerase holoenzyme (Cohen et al. 2007), and the specific Cajal body ribonucleoparticles (scaRNPs). H/ACA snoRNPs are

hetero-pentameric complexes in which dyskerin associates with one molecule of small nucleolar RNA (snoRNA) of the H/ACA class and three highly conserved proteins: NOP10, NHP2 and GAR1 (Kiss et al. 2006). Functional conservation of these H/ACA snoRNP "core" protein components is so notable that archaeal Cbf5p can assemble efficiently with yeast Nop10p protein, consistent with the high sequence conservation observed between archaea and eukarya (Hamma et al. 2005). The specific snoRNA that is recruited by the complex determines both the target recognition and the biological role of snoRNP complexes (see Figure 3). By acting as guide, each assembled snoRNA selects by base complementarity the target RNA and the specific site to be pseudouridylated (Lafontaine and Tollervey 1998). Most common targets are rRNAs, while snRNAs of the U1 spliceosome are modified by a specific subgroup of specimens that do not localize in the nucleoli but in the Cajal bodies, and thus have been named Cajal body-specific RNAs (scaRNAs; Richard et al. 2003). In the pseudouridylation process, dyskerin acts as catalytic pseudouridine synthase, directing the isomerisation of specific uridines to pseudouridines. Furthermore, although the exact molecular mechanism still awaits to be fully elucidated, H/ACA snoRNPs also direct the endonucleolytic cleavages required for rRNA processing, under the guide of U17, E2 and E3 H/ACA snoRNAs, all essential for cell growth. Maturation of 5' end of the 18S rRNA requires the activity, most probably as chaperone, of the U17 snoRNA (also called E1), that in human cells is present in two isoforms, called U17a and U17b. In turn, the snoRNA E2 is needed for the maturation of 3' end of 18S rRNA, whereas the snoRNA E3 drives the maturation of 5' end of the 5.8S rRNA (for a comprehensive review of snoRNAs see http://www-snorna.biotoul.fr; Lestrade and Weber 2006). Finally, a crescent number of "orphan" snoRNAs which lack a known target has been identified, and their functions remain to be defined. Dyskerin-H/ACA snoRNAs association attracted further attention after the discovery that, beside acting in RNA modification processes, snoRNAs can be maturated to produce short regulatory RNAs able to modulate alternative splicing (reviewed by Khanna and Stamm 2010), or microRNAs (miRNAs). This last feature is largely widespread in eukaryotes, since snoRNA-derived miRNAs have been described in Protozoa (Saraiya and Wang 2008), humans (Ender et al. 2008), mouse, Arabidopsis, yeast, chicken (Taft et al. 2009) and Drosophila (Jung et al. 2010). Intriguingly, the percentage of snoRNAs able to be processed into miRNAs has been estimated to range from 60% in humans and mouse to more than 90% in Arabidopsis (Taft et al. 2009). Although the snoRNA-miRNA processing mechanism is mostly unclear, it appears to be Dicer1-dependent but Drosha/DCGR8-independent (Ender et al. 2008; Taft et al. 2009).

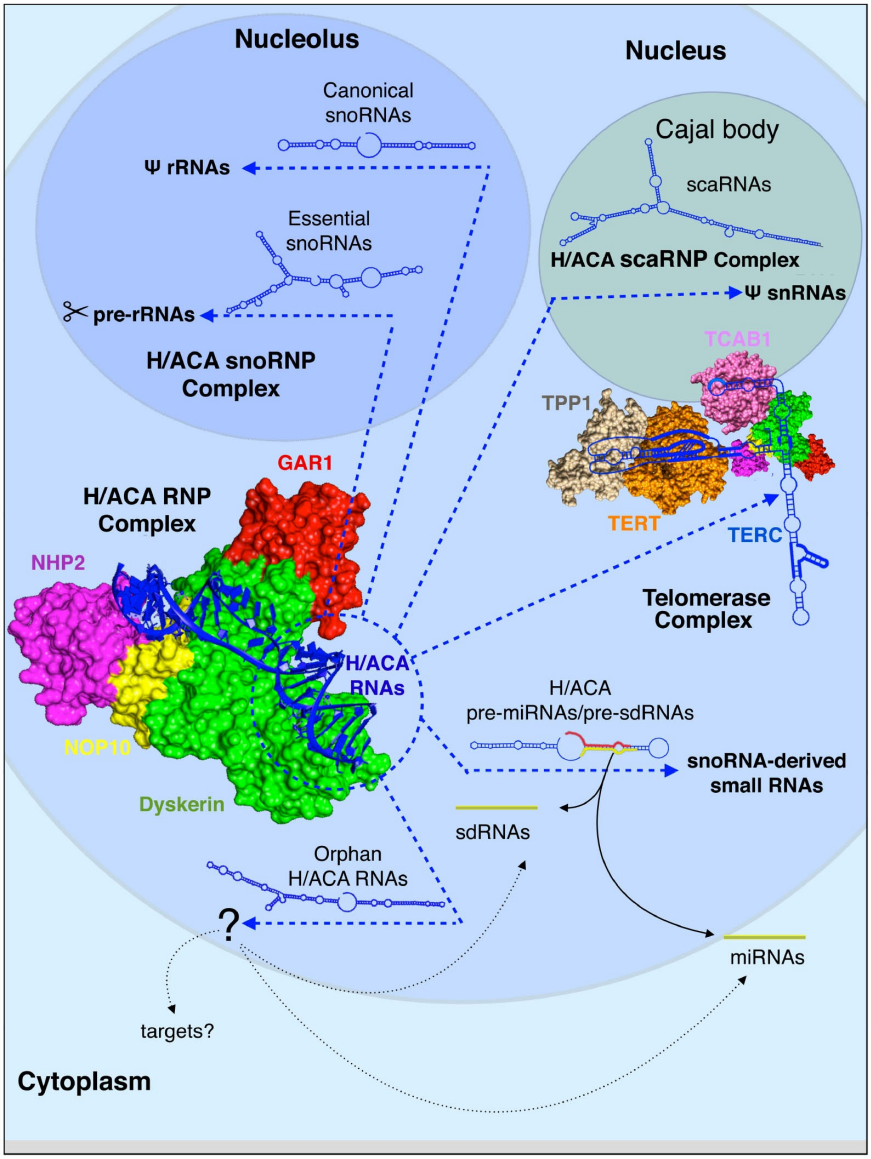

Figure 3. The diverse dyskerin-containing nuclear complexes. Mature H/ACA snoRNPs are composed by a dyskerin-NOP10-NHP2-GAR1 tetramer assembled with a molecule of H/ACA RNA. These complexes localize in the nucleus where, depending on the specific recruited RNAs, play different functions. While RNPs assembled with essential snoRNAs direct pre-rRNA processing, those assembled with canonical snoRNAs direct RNA pseudouridylation. When associated with orphan H/ACA RNAs, that do not have recognized target, these complexes might either guide modification of cellular RNAs or act as precursors of smaller regulatory RNAs (miRNAs/sdRNAs). H/ACA snoRNAs already identified as miRNA/sdRNA precursors are referred to as H/ACA pre-miRNAs or pre-sdRNAs. If assembled with a scaRNA, the dyskerin-NOP10-NHP2-GAR1 tetramer composes the scaRNPs, that localize in the Cajal bodies and direct pseudouridylation of snRNAs. The whole tetramer also participates in the formation of the telomerase active complex, together with the reverse transcriptase TERT, the TCAB1 protein, that directs the complex to the Cajal bodies, and the TPP1 protein, that binds the DNA template. Within the telomerase holoenzyme, dyskerin binds the TERC 3' H/ACA domain.

Given the fundamental role played by miRNAs in post-transcriptional gene regulation, it is expected that dyskerin deficiency might affect a large set of biological processes through the snoRNA-derived miRNA regulatory pathway. Consistent with these expectations, a large variety of developmental defects has been described in *Drosophila* as consequence of dyskerin depletion (Tortoriello et al. 2010). Lastly, through its ability to bind the telomerase RNA component (TERC), which harbours a 3' H/ACA domain, dyskerin participates to the telomerase holoenzyme that is assembled in the Cajal bodies, and thus plays a well established role in maintenance of telomere integrity. This additional function was firstly revealed by Mitchell and co-workers (1999), which found that primary fibroblasts and lymphoblasts from X-DC-affected males had a lower level of telomerase RNA, produced lower levels of telomerase activity and had shorter telomeres than matched normal cells, shedding doubt on the initial view of X-DC as a ribosome deficiency disorder. Subsequently, telomerase RNA deficiency was reported also in the circulating lymphocytes of X-DC patients, indicating that this defect was not due to cell culture (Wong et al. 2004). The involvement of dyskerin in maintenance of the telomere ends was definitively established by Cohen et al. (2007), that identified dyskerin as a component of the telomerase active holoenzyme. Subsequently, mutations in NOP10 and NHP2 that, similarly to dyskerin, participate in both H/ACA snoRNPs and active telomerase complex, were also shown to cause autosomal forms of DC (Savage and Bertuch 2010). Mutations in other genes involved in telomerase activity, as TERC, TERT, TINF2 (that encodes a member of the shelterin complex that protects telomere ends), and TCAB1 (also named WDR79 or WRAP53), that is required for scaRNAs and TERC transit in the Cajal bodies, were also shown to cause DC (reviewed by Mason and Bessler 2011**;** Dokal 2011). Successive works indicated that each TERC molecule associates to two full sets of all four core H/ACA RNP components-dyskerin, NOP10, NHP2, and GAR1 (Egan and Collins 2010).
Overall, this picture lead many researchers to conclude that X-DC was mainly due to compromised telomerase function. However, pathogenic *DKC1* mutations affect not only telomere maintenance, but also rRNA processing and pseudouridylation of cellular RNAs, thus provoking a long-standing question: is X-DC mainly a telomerase disorder, or telomere deficiency is just one of the consequences of perturbed H/ACA snoRNP functions?

1.4 Levels of accumulation of unmutated dyskerin are crucial for X-DC manifestation

Several lines of evidence from different organisms or different mammalian cell lines support the existence of a direct relationship between the amount of

unmutated dyskerin and the efficiency of rRNA processing, RNA pseudouridylation, and telomere shortening. This direct dose-effect relationship was firstly outlined in both yeast and *Drosophila* systems (Cadwell et al. 1997; Zebarjadian et al. 1999; Giordano et al. 1999). Subsequently, a X-DC patient carrying a promoter mutation that affected expression of dyskerin rather than its amino acid sequence was identified (Knight et al. 1999; Salowsky et al. 2002). More recently, by analysing a X-linked pedigree presenting familial pulmonary fibrosis, a symptom showed by 20% of X-DC patients, Parry et al. (2011) found that affected males had either shorter telomeres and reduced levels of TERC and unmutated dyskerin. The authors suggested that a low dyskerin level, in the absence of any coding mutation, can be itself cause of the disorder. A large number of experiments based on *DKC1* silencing or knock-down, in both cultured cells or transgenic model organisms, further supports this view. Collectively, these data pose a crucial question: is the loss of the catalytic activity of dyskerin or the dose of the protein the main cause of X-DC typical defects? Are X-DC pathological mutations acting qualitatively or also quantitatively? In the latter case, any parameter affecting protein accumulation and stability may be critical. Answering to these questions might be relevant for the comprehension of the molecular mechanisms underlying X-DC pathogenesis since, despite their apparent diversity, the ensemble of affected processes could all be related to unique dyskerin ability to ensure sufficient synthesis or steady-state levels of H/ACA snoRNAs, including TERC. According to this view, several dyskerin mutations were found to affect only steady-state TERC levels and not the functionality of the telomerase complex, that in fact can be fully restored by exogenous TERC expression (Zeng et al. 2012). In keeping with previous observations, these results outlined a rate-limiting role for dyskerin in telomerase activity. In turn, the general role of dyskerin in ensuring biogenesis and stability of H/ACA snoRNAs might mediate a wide range of different outcomes (Figure 4). For example, rRNA

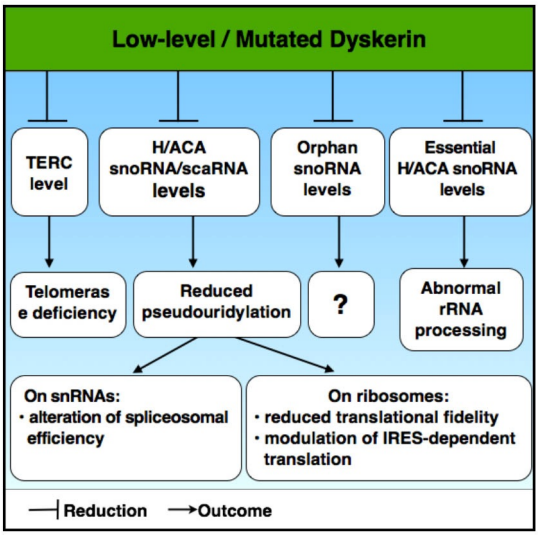

Figure 4. Schematic overview of the variety of effects potentially triggered by dyskerin malfunction. Loss-of-function mutation and *DKC1* gene silencing both cause reduced levels of TERC and H/ACA snoRNAs, being able to trigger the variety of the different outcomes described in latest years.

processing may be affected by reduced levels of snoRNAs essential for its maturation, while reduced pseudouridylation can be a consequence not only of loss of dyskerin catalytic activity, but also of low levels of guide snoRNAs, and a variety of different effects could derive from altered levels of snoRNA smaller processed fragments. Intriguingly, a yet unexplained degree of complexity is generated by the observation that the stability of different snoRNAs can be differentially affected by distinct *DKC1* mutations or by *DKC1* silencing (Mochizuki et al. 2004; Alawi and Lin 2010; Ge et al. 2010; Bellodi et al. 2013); this differential effect extends also to snoRNA-derived miRNA-like molecules (Alawi and Lin, 2010). Although the physiological consequences are presently unknown, it is plausible that some features of X-DC may be related to the functional roles played by these processed molecules.

1.5 Pseudouridylation: a flexible mechanism to modulate gene expression

Pseudouridylation represents the most abundant type of RNA modification occurring in eukaryotic cells. Since pseudouridines promote base stacking interactions and acquire chemical properties that make them able to form hydrogen bridges with bases other than adenine, their presence on RNA facilitates base-pairing, influences folding and increases duplex stability (Davis 1995). All these parameters can logically have a strong impact on both activity and potential interactions of target RNAs. Given that most common targets of pseudouridylation are rRNAs and snRNAs, where pseudouridylated residues are often found at highly conserved functional positions (reviewed by Maden 1990; Yu et al. 2011; Ge and Yu 2013), it was predictable that isomerisation of uridines into pseudouridines could modulate gene expression in a variety of manners. As concerning ribosome structure, it was earlier suggested that this modification not only contributed to rRNA folding and ribosomal subunit assembly, but could also influence translation efficiency and codon recognition (Luzzatto and Karadimitris 1998). Not surprisingly, these predictions have largely been verified in the last decade, since detailed studies on cells in which dyskerin activity was reduced, either by mutations or by specific gene silencing, demonstrated experimentally most of the evoked effects. In 2006, for the first time Yoon et al. revealed that *DKC1* mutations impaired translation from internal ribosome entry sites (IRESs) of specific cellular mRNAs, such as those encoding the apoptotic protein p27 and the antiapoptotic factors XIAP and Bcl-2. The authors suggested that the level of rRNA pseudouridylation could influence the ability of the ribosome to recognize highly structured IRESs, a fundamental step for cap-independent translation. Although active also in physiological conditions, IRES-dependent translation has a key role in

the response to apoptotic stimuli and in cell cycle phases, when cap-dependent translation is reduced (i.e. G_0/G_1 phases). Under-pseudouridylated ribosomes were supposed to affect the ratio between antiapoptotic and proapoptotic factors at the translational level, and this could be one of the causes of bone marrow failure and tumour susceptibility in X-DC patients (Yoon et al., 2006). This conclusion was subsequently supported by the findings that reduced ribosome pseudouridylation, due to either *DKC1* pathologic mutations or reduced dyskerin level, downregulates IRES-mediated translation of p27 and p53 tumour suppressor genes (Montanaro et al. 2010; Bellodi et al. 2010). Further information was recently added by Rocchi et al. (2013) who assayed the translation efficiency of a pool of viral and cellular IRESs in *DKC1* silenced breast cancer cell lines. These authors observed that p53 and CrPV IRES-mediated translation were reduced, while *c-myc*, HCV and EMCV IRES-dependent translation were unaffected. Furthermore, VEGF and HSP70 IRES-mediated translation were upregulated. These results lead to conclude that the level of ribosome pseudouridylation can differently modulate IRES-dependent translation: expression of some specific mRNAs could be repressed, while that of others be either unaffected or upregulated. In addition to modulate IRES-dependent translation, the level of ribosome pseudouridylation can trigger additional and unpredicted effects. In fact, it reduces the binding affinity of aminoacyl-tRNA at both A and P sites, generates translation frameshift, and lead to increase the recognition of *in-frame* stop codons. These effects are conserved from yeast to humans, and result in a decrease of translational fidelity (Jack et al. 2011). Worth noting, effects of reduced pseudouridylation are not limited to rRNA, since also spliceosomal snRNAs represent common targets. Pseudouridylation of snRNAs, that occurs in the Cajal bodies, proved to be crucial for both spliceosomal assembly and mRNA splicing in different organisms as yeast, Xenopus and mammals (reviewed by Wu et al. 2011). Given the significant impact that snRNA pseudouridylation can exert on splicing, it is particularly intriguing that yeast U2 snRNA was found to be inducibly pseudouridylated at two new sites upon stress conditions, (Wu et al. 2011). After this finding, the possibility that pseudouridylation may represent a flexible mechanism able to modulate RNA function in response to cellular signals will be seriously considered. Altogether, these data indicate that this widespread RNA modification can regulate gene expression at different levels and in different ways (see Figure 4).

1.6 Dyskerin and cancer: an intimate but contradictory connection

In 1992 Dokal et al. observed that primary skin fibroblast cultures derived from DC patients were abnormal both in morphology and growth rate (doubling time

about twice the normal) compared to control cells. Since then, many papers have highlighted that dyskerin deficiency perturbs cell cycle progression and proliferation. In particular, a G2/M arrest has been observed in yeast cells with mutated *Cbf5* (Jiang et al. 1993), in transformed dyskerin-depleted cells (Alawi and Lin 2011; Alawi and Lin 2013), in fibroblasts from X-DC patients (Carrillo et al. 2013), and in mouse embryonic fibroblasts expressing only catalytically inactive dyskerin (Gu et al. 2013). Nonetheless, cancer susceptibility represents a main characteristic of X-DC, with head and neck squamous cell carcinomas most frequently observed, followed by skin and anorectal cancer. Cumulatively, the incidence of cancer in X-DC patients was reported around 40%-50% by the age of 50 years (Alter 2009). Considering the functions played by dyskerin as component of H/ACA snoRNPs and telomerase, its deficiency was expected to limit the proliferative capacity of cells, thus making the tumour predisposition observed in the patients difficult to understand. When this aspect was studied in *DKC1* hypomorphic mice (*Dkc1*^{m}), increased susceptibility to tumour formation was observed in first and second generations, when while rRNA pseudouridylation was significantly reduced, even if defects in telomere length were not yet evident (Ruggero et al. 2003). This observation firstly suggested the existence of a link between deregulated rRNA modification and tumour formation, a view subsequently supported by the finding that, as reported above, under-pseudouridylated ribosomes affect translation of a subset of IRES-containing mRNAs that have a key role in cancer (Yoon et al. 2006; Montanaro et al. 2010; Bellodi et al. 2010; Rocchi et al. 2013). By altering the balance between pro- and anti-apoptotic factors, the degree of rRNA pseudouridylation can thus promote neoplastic susceptibility in X-DC cells. Worth noting, dyskerin deficiency may contribute to tumorigenesis also by altering the splicing of specific mRNAs, or by modulating the level of certain snoRNAs. Indeed, fluctuations in the levels of several snoRNAs have been recently observed in various types of cancers, establishing an unexpected link between deregulated expression of these molecules and both cell proliferation and stress response (reviewed by Taulli and Pandolfi, 2012).

1.7.1 *Drosophila* as a model for the study of dyskerin telomerase-independent functions

One of the main challenges posed by the pathogenesis of the X-DC is the understanding of the effects caused by telomere shortening and those caused by altered snoRNPs function. In this respect, the fruit fly is an excellent model organism with which to dissect the telomerese-independent roles of the proteins of the dyskerin family. Indeed, the *Drosophila* homologue of dyskerin,

encoded by the *Nop60B/minifly* (*mfl*) gene, is highly related to its human counterpart, sharing with it 66% identity (Figure 5). The conservation increases remarkably within functional domains (Giordano et al. 1999). In addition, the most frequent missense mutations founded in patients affected by X-DC fall in regions of identity between the *DKC1* and *mfl*. Moreover, *DKC1* and *mfl* genes are positively regulated by Myc oncoproteins, which play an evolutionarily conserved regulatory role in cell growth and proliferation during development. Despite these similarities, telomere maintenance in *Drosophila* is not performed by a canonical telomerase, but by a unique transposition mechanism involving two telomere-associated retrotransposons, HeT-A and TART, which are attached specifically to the chromosome ends (Pardue et al. 2005). The conservation of rRNP/ snoRNP functions, coupled with a different mechanism of telomere maintenance, makes *Drosophila* a useful model system to evaluate the telomerase-independent roles played by pseudouridine synthases. Hypomorphic mutations of *mfl* gene causes developmental delay, defective maturation of rRNA, small body size, alterations of the abdominal cuticle and reduced fertility, while null mutations causes larval lethality.
All of this makes difficult to use the mutants to perform a detailed analysis of

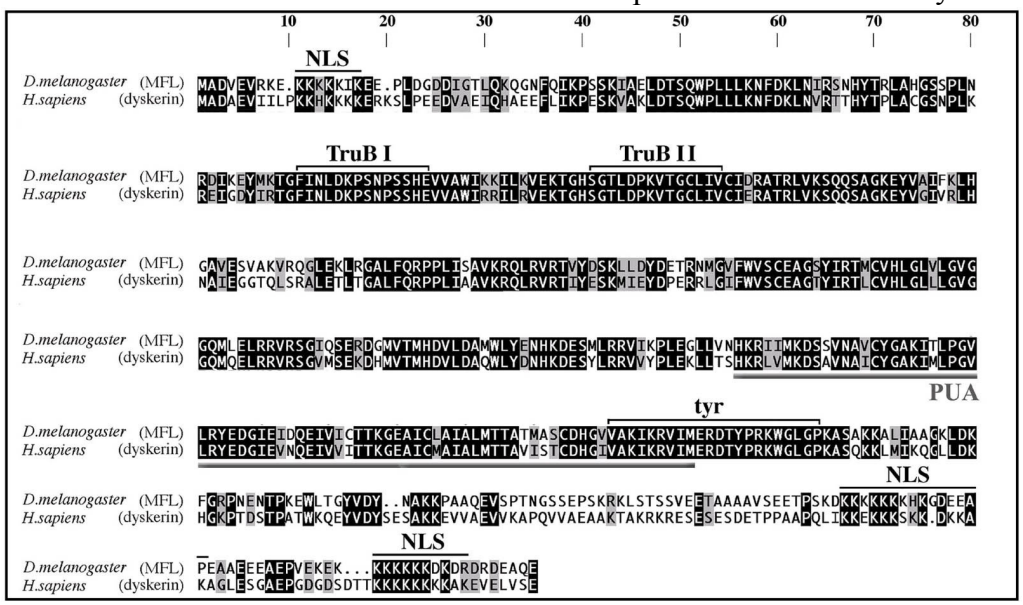

Figure 5. Alignment of *Drosophila* MFL protein and human dyskerin. The two proteins share 66% identity and 79% similarity.

the molecular mechanisms that underlie of the complex phenotypes.
This problem could be overcome by triggering gene silencing by means of RNA interference (RNAi) induced *in vivo* by the yeast Galactose 4 activator protein (Gal4)/yeast upstream activation sequence (UAS) system, routinely used to knock down gene expression in specific regions of the transgenic fly. This approach allowed tissue-specific *mfl* silencing and revealed that MFL

depletion causes specific alterations of developmental patterns (Tortoriello et al. 2010). In directing tissue-specific gene silencing, one anatomical structure of the *Drosophila* can furnish excellent and well studied model to investigate developmental events: the imaginal disc/adult wing system, for the study of patterning, growth, apoptosis and tumorigenesis. The main features of this system is outlined in the following sections.

1.7.2 The imaginal disc/adult wing system

The larval imaginal discs are epithelial structures from which the adult body structures originate. The wing imaginal disc has served as an excellent model to study how morphogens regulate organ patterning and growth. This disc grows from 20-30 cells in the embryo to about 50,000 cells during larval stages; at the third larval stage, it appears as a flattened sac formed by two cell types, the upper squamous peripodial cells and the underneath folded columnar epithelium (Figure 6). Early in their development, imaginal discs are subdivided into spatially distinct and stable units, called compartments, that are developmental fields of cells sharing common ancestry and adhesive properties. The compartment in fact identifies a defined cell population separated from surrounded cells by rigid lineage boundaries (Garcia-Bellido et al. 1973). Signaling between compartments establishes Anterior-Posterior (A-P) and dorsal-ventral (D-V) boundaries (Neto-Silva et al. 2009; Klein 2001). The A-P boundary is defined during the first instal larvae and divides the disco into Anterior and Posterior compartments. The D/V boundary is defined during the second larval instar and divides the disc into Dorsal and Ventral compartments. Imaginal discs begin to intensely proliferate at the second larval instar larvae, and continue to proliferate during third instar, until pupariation. The centrifugal regions of the

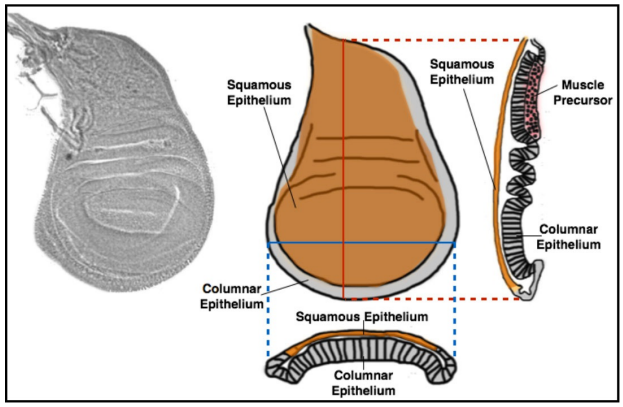

Figure 6. Structure of *Drosophila* wing disc. On the left, representation of a third instar dissected wing imaginal disc as it appears under the stereomicroscope. On the right, schematic representation of the same disc showing the columnar epithelium (in gray, also called pseudostratificated epithelium), the squamous epithelium (in orange, also called peripodial membrane) and the precursors of muscle cells.

imaginal disc five rise to the thorax structures, the notum and the pleura. The middle region gives rise to the hinge region, while the central region is the presumptive territory that will form the wing lamina. At the early pupal stage the peripodial cells undergo apoptosis, while cells of the columnar epithelium undergo an eversion process, forming a Proximal-Distal axis. Specifically, the cells at the centre of the columnar epithelium telescope out to become the most distal region of the wing (the wing blade), while the surrounding cells give rise to the wing hinge, and the outmost cells become the proximal structures (the notum and the pleura; dorsal thorax structures; see Figure 7).

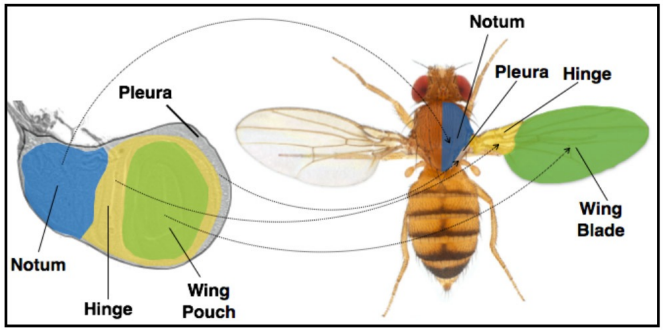

Figure 7. Fate map of third instar wing disc. During metamorphosis, the presuntive regions of pleura (in gray), notum (in blue), hinge (in yellow) and wing pouch (in green) will give rise to the respective adult body regions.

1.7.3 Determination of the Anterior-Posterior axis in the wing disc

One of the first events occurring in the imaginal disc development is the formation of the Anterior-Posterior polarity, that is triggered by the activation of the *engrailed* (*en*) gene (Figure 8). *en* is specifically expressed within the posterior compartment, and its protein induces the expression of *hedgehog* (*hh*) in this compartment (Tabata and Kornberg 1994; Zecca et al. 1995). Hh protein is a morphogen that spreads in a line of cells along the anterior-posterior border, where it induces the expression of another morphogen, Decapentaplegic (Dpp) (Tabata and Kornberg 1994; Zecca et al. 1995). This process is the basis of a complex regulative pathway that leads to the activation and the repression of a large number of regulatory genes. The final result is the definition of the Anterior-Posterior axis and the definition of positional information that leads to the creation of the Anterior-Posterior boundary, as well as the specification of the vein and intervein regions.

1.7.4 Determination of the Dorsal-Ventral axis in the wing disc

Dorsal-Ventral polarity is the second axis to form in a temporal succession. The definition of this axis (Figure 9) occurs at the beginning of the second larval instar (Garcia-Bellido et al. 1973). The dorsal-ventral restriction border

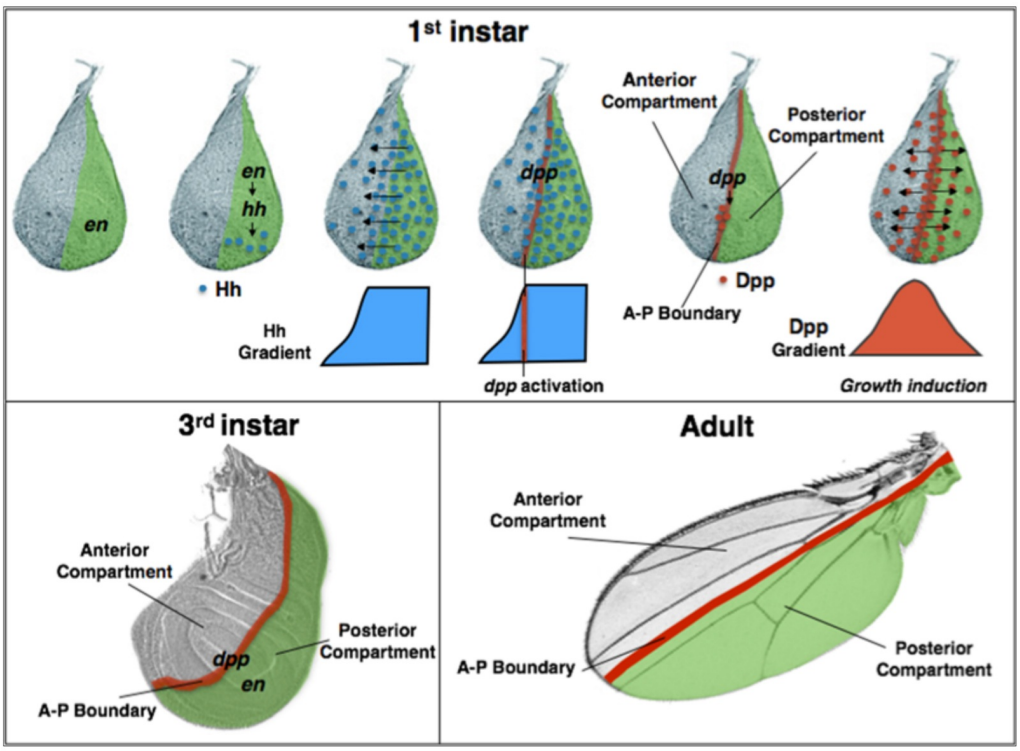

Figure 8. Anterior-Posterior axis formation. At the top, representation of the events that lead, during the first instar larvae, to the specification of Anterior-Posterior axis: *engrailed (en)* expression marks the posterior compartment; *engrailed* expressing cells (in green) also express the segment polarity gene *hedgehog* (*hh*) which encodes a secreted protein (in blue). By inhibiting *dpp* repressors, Hh causes adjacent anterior compartment cells to express *decapentaplegic* (*dpp*). Dpp is a TGF-beta family member that directs growth of the anterior and posterior compartments. Dpp-secreting cells from the Anterior-Posterior axis. At the bottom, representation of the Anterior-Posterior compartmentalization in a third instar wing imaginal disc (at left) and in an adult wing (at right).

depends on the selector gene *apterous (ap)*, that is expressed only in the dorsal compartment (Diaz-Benjumea and Cohen 1993; Blair 1993). The Ap protein induces *fringe* (*fng*) (Irvine and Wieschaus 1994) and *serrate* (*ser*) (Kim et al. 1995) expression in the dorsal cells, while restricts *Delta* (*Dl*) expression to Ventral cells. Delta and Serrate are two Notch (N) ligands (Rebay et al. 1991; de Celis et al. 1996; Milán and Cohen 2000), while Fringe is a secreted glycosil transferase that modifies Notch receptor (N), inhibiting its affinity for unmodified Notch is very low. The final outcome is that in the dorsal compartment the activity of Serrate is inhibited by Fringe, while Delta is ventrally expressed, and can't activate Notch. The only region where Serrate and Delta can both activate Notch is at the Dorsal-Ventral boundary, in two cell stripes (de Celis et al. 1996). At this region, Notch activates the expression of *wingless* (*wg*), *cut* (*ct)* and *vestigial* (*vg*) and, as a consequence, the D/V restriction boundary is formed and the wing blade presumptive territory begins to be defined.

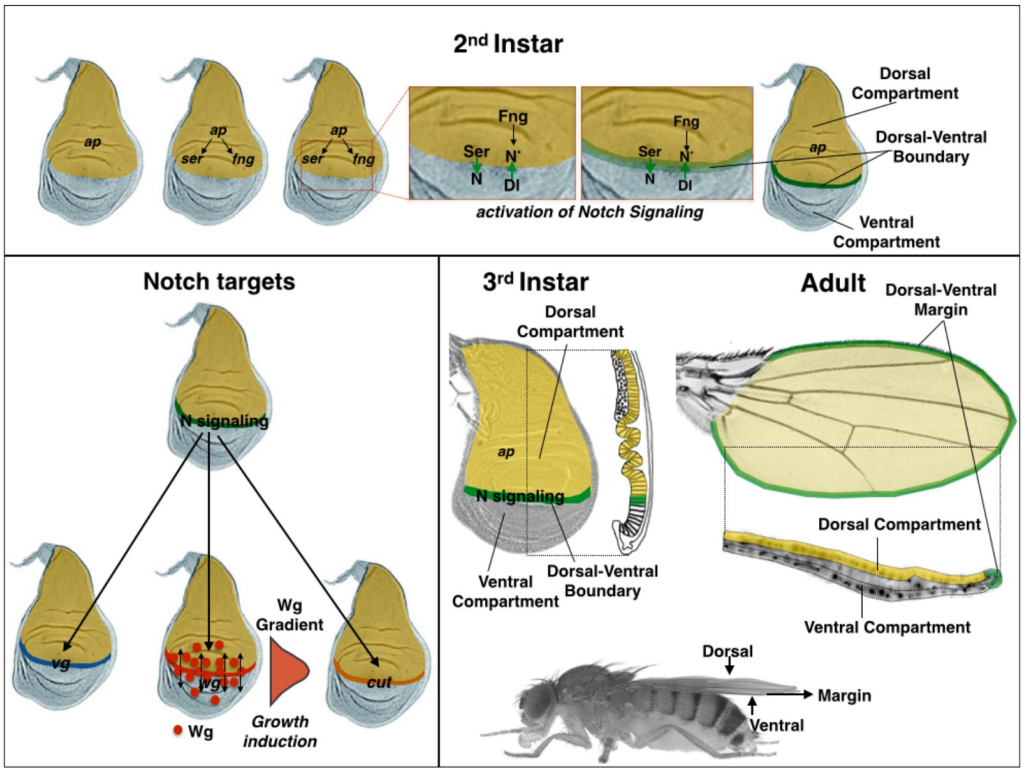

Figure 9. Dorsal-Ventral axis formation. At the top, representation of the events that lead, during the second instar larvae, to the specification of Dorsal-Ventral axis: *apterous (ap)* is expressed in the dorsal compartment (in yellow); Ap protein induces the expression of the glycosil transferase Fringe (Fng) and the Notch ligand Serrate (Ser). Fng performs glycosylation of Notch receipts (N*), making it the highest affinity for Dl (ventrally expressed) and low affinity for Ser (dorsally expressed). The only region where Serrate and Delta can both activate Notch is at the Dorsal-Ventral boundary, in two cell lines. In the cells of the Dorsal-Ventral boundary, the activation of the signaling pathway mediated by Notch (at the bottom left of the figure) leads to the activation of target genes *vestigial* (vg) wingless (wg) and *cut*. Notch target genes contribute to the patterning and growth of the wing disc. The panel at the bottom right shows the Dorsal-Ventral compartmentalization in the third instar wing disc and in the adult wing.

1.7.5 Structural organization of the adult wing

During prepupal and initial pupal stages, the wing imaginal disc everts and folds to form apposed dorsal and ventral epithelia that form the wing blade. The adult wing is thus composed of a plate of epithelial bi-stratified cells in which a ventral and a dorsal surface are present. The proximal region, called hinge, connects the wing to the dorsal (notum) and ventral (pleura) thorax, respectively. The wing lamina, called wing blade (Figure 10), in the anterior border is provided with three series of sensorial bristles, and presents two types of cells that form vein and intervein territories. Five veins are present in each wing blade; these veins are formed by live epithelial cells composing tubular

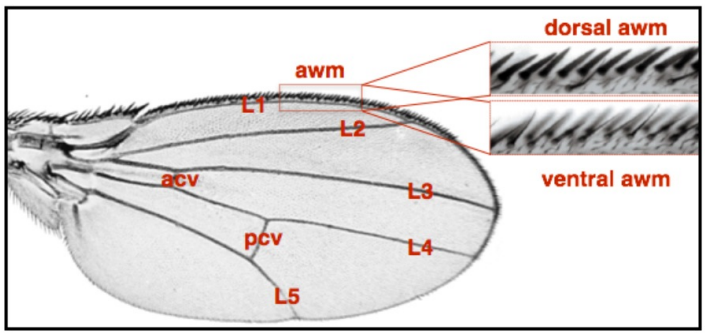

Figure 10. Structural organization of *Drosophila* adult wing. L1-L5: the five longitudinal veins; acv: anterior cross vein; pcv: posterior cross veins; awm: anterior wing margin. awk differentiates three rows of bristles. Two are dorsal (a row of thick mechanosensory bristles adjacent to the compartment boundary and a row of thin curved chemosensory bristles). The ventral row is composed of thin bristles interspersed with chemosensory bristles.

structures that give stiffness to the wing and accomodate the tracheas and the neuronal sheafs. Intervein cells are instead dead and chitinized, and are characterized by the differentiation of a single trichome per cell.

1.7.6 RNAi-mediated gene silencing *in vivo*

Drosophila provide a useful model for the study of developmental events. The genome is fully sequenced, highly annotated and capable of specific manipulation by a variety of techniques. Among others, particularly useful is the binary Gal4/UAS activation system. This system has been adapted from yeast, and relies on the expression of the *Gal4* gene, driven by a specific promoter. Once expressed, the GAL4 protein binds to Upstream Activating Sequences (UAS) and activates the transcription of sequences placed downstream theses sites. This allows for any construct placed downstream of UAS to be expressed in a specific tissue or at a specific time point in development, depending on the wide range of different GAL4 transgenic lines available. Transgenic lines in which GAL4 is under control of specific promoters or enhancers (driver lines) can drive expression of the target UAS-gene in an ubiquitous, temporal/spatial specific or conditional manner. UAS transgenic flies (responder lines) can be used in order to express a particular gene of interest, but also to trigger gene silencing, if transcription of the transgene placed under the UAS control produces a dsRNA able to trigger the RNA interference (RNAi) mechanism. When 'responder' flies are mated to those expressing the Gal4 driver, the resulting progeny (F1) will express the transgene in an expression pattern that will mirror that of the Gal4 driver. For example, *actin-Gal4* or *tub-Gal4* driver lines will allow to express an UAS-trangene (GFP and/or RNAi construct) ubiquitously, while *en-Gal4*, *ap-Gal4*, *vgBE-Gal4 and Omb-Gal4* are driver lines will be active only within specific anatomical regions (Figure 11) and at specific developmental times.

By using the GAL4–UAS system to silence the *mfl* gene *in vivo* in the developing wing disc, Tortoriello et al. (2010) found that knocking-down gene expression by a variety of different drivers was always able to elicit a region-specific size reduction in the corresponding domains of GAL4 expression. The size reduction was achieved either by decreases in cell size or in cell number, depending on the GAL4 driver used. A significant effect on cell size was manifested in the wing pouch, where *mfl* silencing led to markedly higher cell density. Conversely, a decrease in cell number was observed upon silencing in a whole compartment (posterior or dorsal), and this effect was mainly caused by cell death rather than reduced proliferation. Notably, other phenotypes associated with *mfl* knockdown mimicked those caused by impaired Notch signaling, suggesting that the activity of the MFL pseudouridine synthase is required for the normal function of this conserved signaling pathway (Tortoriello et al. 2010). The finding that *mfl* silencing causes phenotypes highly reminiscent of those resulting from defective Notch signaling, perturbing the formation of the D/V boundary, is particularly interesting, as it provides new insights into the mechanisms by which pseudouridine synthases may coordinate cell growth with the developmental programs. During wing development, delineation of the D/V boundary is controlled by the Notch pathway, whose impairment leads to both decreased proliferation and cell affinity changes (Rafel and Milán 2008). Understanding how the loss of function of *Drosophila* snoRNP pseudouridine synthase encoded by the *mfl/*

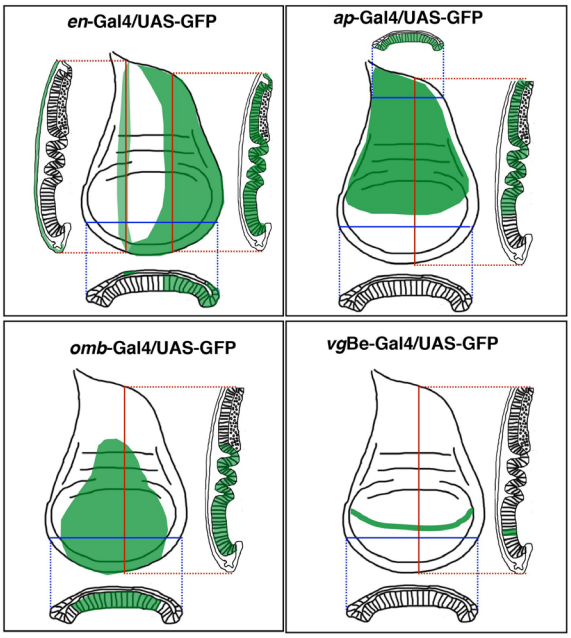

Figure 11. Expression pattern of some of the Gal4 driver lines utilized. The *en*-Gal4 lines expresses Gal4 in the P compartment of the columnar epithelium of the wing disc, but also in same cells of the peripodial membrane (in particular in a stripe of peripodial cells above the A compartment). The *ap*-GAl4 lines expresses Gal4 in the D compartment of the columnar wing disc. The *omb*-Gal4 line expresses Gal4 in the central region of the columnar wing disc. The *vgBE*-Gal4 expresses Gal4 at the D/V boundary of the columnar wing disc., and the *esg*-Gal4 line expresses Gal4 in the AMP, PC and ees esg+ pro+ cells of the larval midgut.

Nop60b gene, can affect Notch signaling is especially important, considering that the Notch pathway is evolutively conserved, controls cell differentiation in many tissues, and regulates binary cell fate decisions and stem cell maintenance (Tien et al. 2009). Using different driver lines, during this work, I have confirmed that MFL depletion causes alteration of Notch signaling and also activation of JNK pathway. A brief summary of the two pathways is shown in the next two sections.

1.8 Notch signaling

The Notch gene encodes a transmembrane receptor that gave the name to the evolutively conserved Notch signaling cascade. It plays a pivotal role in the regulation of many fundamental cellular processes, such as proliferation, stem cell maintenance and differentiation throughout embryonic and adult development. The signaling is based on the binding of two transmembrane proteins presented by neighboring cells: the receiving cells present the Notch receptor, while the sending cells a Notch ligand (DSL: Delta, Serrate, Lag2). DSL-binding of Notch results in the intracellular cleavage of the receptor and the release of its intracellular domain (Nintra). Nintra migrates to the nucleus and binds the transcription factor CSL (Borggrefe and Oswald 2009; Bray and Bernard 2010). The CSL acronym is derived from the fused initials of the human CBF1, the *Drosophila* Suppressor of Hairless [Su(H)], and the C. *elegans* Lag1 factors. By binding a CSL factor, Nintra assembles an activator complex that includes Mastermind (MAM) co-activators (Nam et al. 2006; Wilson and Kovall 2006; Kovall and Blacklow 2010). In vertebrates and in *Drosophila*, this process is antagonized by proteins which transform CSL factors into transcriptional repressors of the Notch target genes (Borggrefe and Oswald 2009; Bray and Furriols 2001). While in vertebrates this co-repressor complex contains SMRT, SHARP (also known as MINT and SPEN) and CtBP, in *Drosophila* it contains Hairless (H), CtBP and Groucho (Gro) (Brou et al. 1994; Morel et al. 2001; Maier 2006; Bray and Bernard 2010; Bray 2006). The Su(H) interacting protein Hairless (H) is the major platform for Su(H) dependent corepressor complex assembly. However, Hairless homolog proteins cannot be identified within higher eukaryotes (Maier 2006), although it has been suggested that a functional homologue might be represented by mammalian SHARP (Oswald et al. 2005; Morel et al.

2001; Barolo et al. 2002). The Figure 12 summarize the main events regulating Notch signaling.

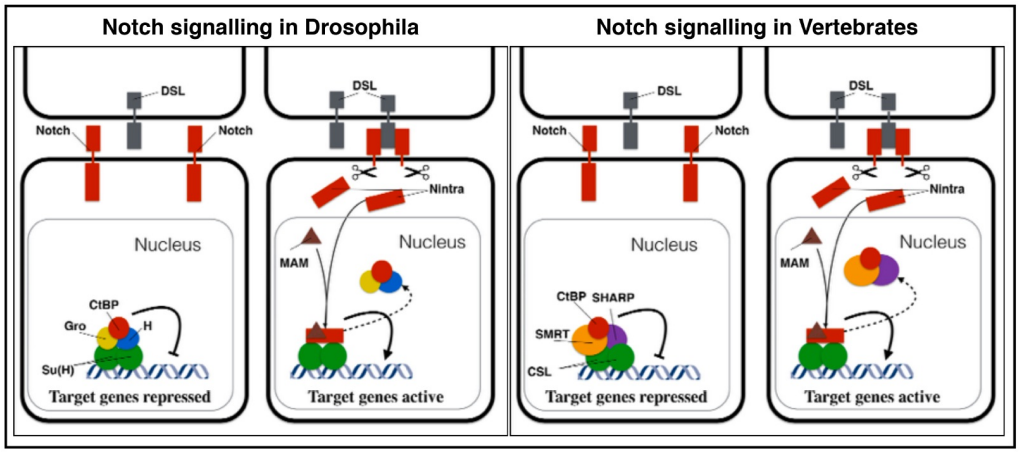

Figure 12. Notch signaling in *Drosophila* and Vertebrates. If there is no interaction between Notch and its ligand (DSL), the target genes are repressed by the co-repression complex. Two co-repressor complexes are illustrated: a *Drosophila melanogaster* complex containing Hairless, CtBP and Groucho (Gro), and a vertebrate complex containing SMRT, SHARP and CtBP. Binding of a DLS ligand of one cell to the Notch receptor of a close cell results in a proteolytic cleavages of the receptor. This proteolytic processing mediates release of the Notch intracellular domain (Nintra), which enters the nucleus and interacts with the DNA-binding CSL (CBF1, Su(H) and LAG-1) proteins. The co-activator Mastermind (Mam; green) is recruited to the CSL complex, and co-repressors are released.

1.9 JNK pathway

The c-Jun N-terminal Kinase (JNK) signaling is an evolutionarily conserved pathway, which is activated in response to many stress (ROS, UV, inflammation, heat) apoptotic signals and proinflammatory cytokine tumor necrosis factor (TNF) (Liu et al. 1996; Moreno et al. 2002; Ryoo et al. 2004; Xia et al. 1995). While the individual components of the JNK signaling pathway are represented by large gene families in vertebrates, the pathway is significantly less complex in flies (Igaki 2009; Johnson and Nakamura 2007). Indeed, *Drosophila*, JNK signal pathway (Figure 13) consists of a number of JNKKKs (including MLK: Mixed Lineage Protein Kinase 2/Slipper; ASK1: Apoptotic signal-regulating Kinase 1; TAK1: TGF-β Activated Kinase 1 and MEKK1: MEK Kinase1), two JNKKs (Hemipterous and dMKK4) and a single JNK (basket). In the activated form of JNK has a number of nuclear and cytoplasmic targets, most prominently transcription factors, including the AP-1 family members Jun and Fos and the Forkhead Box O transcription factor FoxO (Johnson and Nakamura 2007; Weston and Davis 2007). Changes in the cellular transcriptome are thus a major part of the cellular response to JNK

activation (Jasper et al. 2001; Johnson and Nakamura 2007). In *Drosophila*, an important target gene of AP-1 is puckered (*puc*), which encodes a JNK-specific phosphatase that restricts JNK activity in a negative feedback loop (Martin-Blanco et al. 1998; McEwen and Peifer 2005). Selected genes that are transcriptionally regulated in response to JNK activation, and that mediate specific physiologic consequences of JNK activation, such as apoptosis, cytoprotection, autophagy, metabolism and growth, cell proliferation, regeneration and tissue repair.

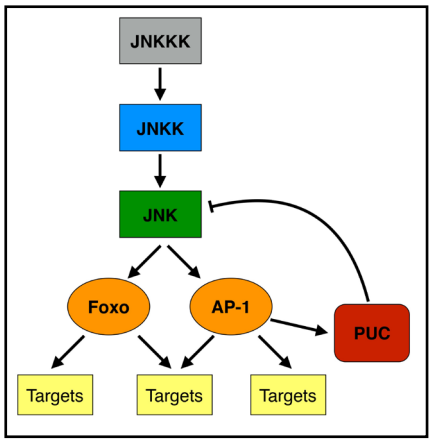

Figure 13. JNK signal pathway in *Drosophila*. Into *Drosophila* genome many JNKKK proteins are present, including MLK/Slipper; ASK1; TAK1 and MEKK1. JNKKK proteins phosphorilate the two JNKK proteins (Hemipterous and dMK4) that phosphorilate the only JNK protein called Basket. In the activated form of JNK has a number of nuclear and cytoplasmic targets, most prominently transcription factors. An important target gene is *puckered* (*puc*), which encodes a JNK-specific phosphatase that restricts JNK activity in a negative feedback loop.

2. AIMS OF THE STUDY

Eukaryotic pseudouridine synthases compose a highly conserved protein family, whose best characterized members are yeast Cfb5p, rat NAP57, *Drosophila* MFL/Nop60b, and mouse and human dyskerins (for a review, see Angrisani et al. 2014). All members of the family localize mainly in the nucleolus, and are components of the H/ACA snoRNP complex that is involved in a variety of essential cellular functions, including ribosome biogenesis, pseudouridylation of cellular RNAs, modulation of the efficiency of internal ribosomal entry (IRES)-dependent translation, and biogenesis and stability of H/ACA snoRNAs. In humans, the pseudouridine synthase dyskerin is also an essential component of the active telomerase complex and therefore has a relevant role in maintenance of telomere integrity. Loss of function mutation in the dyskerin encoding gene (h*DKC1*) are responsible for the X-Linked Dyskeratosis Congenita (X-DC), a disorder characterized by mucocutaneous features, premature aging, bone-marrow failure and increased susceptibility to cancer. The distinction between the effects caused by telomere shortening and those related to impairment of other dyskerin functions is one of the main challenges posed by the pathogenesis of this disease and is still on debate. *Drosophila* may represent an attractive model system with which to dissect the telomerase-independent roles played by members of eukaryotic

pseudouridine synthases. The *Drosophila* protein, encoded by the *Nop60B / minifly* (*mfl*) gene, is highly related to dyskerin, its human counterpart, sharing with it 66% identity and 79% similarity (Giordano et al. 1999). In addition, the most frequent missense mutations identified in X- DC patients fall in regions of identity between the human *DKC1* and the *mfl Drosophila* gene. However, despite these similarities, telomere maintenance in *Drosophila* is known not to be performed by a canonical telomerase, but by a unique transposition mechanism involving two telomere-associated retrotransposons, HeT-A and TART, which are attached specifically to the chromosome ends (Pardue et al., 2005). The purpose of this study was that of using *Drosophila* as a model organism to obtain more detailed information about the telomerase-independent roles of eukaryotic pseudouridine synthases, in order to increase the knowledge of the molecular mechanisms underlying the X-DC pathogenesis. Previous work (Tortoriello et al. 2010) and my preliminary experiments showed that *in vivo* silencing of the gene by localized RNAi did not impeded protein synthesis or cell proliferation (no significant alteration in the levels of tubulin or other constitutive proteins between the silenced and unsilenced areas; efficient GFP expression in the silenced tissues, etc.) suggested that gene silencing may specifically affect key devolpemental pathways. I thus focussed my research activity to analyze the effects of *mfl* gene silencing on the development of the wing imaginal disc, which represents an excellent model to study the morphogenetic regulation of organ growth and patterning. Experiments reported in this thesis document the effects triggered by gene silencing on the activity on important and highly conserved developmental pathways, such as those of Notch, Wg/Wnt and JNK signaling, with the main aim to define how pseudouridine synthases could regulate tissue growth and differentiation. A major attempt was that to gain more information about the puzzling issue: how X-DC patients, who carry loss-of-function mutations in a gene involved in ribosome biogenesis, and thus is essential for cell growth and proliferation, can acquire a paradoxical high predisposition to develop cancer?

3. MATHERIALS AND METHODS

3.1 *Drosophila* strains

Flies were raised on standard *Drosophila* medium at 25 °C. UAS-IR*mfl* RNAi *mfl*-silencing lines (v46282 and v46279) were from the VDRC RNAi collection. The following strains: # 30730 (UAS-DCR2/UAS-DCR2; *en*-Gal4, UAS-myrRFP, NRE-GFP/Cyo), # 30728 (NRE-GFP/NRE-GFP on 3rd Chromosome), #25752 (*en*-Gal4, UAS-GFP/Cyo); #6819 (*vg*BE-Gal4; TM2/ TM6B) were obtained from Bloomington Drosophila Stock Center at Indiana University. *en*-Gal4/Cyo and UAS-p35/TM3 was kindly provided by L.

Johnston (Columbia University, USA). UAS-HAflII/TM3sb over-expressing Hp120 construct, *puc*-lacZ/TM3 reporter, *omb*-Gal4/FM7 driver line and *omb*-Gal4/*omb*-Gal4;*vg*BE-lacZ/*vg*Be-lacZ combined line were kindy provided by A. Preiss (University of Hohenheim, Germany).

3.2 Mounting adult wings

Wings were removed from adult flies and dehydrated in 100% ethanol for 5 min. The wings were placed on a microscope slide, and ethanol allowed to evaporate. A small drop of Euparal Mounting Medium was dropped onto the wing and a glass coverslip placed on top. Images were captured with a Spot digital camera and a Nikon E1000 microscope. For the monitoring of the NRE-GFP reporter, the adult wings were detached, placed dried on a slide and imaged in with an epifluorescence Nikon E1000 microscope.

3.3 In vivo Notch signaling activity functional assay

Immediately after dissection, wing imaginal discs from third instar larvae were placed in a drop of PBS + DAPI and imaged with an epifluorescence Nikon E1000 microscope. The raw pictures were analyzed with ImageJ v1.440 software.

3.4 Immunofluorescence stainings

Wing discs were dissected, fixed and immunostained as described in Tortoriello et al. 2010. Antibodies used were: customer rabbit polyclonal antibody against MFL (Sigma-Aldrich Inc., St. Louis, MO, USA; dilution 1 : 100); mouse monoclonal antibodies against Wingless, Cut, Arm, Mmp1, β-Galactosidase (Hybridoma Bank, University of Iowa, Iowa City, IA, USA; dilution 1 : 50 anti-Wg, 1:100 anti-Cut; 1:50 anti-Arm, 1:50 anti-Mmp1 and 1:250 anti-β-Gal); rabbit polyclonal antibodies against Phospho-Histone H3 and cleaved Caspase-3 (Cell Signaling Tech., Danvers, MA, USA; dilutions 1 : 100 anti-PH3 and 1 : 500 anti-Cas3); guinea pig polyclonal antibody against Hairless central domain (anti-H_{CD}, gift, from A. Preiss and D. Maier, Hohenheim University, Stuttgart, Germany; dilution 1:500); rat polyclonal antibodies against Groucho and CtBP (gift from AC Nagel, Hohenheim University; dilution 1:500 for both antibodies); rabbit polyclonal antibody against Twist (gift from AC Nagel; dilution 1:50). Fluorescent secondary antibodies were from Jackson ImmunoResearch (Dianova, hamburg, Germany) and used at a final dilution of 1 : 200. Rhodamine Phalloidin Conjugate for actin cytoskeleton staining were obtained from Molecular Probes (Eugene, OR;

dilution 1:250). Confocal images were obtained with a Bio-Rad MRC1024 or Zeiss LSM510 confocal microscope.

3.5 Z-stack analysis

All captured pictures (in RAW format) have been analyzed and processed with ImageJ v1.440 software Z-stack analysis was performed by using STACK> ZProjection and STACK>Othogonal views ImageJ plug-in.

3.6 Wg gradient analysis.

To quantify the amount of Wg protein secreted by D/V boundary cells, for each imaged stained discs were captured many focal planes (from the base of the pseudo stratified epithelium to the base of the peripodial membrane). All focal planes were added with STACK> ZProjection ImageJ plug-in. On each ZProjection pictures, two areas of 100 x 150 pixels centered on the D/V boundary, one in the posterior region and the other in the anterior region, were selected. For each of the two areas the luminance histogram of the Wg signal was drawn using PlotProfile algorithm of ImageJ. The area of each histogram, that reflects the amount of Wg secreted by D/V boundary cells ($[Wg]_{D/V\ boundary}$), was calculated with the algorithm Measure of ImageJ. For 5 discs of each genotype the ratio $[Wg]_{Posterior\ D/V\ boundary}$ /$[Wg]_{Anterior\ D/V\ boundary}$ was calculated. The obtained values obtained were subjected to One-way ANOVA analysis.

3.7 In situ hybridizations

In situ hybridizations was carried out as described in Giordano et al. 1999. Cut single-stranded DIG-labeled probe was prepared from plasmid pGEM-T easy vector (Promega) from plasmid pGEMT-easy carrying *cut* gene-specific genomic fragments obtained by PCR amplification using specific oligo primers designed with Primer3 software and sequence date available in Flybase (flybase.org)(primer sequences: F 5'-TGCACATATCCTCAGCGAAG- 3'; R 5'-CCTGGTAGAGACGAGCCATC-3')

3.8 Protein extraction and western blot analyisis of embryo lysates

Embryos were dechorionated in 50% Chlorix (2 minutes) and washed in 0,7% NaCl + 0,002% Triton X-100 solution. 100 dechorionated embryos of each genotype were homogenized in 80 µl of RIPA I buffer (50 mM TRIS-HCl pH 7.5, 150 mM NaCl, 1% Triton X-100, 0.1% SDS, protease and phosphatase inhibitor cocktail (roche Diagnostics, Basel, Switzerland)) on ice. After thermal denaturation (5 minutes at 100 ° C) and centrifugation, a loading buffer was

added to the supernatant and the samples were loaded onto an SDS-Page followed by western blotting. Rabbit polyclonal anti-MFL antibody (1:100) and guinea pig polyclonal anti-H_{CD} (1:1000) were used. The mouse monoclonal anti-α-tubulin (1:500, AA4.3 Hybridoma Bank) was used as a loading control. The secondary antibodies were coupled with alkaline phosphatase (Jackson ImmunoResearch).

3.9 Laser microdissection

Laser microdissection applied to achieve a compared RNA transcript profiling of silenced and unsilenced areas of the *Drosophila* wing discs was performed as described in Vicidomini et al. 2010. Leica LMD6000 equipment was used to collect 100 areas of about 5000 μm^2 from both anterior and posterior compartment of wing discs. Extraction of total RNA from microdissected areas and subsequent reverse transcription with random hexamers were performed. Accuracy of the laser cut was controlled by checking the *GFP* expression by RT-PCR. Quantification of the accumulation levels of *mfl* and *puc* mRNAs was evaluated by Real Time PCR, using *α-tub* mRNA as normalized an the anterior compartment as internal control.
The primers used (designed by Primer3 software and sequences data in flybase) are as follows:

-*GFP*: Forward 5'-GTCAGTGGAGAGGGTGAAGG-3'
Reverse 5'-TACATAACCTTCGGGCATGG-3'
-*mfl*: Forward 5'-GAACCCAGCAAACGCAAGTT-3'
Reverse 5'-CTTGGAAGGAGTCTCCTCGGATA-3'
-*puc*: Forward 5'-AAATACCTGCCAGCGATACG-3'
Reverse 5'-CAGGGAGAGCGACTTGTACC-3'
-*α-tub*: Forward 5'-GTGAAACACTTCCAATAAAAACTCAATATG-3'
Reverse 5'-CCAGCAGGCGTTTCCAAT-3'

3.10 Prediction of RNA secondary structures

The prediction of secondary structure of the first exon of the *hairless* gene construct and of the of UAS-HAflII construct was performed by RNAfold software at the http://rna.tbi.univie.ac.at/cgi-bin/RNAfold.cgi site. For the calculation of the most stable structure was set to a temperature of 25 ° C.

4 RESULTS AND DISCUSSION

4.1 Depletion of MFL protein causes up-regulation of Notch signaling in the wing disc

mfl RNAi directed by *en*-Gal4 (Figure l4A) or *vg*BE-Gal4 (Figure 14B) driver produces adult wings exhibiting "Notched" margins typical of loss of function *Notch* phenotype (Tortoriello et al. 2010), and thus suggested a reduction of this signaling at the D/V wing margin. In order to confirm this effect, I used a functional *in vivo* assay based on the use of a NRE-GFP reporter transgene (Notch-Response-Element-GFP reporter; Saj et al. 2010) derived from the *Enhancer of Split* [*E(spl)*] Notch-responsive gene (de Celis et al. 1996). In this reporter, the *E(spl) Notch Response Element* drives GFP expression (Figure 15A). In transgenic flies carrying the *NRE:GFP* construct (obtained by Bloomington *Drosophila* Stock Center, Indiana University), GFP expression marks cells with active Su(H)-dependent Notch signaling along the dorsal ventral (D/V) boundary of the wing imaginal disc. By suitable crosses, I introduced the *NRE:GFP* transgene in a *en*-GAl4, UAS-myrRFP, UAS-DCR2 genetic background (the UAS-DCR2 construct is routinely used to increases RNAi efficiency). This line was then crossed to a *mfl*-RNAi line (UAS-IR*mfl*) to obtain a progeny in which depletion of MFL protein was limited to the posterior compartment of the wing disc (RFP-marked), while the anterior compartment served as an internal *wild-type* control. Immediately after dissection, wing imaginal discs from third instar larvae of UAS-DCR2/+; *en*-GAl4, UAS-myrRFP, *NRE:GFP*/+ (control) and UAS-DCR2/+; *en*-GAl4, UAS-myrRFP, *NRE:EGFP*/UAS-IR*mfl* (silenced in the P compartment) genotypes were placed in a drop of PBS + DAPI on a microscope slide for epifluorescence analysis (Figure 15B).

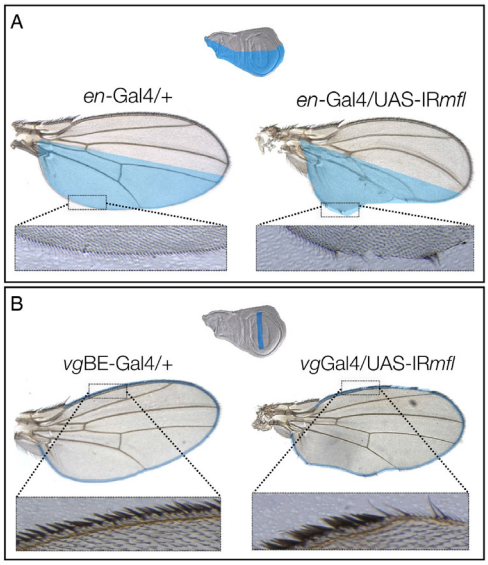

Figure 14. Effects of *mfl* localized RNAi in vivo. (A) *mfl* RNAi directed by en-Gal4 causes a reduction of silenced posterior compartment, alteration of wing vein pattern and alteration of wing margin. **(B)** *mfl* RNAi directed by *vg*BE-Gal4 causes alteration of wing margin. The alteration of wing margin are a typical Notch loss of function phenotype.

In the control discs (Figure 15C, left), the levels of the Nintra activity, localized at the D/V boundary, do not show significant differences between anterior and posterior compartment. Surprisingly, Notch signaling was instead found strongly up-regulated in the D/V boundary cells upon *mfl* silencing

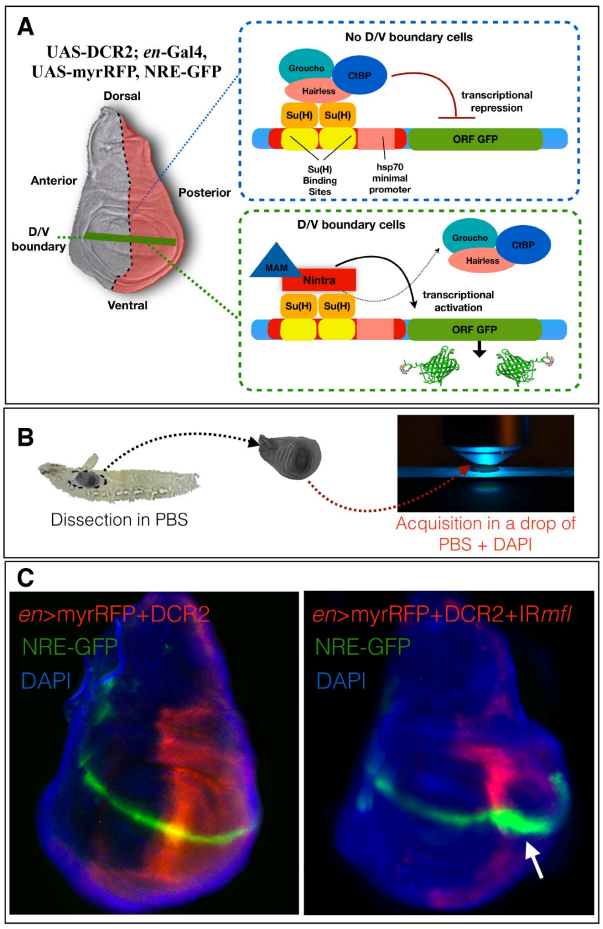

Figure 15. *mfl* RNAi causes Notch signaling up-regulation. (A) structure and functioning of the NRE-GFP transgene: the GFP is placed under the control of a *hsp70* minimal promoter and two *Su(H)* binding sites; in the absence of activation of the Notch receptor, GFP transcription is blocked by the co-repressor complex consisting of Groucho, CtBP and Hairless; in the D/V boundary cells, the Notch receptor is activated, Nintra translocates to the nucleus and, together with MAM, activates GFP transcription. As result, the GFP signal marks Nintra activity at the D/V boundary. **B)** *in vivo* functional assay: immediately after dissection, wing imaginal discs from third instar larvae were placed in a drop of PBS + DAPI and analyzed by fluorescent microscopy. **C)** on the left, expression of the NRE-GFP reporter in wild-type control discs; on the right, upon *mfl* silencing, the expression of the NRE-GFP reporter is strongly increased in the P-silenced compartment.

(Figure 15C, right); the GFP signal was strongly and specifically increased upon *mfl* RNAi in all wing discs inspected (n>20).
Therefore, *mfl* knockdown induced opposite Notch phenotypes during wing development: in fact, while in the adult wings loss-of function defects were observed (Figure 14), hyperactivation of the signaling was observed in the silenced discs (Figure 15). These findings could imply a reversion of Notch up-regulation during development, suggesting that up-regulation of the signaling during early development can be translated into its down-regulation at later stages.
To test this possibility, freshly dissected, unfixed adult wings were analyzed by epifluorescence microscopy and tested for NRE-GFP expression. As reported in Figure 16, in control wings (left panel), Notch reporter (NRE-GFP) expression appears very weak at the posterior D/V boundary; in contrast, upon *mfl* silencing directed by *en-Gal4*, the reporter activity appears to be highly active at the D/V margin and, in addition, ectopically activated in the posterior compartment of the wing blade. The ectopic expression of the NRE-GFP reporter could be due to due to persistence of high Notch activity at the D/V boundary throughout metamorphosis or to loss of Notch repression by defective lateral inhibition into the specification of the veins-interveins terittories. In every case, the observed ectopic activation of Notch signaling is

likely to contribute to the alterations of wing veins pattern shown by *en*-Gal4/ UAS-IR*mfl* adult silenced wings (Figure 14A and 16A). More importantly, the finding that Notch up-regulation persisted along development raises the possibility that coexistence of both gain and loss-of-function phenotypes could be due to a misfunctioning of nonetheless costantly hyper-activated Notch pathway.

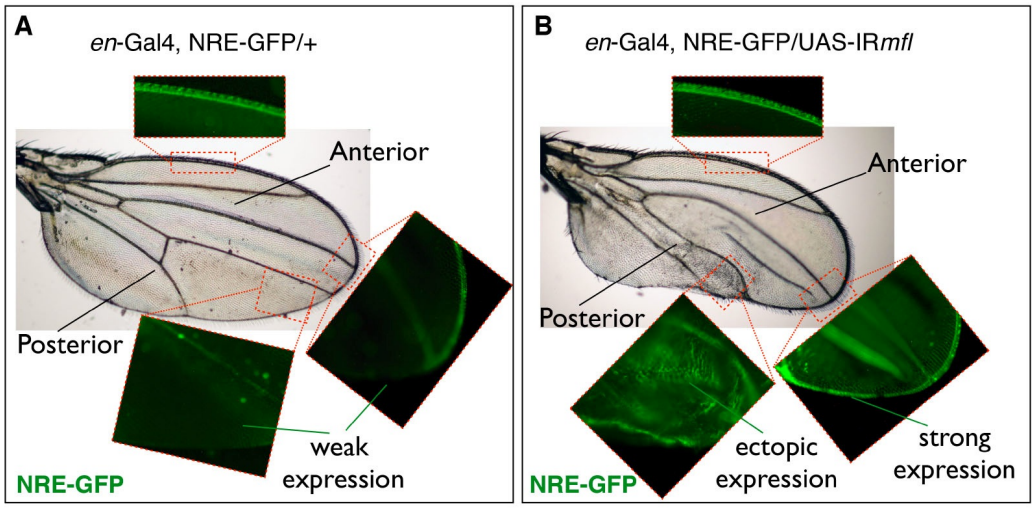

Figure 16. NRE-GFP expression in adult wings. A) In the control wings the expression of NRE-GFP reporter appears high beside veins; vein L1 coincides with the anterior D/V margin. Expression of the NRE-GFP is almost undectectable in the posterior compartment, and along the D/V margin. Upon *mfl* silencing **(B)**, the NRE-GFP reporter is highly active along the posterior D/V margin; in addition, it is also ectopically activated in the posterior silenced compartment; abnormal vein patterning is also evident.

4.2 The *mfl* gene acts as a Notch modifier

The finding that *mfl*-silenced adult wings showed Notch loss of function phenotypes ("notched" wing margin), in contrast with a constant hyperactivation of the signaling, suggested that, although hyperactivated, the pathway could be misfunctional. I thus decided to monitor the expression levels of some Notch gene targets known to be induced in the wing disc at the D/V boundary, such as *wingless* (*wg*), *vestigial* (*vg*BE), and *cut* (Neumann and Cohen 1996), upon *mfl* knockdown.

The activity of the Wg signaling pathway is known to be required for the specification, growth, patterning, and morphogenesis of the wing pouch (reviewed by Gonsalves and DasGupta 2008), and its expression in the wing disc is complex. Two rings of *wg* expression mark the presumptive hinge territory; the wing pouch primordium lies within the inner ring, while the notum is formed from tissue outside the outer ring (Baker 1988; Wu and Cohen 2002). *wg* is known to be a Notch target at the D/V boundary (Williams et al. 1993); upon Notch activation, the Wg protein is secreted and acts as

morphogen: it forms a long-range gradient that induces target gene expression in the surrounding cells (Zecca et al. 1996). To quantify the amount of Wg protein secreted by D/V boundary cells I performed a statistical analysis of its accumulation levels in both control and silenced wing discs. After immunostaining with anti-Wg specific antibody, two equivalent areas of 100 x 150 pixel centered at the D/V boundary (one in the posterior region and the other in the anterior region), were selected from Z-projection confocal microscopy analysis (Figure 17). For each of the two areas, the luminance histogram of the Wg channel was drawn (in gray scale) using Plot Profile algorithm of the ImageJ v1.440 software. These histograms reflected the profile of the Wg gradients, with the area of each histogram depending on the amount of Wg protein produced at the D/V boundary. Specifically, the amounts of Wg protein secreted from the D/V boundary cells in the anterior (unsilenced) and the posterior (silenced) compartments were calculated according to the following formulas:

$$[Wg]_{\substack{\text{Anterior}\\ \text{D/V boundary}}} = \int_{a=0}^{d=100} L(D)\, dD \qquad \text{and} \qquad [Wg]_{\substack{\text{Posterior}\\ \text{D/V boundary}}} = \int_{a'=0}^{d'=100} L(D)\, dD$$

where L is the luminance and D is the distance, while the fraction:

$$[Wg]_{\substack{\text{Posterior}\\ \text{D/V boundary}}} / [Wg]_{\substack{\text{Anterior}\\ \text{D/V boundary}}}$$

represents the ratio between the amount of Wg protein secreted by D/V boundary cells in the P and A compartments; for each wing disc this ratio was calculated on Z-stack projection (35-40 optical slices). In total, I analyzed 5 control discs (*en*-Gal4, UAS-GFP/+), 5 discs silenced in the posterior compartment (the anterior compartment serves as internal control) (*en*-Gal4, UAS-GFP/UAS-IR*mfl*) and 5 discs silenced in the posterior compartment in UAS-Dcr2 background (to increase RNAi efficiency) (UAS-Dcr2/+;*en*-Gal4, UAS-myrRFP/UAS-IR*mfl*). Table 4 summarizes the values obtained from the three genotypes. The statistical one-way anova analysis (Table 5) shows that these mean ratios $[Wg]_{\text{Posterior D/V boundary}}$ /$[Wg]_{\text{Anterior D/V boundary}}$ were significantly different (Figure 18). Indeed, the $[Wg]_{\text{Posterior D/V boundary}}$ / $[Wg]_{\text{Anterior D/V boundary}}$ ratio increases upon *mfl* silencing, indicating that MFL depletion correlates with an increase of the amount of Wg protein secreted at

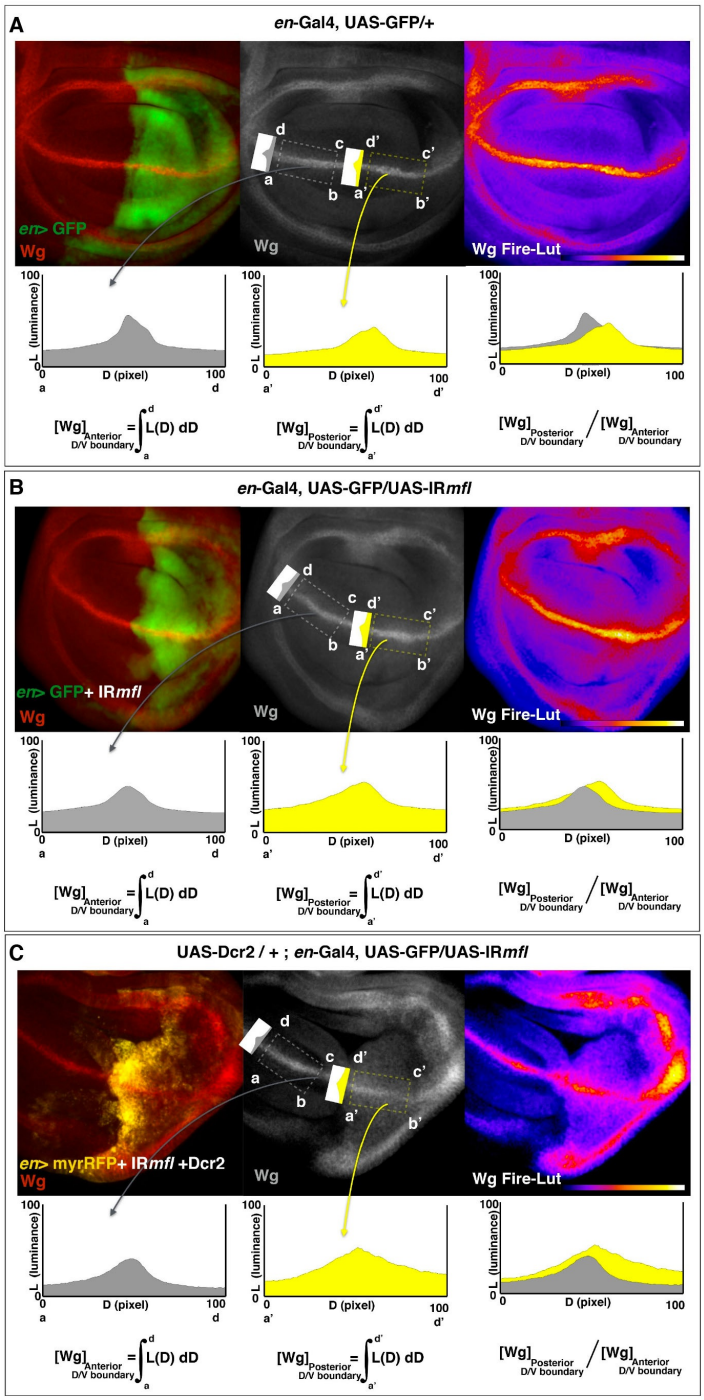

Figure 17. Analysis of Wg expression at the D/V boundary. To quantify the amount of Wg protein secreted by D/V margin cells, two equivalent areas of 100 x 150 pixels centered at the D/V boundary (one in the P region and the other in the A compartments), were selected from confocal microscopy images; for each of the two areas the luminance histogram of the Wg signal was drawn. These histograms reflected the profile of the Wg gradients, and the area of each histogram reflected the amount of Wg protein. A) control discs. B) discs silenced by the *en*-gal4 driver. C) discs silenced by the *en*-gal4 driver in the UAS-DCR2 background. A significant increase of Wg protein was observed at D/V boundary in the posterior compartment of the silenced discs, with or without the UAS-DCR2 transgene.

the D/V boundary. This finding is fully compatible with the observed up-regulation of Notch signaling. Noticeably, a strong overexpression of the Wg morphogen is also detected at either dorsal and ventral hinge areas along the inner Wg-expressing ring; this over-expression becomes even more evident in the UAS-Dcr2 background (Figure 19).

I then tested the expression of *cut,* an additional target gene activated by Notch at the D/V of the wing disc (de Celis et al. 1996; Micchelli et al. 1997;

Table 4. $[Wg]_{\text{Posterior D/V boundary}} / [Wg]_{\text{Anterior D/V boundary}}$

en-Gal4/+	*en* >IR*mfl*	*en* >IR*mfl*+DCR2
0,80	1,21	2,14
0,89	1,18	1,56
0,87	1,09	2,28
0,81	1,10	1,63
0,82	1,07	1,32

Table 5. One-way analysis of variance

P value	0,0001
P value summary	***
Are means signific. different? (P<0,05)	YES
Number of groups	3
F	20,70
R squared	0,7753

Neumann and Cohen 1996). *cut* encodes an evolutionarily conserved protein containing DNA binding domains (homeodomain and cut repeats); proteins of the Cut family are transcription factors (generally repressors) involved in cell-type specification, morphogenesis, and cell cycle progression (reviewed by Nepveu 2001). In control discs, (Figure 20 upper-left panel), Ct protein is uniformly expressed within D/V boundary cells; conversely, upon *mfl* silencing the accumulation of the protein at the D/V boundary is abolished in the posterior silenced compartment. Worth noting, this result can account for the "notched" phenotype exhibited by adult wings, since *cut* loss of function mutants are known to cause wing margin defects ("notches"; Jack et al. 1991; Dorsett 1993). Hence, Hence, Notch-up-regulation triggered by *mfl* silencing, although it is transduced in activation of the downstream *wg* gene, fails to induce *cut* expression. Taken together, these results demonstrated that *mfl* acts as a Notch modifier, and its knockdown can dysregulate this signaling. Moreover, the concomitance of Wg activation with Cut loss at the silenced D/V margin can nicely explain the mixture of Notch loss and gain of function phenotypes that are triggered by *mfl* silencing.

To learn more about the loss of Cut protein accumulation, I

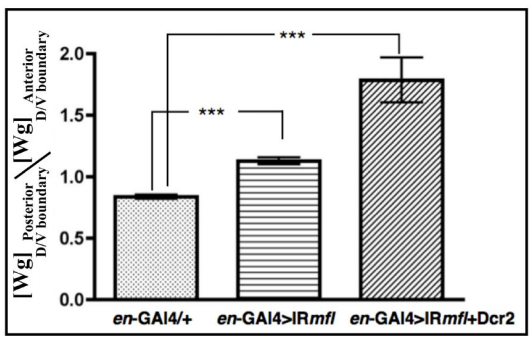

Figure 18. Histograms of the mean $[Wg]_{\text{Posterior D/V boundary}} / [Wg]_{\text{Anterior D/V boundary}}$ ratios. After *mfl* silencing, the amount of Wg protein secreted at the D/V boundary increases, in parallel with the RNAi efficiency (UAS-Dcr2 background).

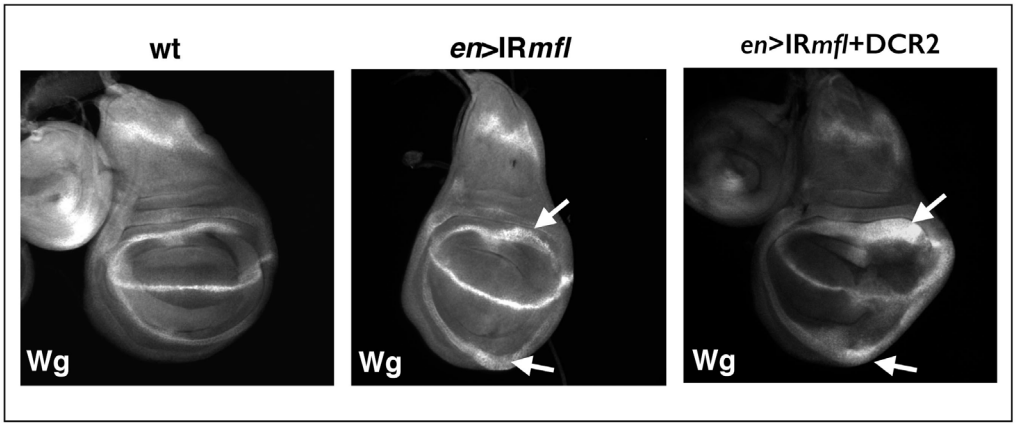

Figure 19. *mfl* silencing induces Wg up-regulation at the inner ring. Upon *mfl* silencing, overexpression of the Wg morphogen is also detected in the hinge, at either dorsal and ventral areas of the inner Wg-expressing ring; this effect becomes more evident in the UAS-Dcr2 background.

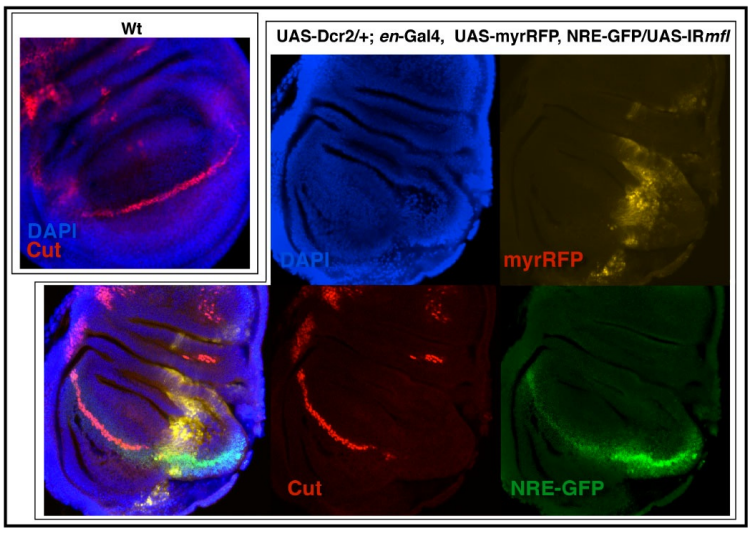

Figure 20. *mfl* silencing causes loss of Cut protein accumulation at the D/V boundary. In wild-type third instar discs (upper-left panel), Ct Protein is expressed within all D/V boundary cells; conversely, upon *mfl* silencing directed by *en*-Gal4 in the posterior compartment, the accumulation of the protein is abolished in the posterior compartment at D/V boundary. The anterior compartment serves as internal control.

performed an *in situ* hybridization experiment to assess the levels of *cut* mRNA at the D/V boundary of the silenced discs. As shown in Figure 8 (left panel), in the control discs *cut* mRNA marks the D/V boundary, and accumulates uniformly in both A and P compartments. In contrast, in wing discs in which *mfl* silencing was directed by the *en*-Gal4 driver (Figure 21, right panel), an almost total absence of *cut* mRNA was observed in the silenced (posterior) compartment. This finding is compatible with either defective transcription, or with extensive degradation of *cut* mRNA in the silenced cells. Even if these aspects remain to be defined, this result

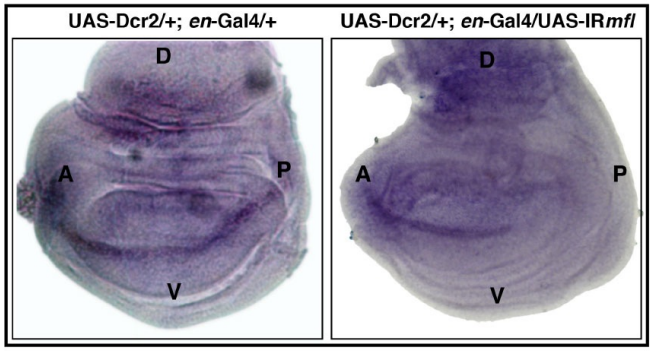

Figure 21. *mfl* silencing represses accumulation of *cut* mRNA at the D/V boundary. *In situ* hybridization with *cut* antisense RNA probes. Discs are orientated with the posterior compartment on the right. In the control discs (left panel), accumulation of *cut* mRNA marks the whole D/V boundary. In discs in which *mfl* was silenced by the *en-Gal4 driver* (right panel), *cut* mRNA fails to accumulate in the silenced posterior compartment (anterior compartment serves as internal control).

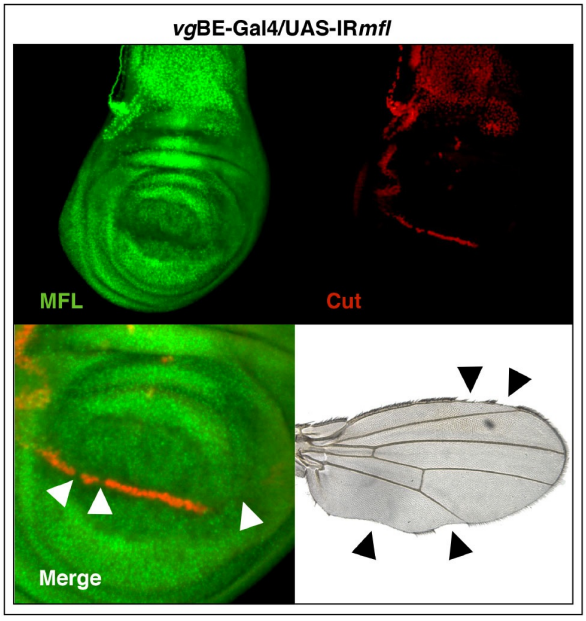

Figure 22. *mfl* RNAi driven by *vg*Be-Gal4 leads to the gaps in Cut expression at the D/V boundary. Third instar wing imaginal discs stained with anti-MFL (green) and anti-Cut (red). Cut protein expression at the D/V boundary present gaps (indicated by white triangles). These gaps are responsible for the wing margin defects shown by adult wings (black triangles).

confirmed the depletion of Cut protein, and revealed that it did not depend on translational or post-translational defects. Worth noting, the view that the loss of *cut* expression may depend on defective transcriptional induction can be in keeping with the model proposed by Bray and Furriols (2001), that suggested to divide Notch target genes into two classes: the class of permissive genes, for which the Notch primary function is to relieve the repression operated by the Su(H) complex, and that of instructive genes, for which Notch plays an essential activation role by recruiting specific coactivators. These differences may presumably depend on the combinatorial code of transcription factors that regulate each promoter. For example, it has been observed that Med12 and Med13 factors are required for *cut* (an instructive Notch target) activation at the wing margin, while they are required for *wg* and *vgBE* repression (two permissive targets; Janody and Treisman 2011). According to this view, it is plausible that Notch hyperactivation triggered by

mfl-RNAi may result in a loss of repression of permissive target genes, while the lack of appropriated co-activators would impede the expression of instructive targets. Alternatively, the loss of *cut* mRNA accumulation could be due to an increased instability or a selective degradation. I then wondered whether the loss of Cut expression could be a cell-autonomous phenomenon. To this goal, *mfl* was silenced by the *vg*BE-Gal4 driver (that is activated by Notch through the boundary

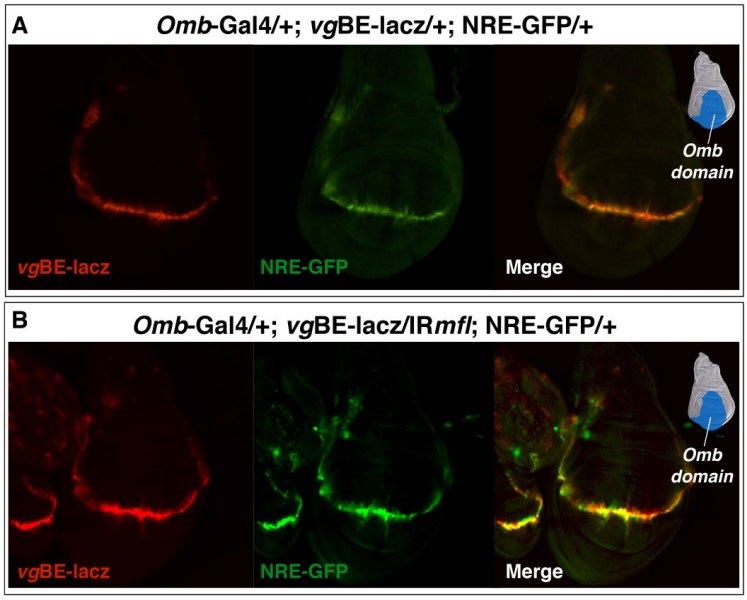

Figure 23. *mfl* RNAi causes *vg*BE-lacz up-regulation. Expression of the vgBE-lacZ reporter gene was determined by anti-β-galactosidase staining (red) on third instal wing discs. Control discs (**A**) shows the vgBE typical expression in a thin strip of cells along the D/V boundary (red). *mfl* RNAi (**B**) causes up-regulation of *vg*BE transcription. Note that up-regulation of *vg*BE and NRE-GFP (in green) reporters overlaps.

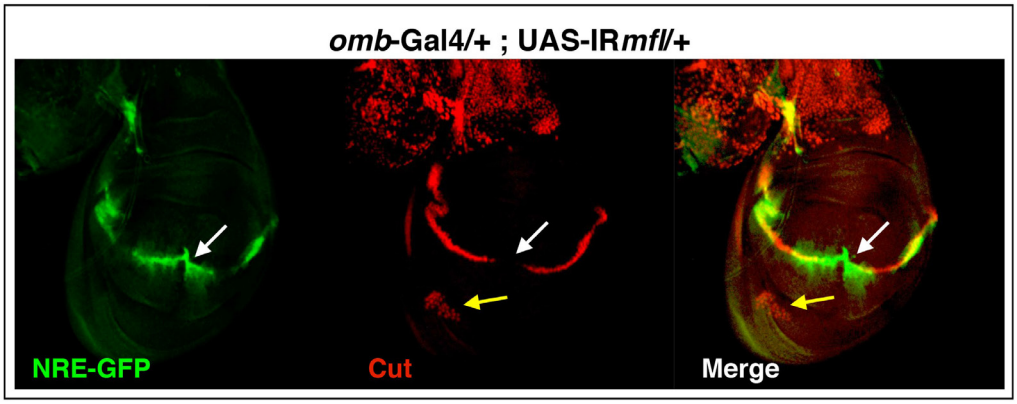

Figure 24. *mfl* silencing triggered by the *omb*-Gal4 driver causes loss of Cut expression at the D/V boundary. White arrows marks the central region of the D/V boundary where the NRE-GFP is upregulated, and Cut expression is abolished. The yellow arrow marks an unexpected ectopic expression of Cut in the ventral area of the disc.

enhancer *vg*BE specifically in the D/V boundary cells), and silenced discs were immunostained with anti-Cut and anti-MFL antibodies. This approach

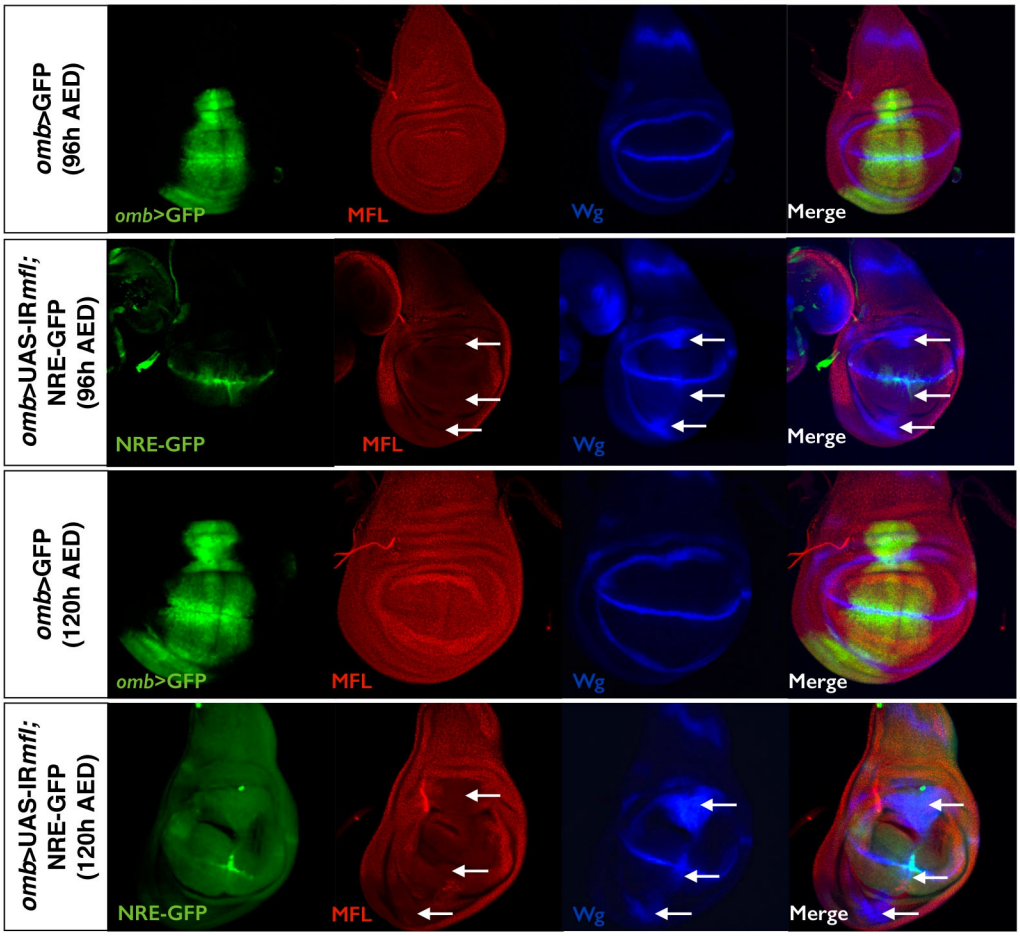

Figure 25. MFL-depleted cells overexpress Wg at the inner ring. *omb*-Gal4/+; UAS-GFP/+ control discs and *omb*-Gal4/+; UAS-IR*mfl*/+; NRE-GFP/+ silenced discs were stained with anti-MFL and anti-Wg antibodies. Orentation of discs is ventral at the bottom and the posterior at right. At both 96h AED and 120h AED, all examined silenced discs (n = 10) over-produce Wg protein at D/V and at the ineer ring (white arrows).

confirmed that gene silencing causes loss of Cut (Figure 22) expression, although in this context the loss was found discountinous and did not occur in all the silenced cells. This effect is likely due to *vg*BE-Gal4 late developmental expression pattern, that can result in a weaker silencing. Importantly, "gaps" of Cut expression are not restricted to the posterior compartment, indicating that D/V boundary cells of both A and P compartment are sensitive to MFL depletion. Finally, since the *vg*BE-Gal4 driver expression is restricted to D/V boundary cells, we concluded that *mfl* silencing induces loss of Cut expression in the D/V cells in a cell-autonomous manner. I then used of the X-linked *Omb*-Gal4 driver line (Figure 23), whose expression domain is restricted to the central area of the A compartment (see background section), to check the effects triggered by *mfl* silencing on the *vg* boundary enhancer (*vg*BE) that is activated by Notch specifically in D/V cells.

In these experiments, I used the *vg*BE-lacZ transgenic line, in which *vg*BE was fused to β-Galactosidase (Williams et al. 1994; Kim et al. 1996) to check its expression by anti-β-Galactosidase staining, and the NRE-GFP to monitor Notch activity in both control and *Omb*-Gal4 *mfl* silenced discs. While in the control discs (Figure 23A) both *vg*BE-lacz and NRE-GFP expression appears rather uniform at the D/V boundary, after *mfl* knockdown both reporters were strongly up-regulated in the central region of the *Omb* expression domain. Hence, the use of this additional driver confirmed that gene silencing induces up-regulation of Notch signaling, and shows that this effect is transduced in efficient *vg*-BE activation. Cut loss and Wg overexpression were also effectively reproduced when silencing was triggered in the *omb*-Gal4 expression domain (Figure 24 and 25). Intriguingly, Wg overexpression along the inner ring was markedly enhanced in this context, and detected also into the wing poutch, along the A/P boundary (Figure 25). As shown in the figure, double staining with anti-Wg and anti-MFL proteins clearly showed that MFL-depleted cells (and not the surrounding unsilenced cells) are those secreting large amounts of Wg protein, indicating that these cells are increasing the specific synthesis of this morphogen. Given the role of MFL protein in the ribosome biogenesis, the finding that depleted cells synthetize high-level of this morphogen and actively proliferate was unexpected.

4.3 Effects of *mfl* silencing on wing disc growth

Considering the high-level Wg expression, I checked the effect triggered by *mfl* silencing on cell growth. To determine the effects of MFL depletion on both cell proliferation and death along the development, I stained *omb*> IR*mfl* wing discs dissected at two different developmental times, that is at 96h and 120h after egg deposition (AED), with anti-pH3 (antibody against phospho-Histone H3) to mark mitotic cells, and with anti-Cas3 (antibody against activated Caspase3), to monitor apoptotic cells. At 96h AED, staining of wild-type discs with anti-pH3 (*omb*-Gal4/UAS-GFP; n = 10) showed frequent mitotic spots along the A/P axis (Figure 26A, yellow dashed area). In contrast, all examined silenced discs (*omb*-Gal4/+; UAS-IR*mfl*/+; NRE-GFP/+ ; n = 10) had in the same area very few mitotic spots, indicating a strong reduction of cell proliferation (Figure 26A', yellow dashed area). A reduction of mitotic spots along the A/P boundary was again observed at the subsequent developmental time (120h AED; Figure 26B, B', yellow dashed area).

However, at this later stage the same discs (n = 10) showed an increase in the number of mitotic spots, compared to wild type controls (n = 10), in both a hinge ventral (26B,B' blue dashed area) and dorsal area (purple dashed area), of the *omb* domain. This hyper-proliferation causes evident morphological

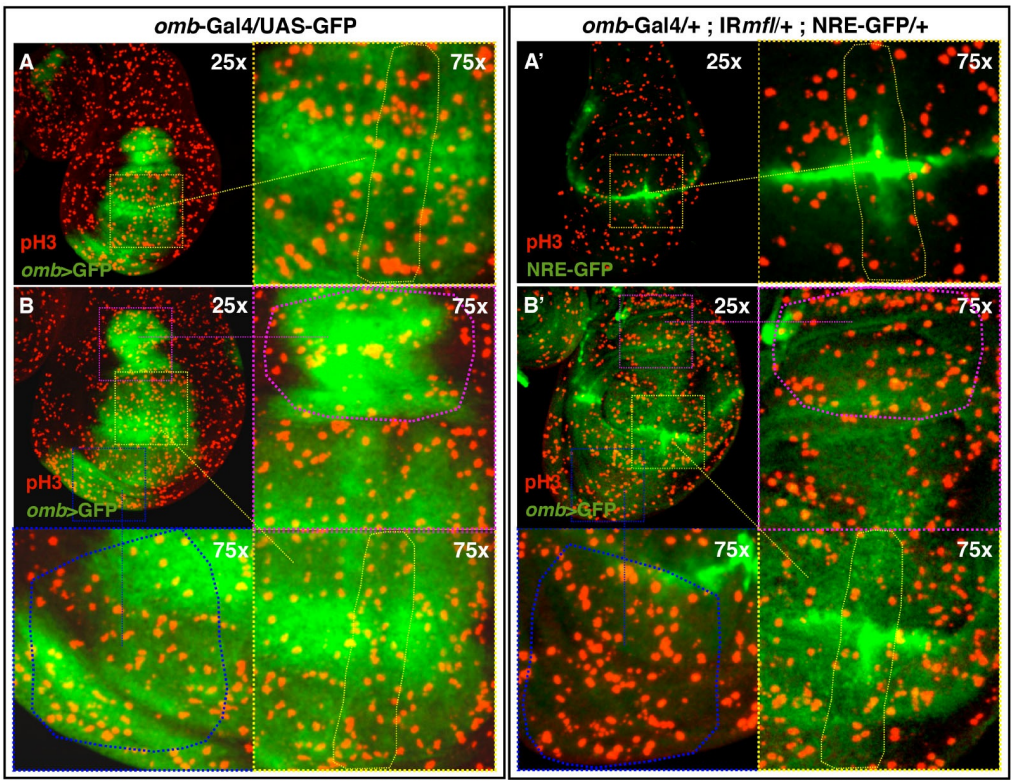

Figure 26. *mfl* RNAi driven by *omb*-Gal4 causes alteration of the proliferation. All discs were stained with anti-pH3. The discs are placed with the ventral at the bottom and the posterior at right. For each stage and genotype, 10 discs (n = 10) were analyzed. **(A)** Control discs with *omb*-Gal4/UAS-GFP genotype at 96h AED. At this stage, frequent mitotic spots are detectable at the A/P axis (yellow dashed area). **(B)** Control discs at 120h AED. **(A')** Silenced discs with *omb*-Gal4/+; UAS-IR*mfl*/+; NRE-GFP/+ genotype at 96h AED. In this discs very few mitotic spots are detectable at the A/P axis. **(B')** Silenced discs at 120h AED. These discs compared to control discs (B), present an increased frequency of mitotic spots in a ventral area (blue dashed area) and a dorsal area (purple dashed area).

alterations of the central region of the disc that triggers a deformation of the D/V boundary, although a strong up-regulation of the NRE-GFP reporter at this margin remains still evident (Figure 27). Hence, MFL depletion within the *omb* domain causes unexpected opposite effects: a strong reduction of proliferation occurs in the central region of the wing pouch, while a simultaneous proliferative increase is observed into ventral and dorsal hinge areas.

I then co-stained the silenced discs with anti-Wg and anti-Cas3 antibodies. Indeed, at 96 AED all silenced discs (n = 10) show presence of apoptotic spots along the A/P boundary (Figure 27A), consistent with the noticed localized reduction of PH3-labeled mitotic spots. In the same discs, over-production of the Wg morphogen it is detected along the A/P boundary and at the hinge dorsal and ventral regions of the inner ring. At subsequent developmental time (120h AED; n=10), the apoptosis spreads troughout the wing pouch, and

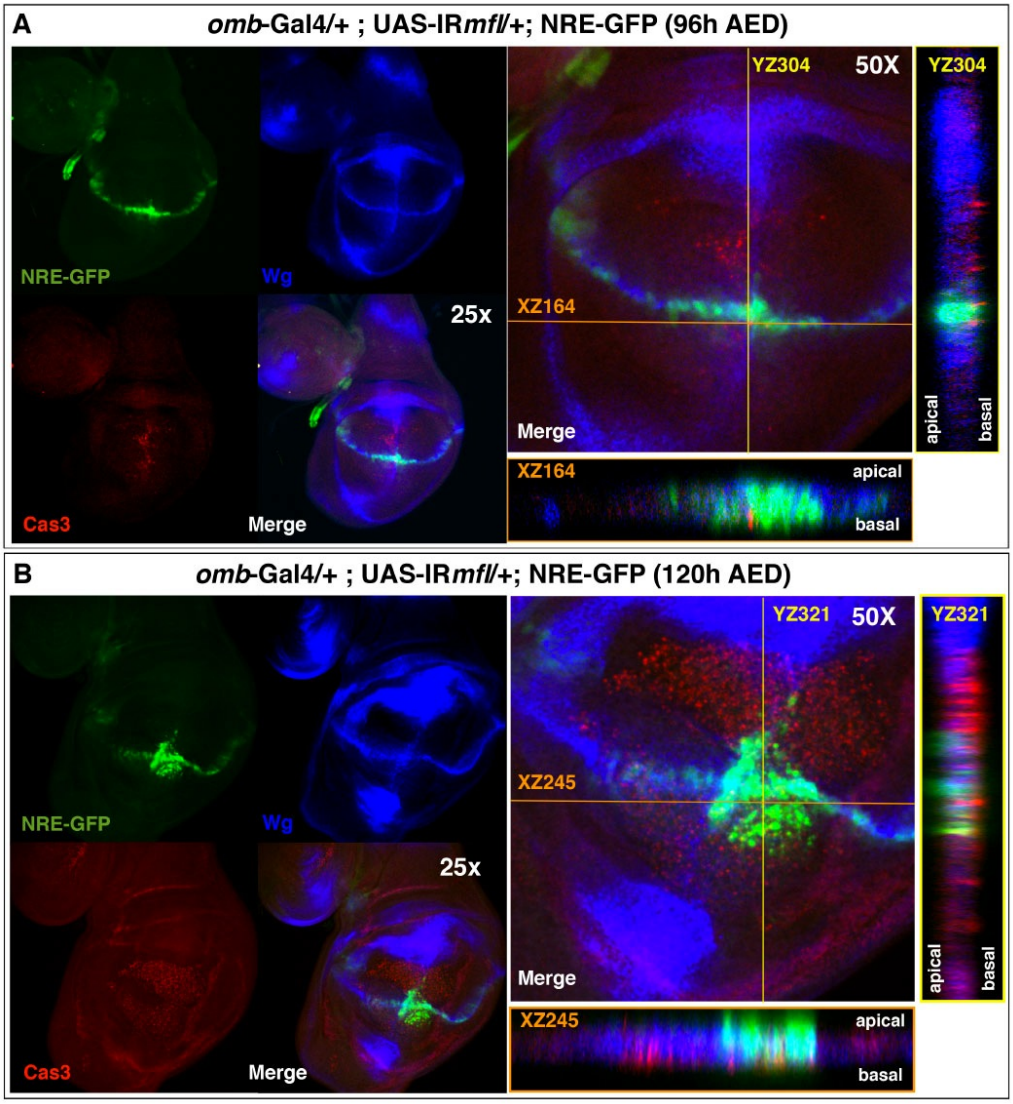

Figure 27. *mfl* RNAi driven by *omb*-Gal4 causes apoptosis and Wg overexpression. *omb*-Gal4/+; UAS-IR*mfl*/+; NRE-GFP/+ wing discs were stained with anti-Cas3 and anti-Wg antibodies. Orientation is ventral at the bottom and posterior on the right. **(A)** At 96 AED, all discs (n = 10) show apoptotic spots along the A/P axis, and Wg overexpression around the A/P axis and at dorsal and ventral hinge regions. The Z-stack analysis (right panel) shows that Wg is secreted by the non- apoptotic cells. The D/V boundary cells do not undergo apoptosis, and the NRE-GFP reporter is up-regulated in the central region of the D/V boundary. **(B)** At 120h AED, all discs (n = 10) show massive apoptosis into the wing pouch and an increased Wg production into surrounded tissues. Overall structure of the disc is strongly altered, and the D/V boundary, marked by NRE-GFP, is deformed. The Z-stack analysis (right panel) shows that the apoptotic cells are basal, while Wg accumulation is more apical.

Wg production markedly increases (Figure 27B). Worth noting, the areas marked by Wg accumulation overlap those where an increased number of PH3-lebeled mitotic spots is observed (see Figure 26).

Noticeably, Z-stack analysis of the optical sections captured show that Wg overexpression is never due to apoptotic cells. Although dying cells are contiguous, they lie more basally than those releasing the Wg signal (Figure 27A, right panel). Based on these data, I concluded that at early developmental stages (96h AED) the silenced cells along the A/P margin undergo apoptosis; however, simultaneous Wg overexpression occurs in the surrounding cells. At subsequent developmental time (120h AED), apoptosis within the wing pouch becomes more massive; in parallel, Wg secretion strongly increases, and these two concomitant but opposite processes result in a strong alteration of the disc morphology. Considering their spatial overlapping, it is reasonable to suppose that the Wg signal is responsible for the increased cell proliferation rate testified by the high number of PH3-labelled cells.

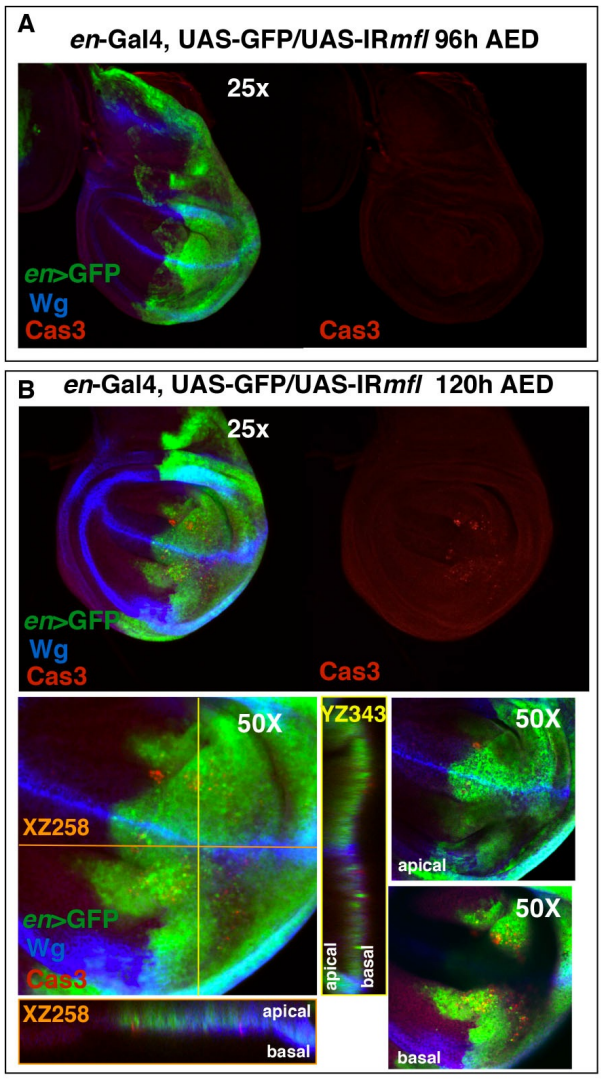

Figure 28. *mfl* silencing directed by *en*-GAl4 causes only weak apoptosis at 120h AED. *en*-Gal4,UAS-GFP/UAS-IR*mfl*/+ wing discs were stained with anti-Cas3 and anti-Wg antibodies. **(A)** At 96h AED, no apoptotic spots were detected. **(B)** At 120h AED, some apoptotic spots were detected in the P silenced compartment. The Z-stack analysis shows that cells of the D/V boundary (marked by Wg) do not undergo apoptosis. In addition, apoptotic cells are located basally in the pseudostratified epithelium. The two smaller panels (magnification 50x) represent the sum of 10 most apical focal planes and 10 most basal focal planes, respectively.

In conclusion, these results show that patches of silenced cells around the A/P margin start to undergo apoptosis, while surrounding patches of silenced cells, located more distally respect to the A/P boundary, secrete Wg and stimulate proliferation, as a sort of homeostasis

compensatory mechanism. These coupled phenomena typically occur in regenerative processes (Schubieger et al. 2010). I noticed that, although *mfl* silencing drived by either *en*-Gal4 or *omb*-Gal4 lines triggered identical effects at the D/V boundary (loss of Cut, NRE-GFP and Wg up-regulation), the growth defects caused by the *omb*-Gal4 driver were markedly more pronounced (Figure 27), and the apoptosis was scarsely induced by the en-Gal4 driver. In fact, a very few apoptotic spots are observed only at later developmental time (120h AED; Figure 28A,B). I reasoned that this difference cannot be related to the driver strength or a more precocious activation, since *omb*-Gal4 is known to be almost as strong as *en*-Gal4, and its activation occurs at later developmental time. I thus speculated that the stronger effects exherted by the *omb*-Gal4 driver could be related to its expression domain, that includes the cells composing the A/P boundary. Indeed, *omb*>IR*mfl* triggered apoptosis starts along the A/P axis, suggesting that these boundary cells could be more sensitive to depletion of the MFL protein.

4.4 *mfl* silencing causes epithelial remodeling

Considering the important organizative role exerted by the A/P boundary, the loss of its integrity could cause massive apoptosis and subsequent tissue remodeling in the wing disc. To further document these aspects, I followed two markers of the epilethial tissue organization: the apical/basal distribution of the Drosophila β-Catenin/Armadillo (Arm), and the levels of polymerized F-actin. β-catenin/Arm protein is a known effector of Wg signaling and plays the dual role of component of the cell adherens junctions and of nuclear transcription factor able to transduce Wg signaling. Within the wing disc, Arm is ubiquitously expressed but is strongly stabilized in two stripes surrounding the D/V boundary (Couso et al. 1994). Arm concentrates apically, where it binds transmembrane glycoproteins cadherins to build up the adherens junctions that connect actin filaments across polarized epithelial cells. Upon *mfl* silencing triggered by the both *en*-Gal4 and *omb*-Gal4 drivers (Figure 29), Arm accumulation results strongly reduced within all the silenced areas. This reduction is most evident at the D/V boundary, where the apical accumulation of the Arm protein is clearly abolished, suggesting a loss of cell polarity. In the wing cells, Wg activation induces a transient reduction of membrane-associated Arm, thus causing an immediate reduction of cell adhesion that facilitates changes in cell shape, structural reorganization of the cytoskeleton and cell mobility. At subsequent times, Arm levels are stabilized (Wodarz et al. 2006). The loss of apical localization of Arm protein is clearly restricted to the silenced cells, so that the planar cell polarity (PCP) of the overall epithelium was also disrupted (see Figure 29). PCP is a process that ensures the uniform

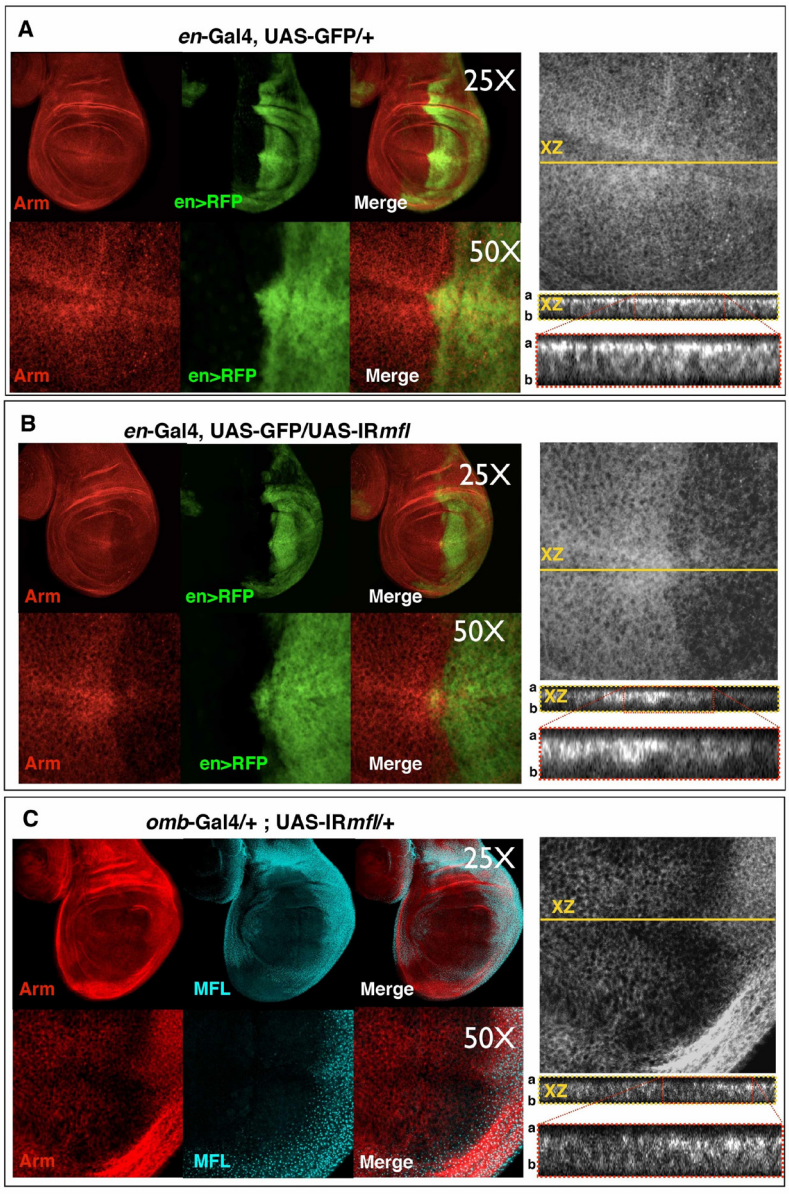

Figure 29. *mfl* RNAi reduces Arm/β-Catenin apical accumulation. In the *en*-gal4, UAS-GFP/+ control discs **(A)**, the Arm protein strongly concentrates in two stripes of cells adjacent to the D/V boundary, where it localizes apically. In the *en*-Gal4>IR*mfl* **(B)** and *omb*-Gal4>IR*mfl* silenced disc **(C)**, Arm accumulation is strongly reduced within the silenced areas; Z-stack analysis (right panel) shows that in the silenced areas the apical localization is clearly abolished, indicating disruption of the apical-basal polarity.

polarization of a group of cells, establishing a common global directional mechanism. Worth noting, Wg signaling is known to activate a non canonical pathway correlated with PCP regulation, tissue remodeling and cytoskeletal reorganization (reviewed by Komiya and Habas 2008; Gao 2012). Indeed, cytoskeletal remodeling within the silenced areas was further suggested by phalloidin staining, that similarly indicated a strong F-actin reduction at the D/V margin. As shown in Figure 30A, in wild-type discs the F-actin concentrates at the adherens junctions within two stripes adjacent to the D/V boundary, similarly to Arm (Major and Irvine 2005); in contrast, F-actin

accumulation at this region was strongly reduced in the silenced discs (Figure 30B). Since the Jun-N-terminal Kinase signaling pathway (JNK; see the background section) is also known to be involved in cytoskeletal remodeling, triggering both apoptotic (Adachi-Yamada et al. 1999; McEwen and Peifer 2005) and regeneration phenomena (Bosch et al. 2005; Bosch et al. 2008; Lee et al. 2005; Mattila et al. 2005), and is also part of the PCP pathway (reviewed by Bikkavilli and Malbon 2009). To test whether it could be specifically activated upon *mfl* silencing, I analyzed the expression of *puckered*, a JNK downstream effector, into *omb*>IR*mfl* wing discs by using a *puc*-lacz reporter line (Ring and Martinez Arias 1993). As described, in the *omb*-Gal4/+; +/+; *puc*-lacz/+ control discs, *puc* expression was detected only in the stalk region (Figure 31A), where wing discs are connected to the larval epidermis (Agnès et al. 1999). Surprisingly, upon *mfl* RNAi a strong *puckered* expression was observed within the *omb* domain, where MFL protein was depleted (Figure 31B), indicating that

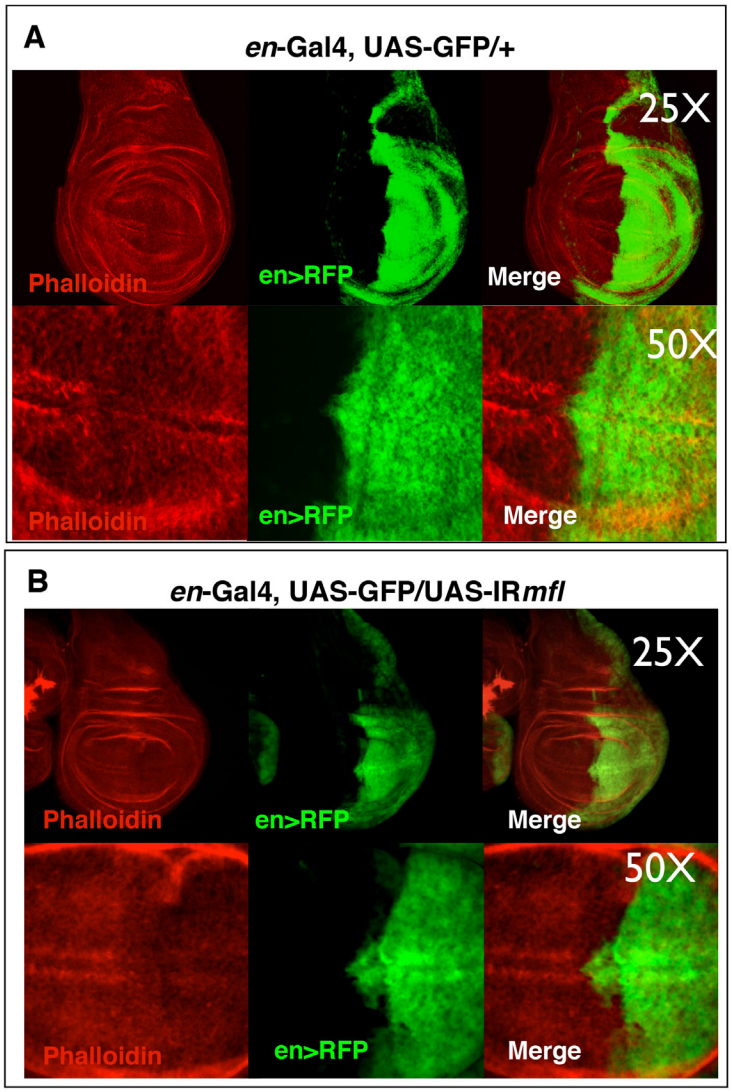

Figure 30. *mfl* RNAi reduces F-actin at the D/V margin. In the *en*-Gal4, UAS-GFP/+ control discs **(A)**, F-actin concentrates in two stripes of cells adjacent to the D/V boundary . In the *en*-Gal4, UAS-GFP/UAS-IR*mfl* silenced discs **(B)**, F-actin accumulation is strongly reduced in the Posterior silenced compartment, indicating reduced actin polymerization.

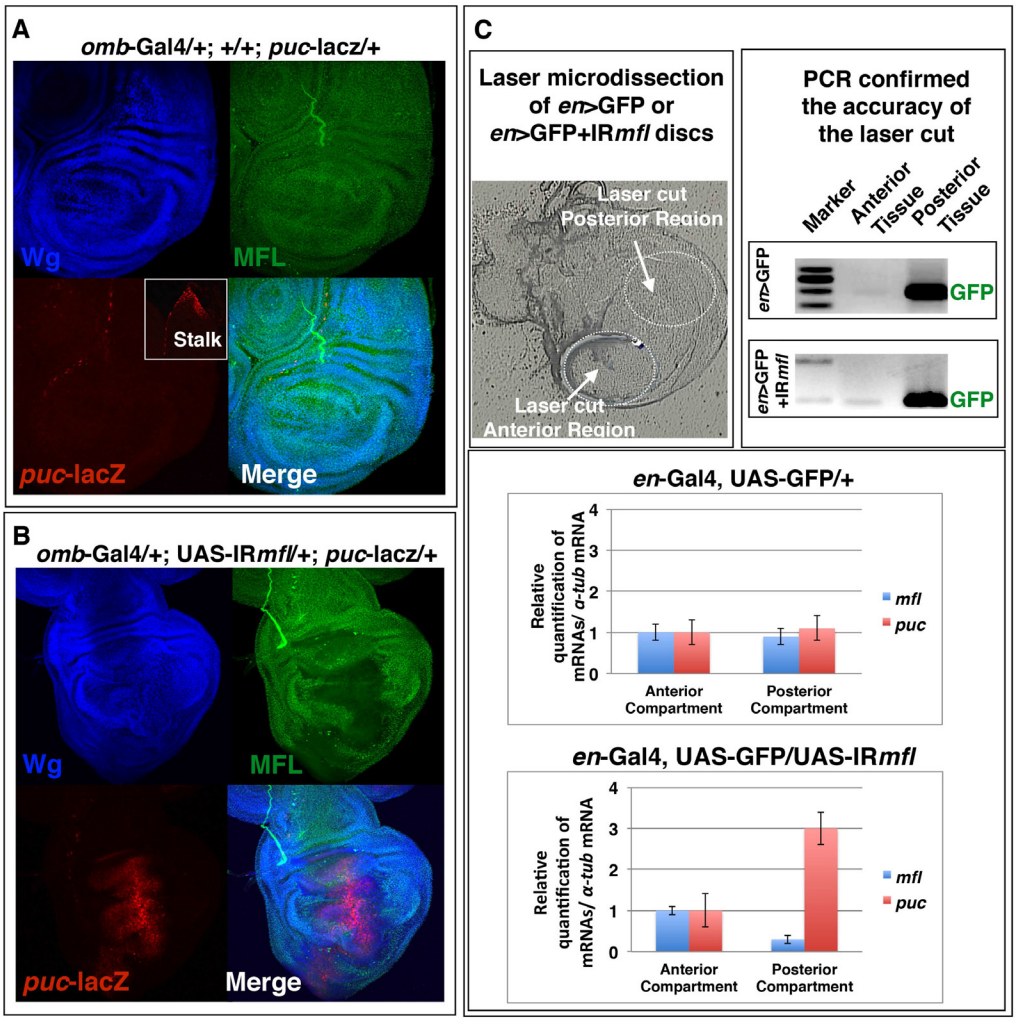

Figure 31. *mfl* RNAi causes JNK activation. (A) *omb*-Gal4/+; +/+; *puc*-lacZ/+ control discs stained with DAPI, anti-MFL and anti-β-gal. In these discs, the JNK pathway is activated only in the stalk cells (shown in the inset). **(B)** *omb*-Gal4/+; UAS-IR*mfl*/+ ; *puc*-lacZ/+ discs stained with anti-MFL and anti-β-gal. A strong *puc* expression was detected in the *omb*-Gal4 domain where MFL was depleted. **(C)** Laser microdissection applied to achieve a compared RNA transcript profiling of silenced and unsilenced areas of the *Drosophila* wing disc. *en*-Gal4, UAS-GFP/+ discs were used as control. Equivalent areas of the posterior compartment (marked by GFP) and the posterior compartment were separated by laser cutting. From the two tissue fractions (Anterior and Posterior) was extracted RNA total, was made a reverse transcription and, finally, a Real Time PCR. The same was done on *en*-Gal4, UAS-GFP/UAS-IR*mfl* discs. The accuracy of laser microdissection was controlled by checking the GFP expression in the two samples by RT-PCR. The quantitative Real Time PCR showed that in the control discs, there are not significant differences in the mfl RNA accumulation levels between posterior tissue and anterior tissue (used as internal control). The same is true of *puc* mRNA accumulation levels. In *en*-Gal4, UAS-GFP/UAS-IR*mfl* silenced discs, the Real Time PCR showed a mfl RNAi efficiency of the 80% and increased *puc* mRNA accumulation levels in the posterior silenced compartment (3 fold increase). This confirms that the *mfl* RNAi causes activation of JNK signal pathway.

mfl silencing induces ectopic activation of JNK signal pathway. This activation

was confirmed also upon *mfl* RNAi driven by *en*-Gal4 driver. In this case, I analyzed the accumulation levels of *puc* mRNA by q-RT PCR analysis of total RNA preparation obtained by laser-microdissection of posterior and anterior areas of silenced and unsilenced wing discs. Laser microdissection can successfully be applied to the validation of putative targets of diverse regulatory pathways, and we had previously shown that gene expression profiling of discrete subsets of cells of wing imaginal discs can precisely be determined after laser-mediated microdissection, using the fluorescent GFP signal to guide laser cut (Vicidomini et al. 2010). I then dissected equivalent

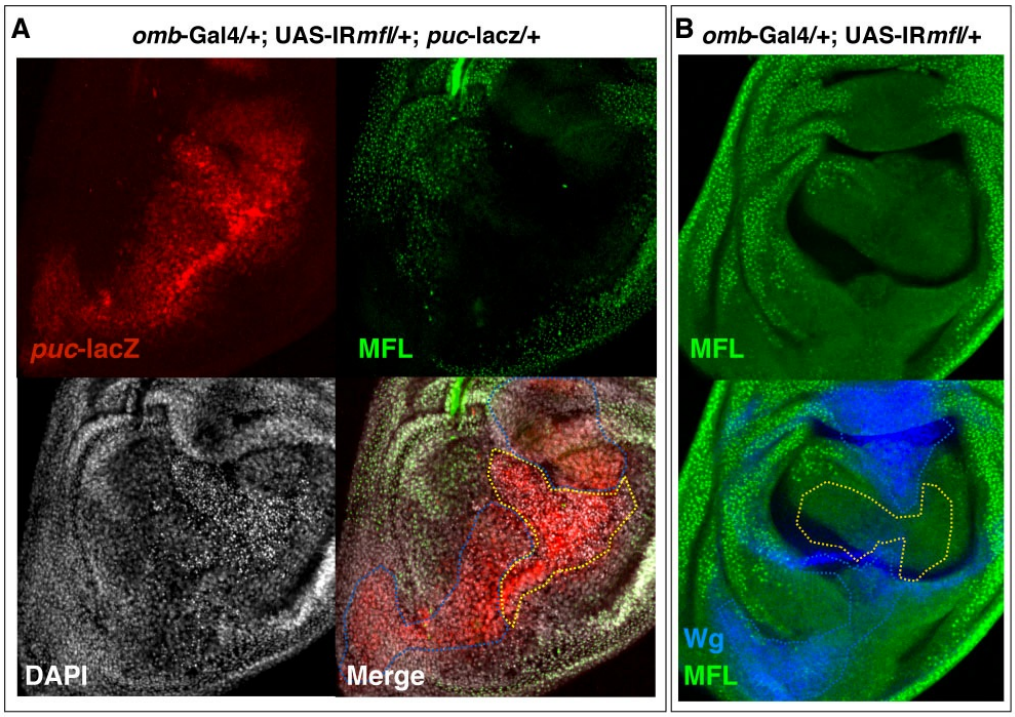

Figure 32. Activation of *puc*-lacZ reporter in the apoptotic and non apoptotic MFL depleted cells. (A) *omb*-Gal4/+; UAS-IR*mfl*/+; *puc*-lacZ/+ discs stained with DAPI, anti-MFL and anti-β-gal. The DAPI staining shows that apoptotic pyknotic nuclei located in the center of the wing pouch (dashed yellow area). The *puc*-lacZ reporter is activated in the apoptotic central region and in the surrounding regions (dashed blue areas), where apoptosis never spreads. These regions have previously found to secrete the Wg morphogen. **(B)** *omb*-Gal4/+; UAS-IR*mfl*/+ discs stained with anti-MFL and anti-Wg. Wg is secreted in response to the apoptosis by MFL depleted cells. Dashed blue areas indicate proliferative regions, dashed yellow area indicates the apoptotic region. The JNK is activated in either apoptotic and proliferating regions.

areas of the disc from the posterior (labelled by GFP expression), and the anterior (unlabelled) compartment upon *mfl* silencing driven by *en*-Gal4. RNA was extracted from microdissected silenced and unsilenced areas and comparative gene expression profiling determined by quantitative qRT-PCR. In the *en*-Gal4, UAS-GFP/+ control discs no significant differences were

observed between the anterior (that serves as internal control) and the posterior compartment about the accumulation levels of both *mfl* and *puc* mRNAs (Figure 31C). Although the *puc* gene is not normally expressed into pseudostratified epithelium of wing disc, it is expressed in peripodial cells (Agnes et al. 1999). This expression pattern accounts for the successful amplification of *puc* RNA in the anterior compartment. In the *en*-Gal4, UAS-GFP/UAS-IR*mfl* silenced discs, the accumulation levels of *puc* mRNAs in the P compartment increases of about 3 fold compared to the anterior compartment (used as internal control; Figure 31C). This finding confirms that the *mfl* silencing induces *puc* transcriptional activation through the JNK signal pathway. Worth noting, the JNK pathway is involved not only in apoptosis and regeneration, but also in cell shape changes and cell migration during normal development. For example, in flies the embryonic dorsal closure, follicle cell morphogenesis, thorax closure and male genitalia disc rotation/closure during metamorphosis all require JNK activation (Agnès et al. 1999; Martın-Blanco et al. 2000; Dobens et al. 2001; Macías et al. 2004; Rousset et al. 2010). Ventral closure, in *Caenorhabditis elegans*, and hindbrain closure in vertebrates, together with vertebrate wound healing, also use the JNK pathway (Martin and Parkhurst 2004; Belacortu and Paricio 2011; Gorfinkiel et al. 2011). Intriguingly, a detailed analysis of the expression of the *puc*-lacZ reporter suggested the possibility that JNK activation elicited opposite effects on different subpopulations of wing pouch cells. In fact, I noted that the DAPI staining marked presence of apoptotic pyknotic nuclei only in the central area of the wing pouch; the expression domain of the activated *puc*-lacZ reporter was instead markedly wider, and extended into areas where Wg overexpression was noticed (Figure 32). Given the role of the JNK pathway in regeneration, I hypothesize that its activation may triggers opposite effects: push the cells located along the A/P margin to dye, and the surrounding cells to secrete the Wg regenerative signal. Since dying and Wg-producing cells are similarly MFL-depleted, it can be concluded that the gene silencing can triggers opposite outcomes in different cell populations, so that its effects can be strictly context-dependent. In *Drosophila*, the JNK signaling pathway is known to induce production of the *Drosophila* Matrix metalloproteinase1 (Mmp1), that is required in the epidermis to facilitate reepithelialization after wound healing, remodeling the basement membrane, promoting cell elongation, actin cytoskeletal reorganization, cell migration, and activating extracellular signal-regulated kinase signaling (Stevens and McCawa 2012). Matrix metalloproteinases (MMPs) are extracellular proteases that are generally highly expressed at wound sites during regeneration and are known to be involved in tumor invasion (reviewed by Reuben and Cheung 2006). Not surprisingly, I found strong ectopic Mmp1 activation in the *mfl*-silenced area, that appeared

more marked in the ventral area of the *omb*-gal4 domain (Figure 33). Taken together, the data obtained clearly indicate that *mfl* silencing induces cell death and regenerative reepithelialization, as demonstrated by reduction of F-actin and apical accumulation of Arm, as well as by JNK and Mmp1 activation. All these effects result in massive remodeling of the growing disc, and point out that the gene can play an important role in both developmental and regenerative phenomena. Moreover, the high-level Mmp1 induction raised the possibility that the silenced cells can aquire a migrative behavior and/or undergo a Epithelial Mesenchymal Transition (EMT), an event known to occur in both physiological developmental events as well as in pathological conditions leading to tumorigenesis (reviewed by Radisky and Radisky 2010).

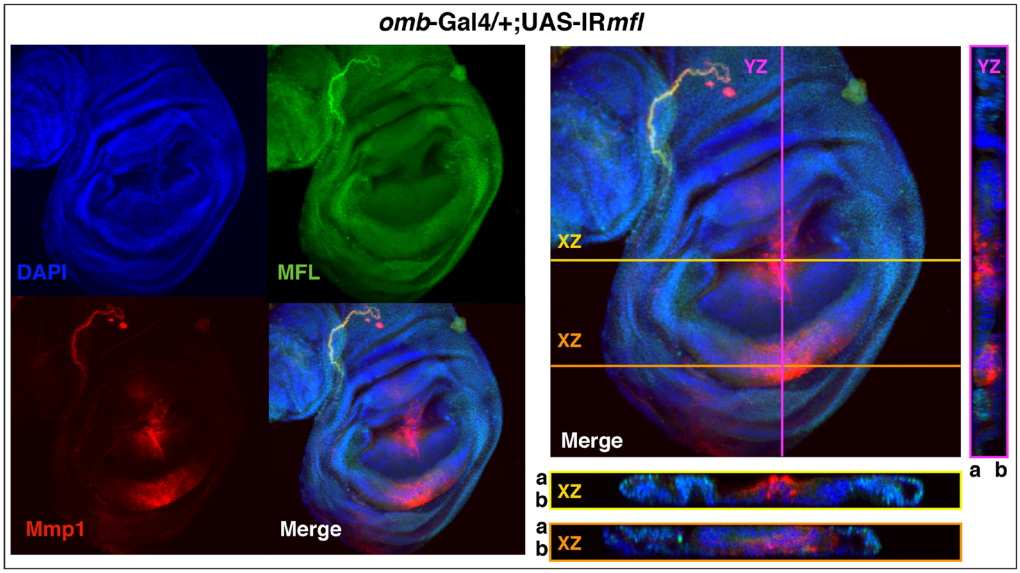

Figure 33. Matrix metalloproteinase1 (Mmp1) expression in *omb*>IR*mfl* silenced discs. Upon *mfl* silencing, Mmp1 expression is induced within the silenced area, consistent with active reorganization of the epithelium and increased cell motility.

4.5 *mfl* silencing induces EMT

As showed in the previous sections, the expression domain of the *omb*-Gal4 driver lies in the central area of the wing pseudostratified epithelium (as showed above); however, it do not include the corresponding area of the above peripodial membrane. In fact, upon *mfl* RNAi directed by this driver, the MFL protein is depleted in the central area of the pseudostratified epithelium, but accumulates actively into nucleoli of the above peripodial membrane cells (Figure 34). This expression pattern allowed to detect an unexpected cell non-autonomous effect. In fact, I noticed that gene silencing drived by *omb*-Gal4 not only caused loss of Cut protein at D/V boundary of the silenced

pseudostratified epithelium, but it also induced Cut ectopic expression (Figure 34C,D). This ectopic expression was detected in almost 95% of the discs examined (n = 20), and could be unambiguously attributed to cells of the peripodial membrane by careful Z-stack confocal analysis.

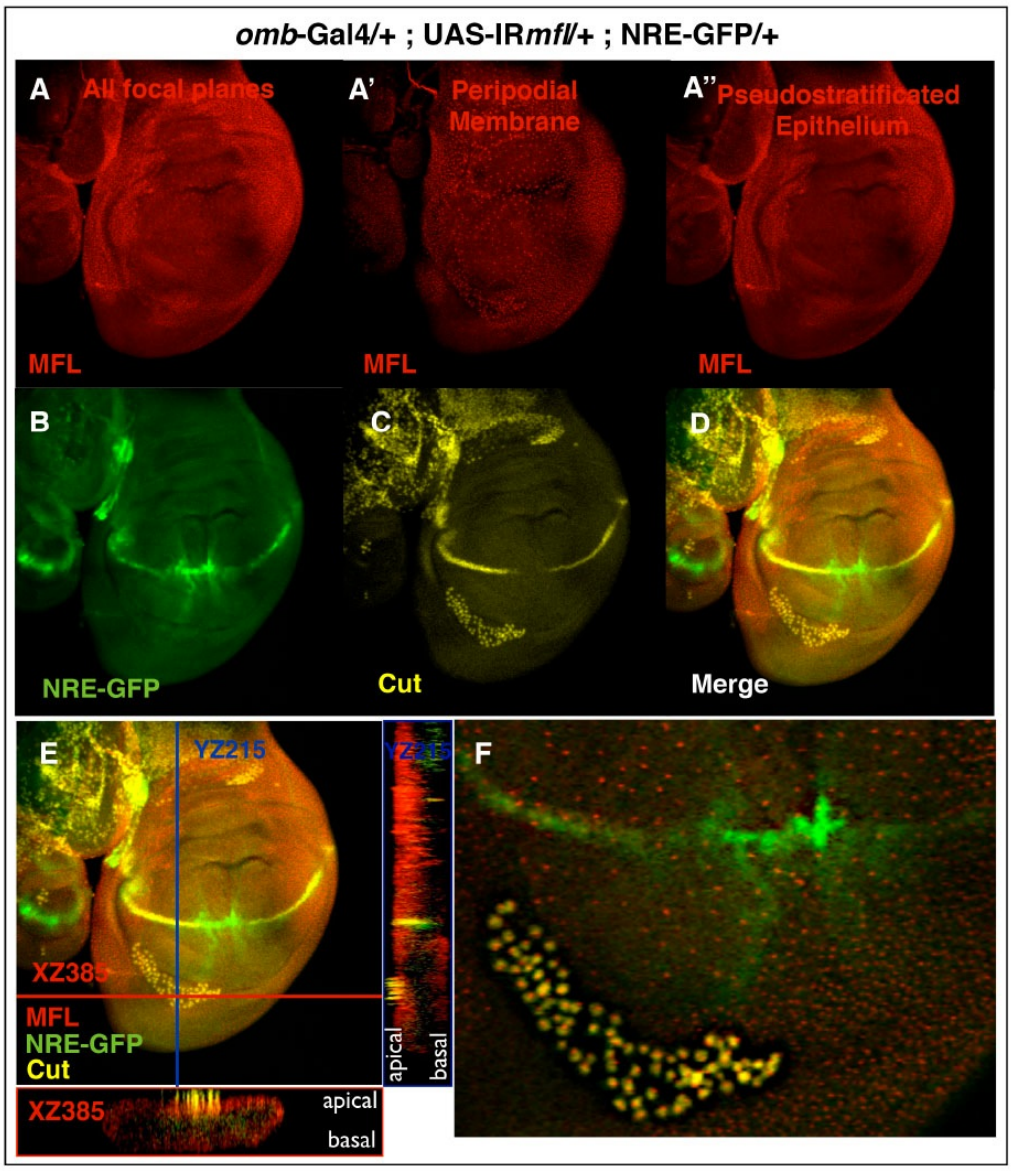

Figure 34. *mfl* RNAi causes cell non-autonomous Cut expression in same peripodial membrane cells. Third instar wing imaginal discs with *omb*-Gal4/+, UAS-IRmfl/+; NRE-GFP/+ genotype stained with anti-MFL and anti-Cut antibodies. Upon *omb>mfl* RNAi, MFL protein is absent into central domain of pseudostratified epithelium **(A")** but is present into nucleoli of peripodial membrane cells **(A')**. **A** is the sum of **A'** and **A"** sections. NRE-GFP is up-regulated in the central part of D/V boundary (B). Cut protein is absent where NRE-GFP is up-regulated (C), but is ectopically expressed in patches of ventral cells. Confocal z-stack analysis (E) shows that these cells are located in the peripodial membrane, and the MFL protein accumulates in their nucleoli (F).

Since Cut expression in the wing disc marks the muscle cells basally associated with the notum (Sudarsan et al. 2001), I wondered whether the Cut ectopically expressing cells had acquired a muscle identity, in keeping with what expected for EMT occurrence. To assess this point, I used an antibody against Twist protein, that typically marks *Drosophila* muscle cells (Ghazi et al. 2000). In addition to be a typical mesenchymal marker, Twist is known to act as a Notch coactivator on Cut induction in muscle cells (Bernard et al. 2010). When I performed an anti-Cut and anti-Twist co-staining of the silenced discs, the peripodial cells that ectopically express Cut were found to similarly express Twist (Figure 35). This finding provided clear evidence that MFL depletion into the below pseudostratified epithelium had induced epithelial-mesenchymal transition in the above peripodial cells. Although it remains to be defined whether Twist-expressing peripodial cells had undergone EMT as a cell non-autonomous phenomenon, or they had migrate from the silenced pseudostratified, it seems very likely that this effect is induced by the high-level secretion of Wg, that is known to be an EMT inducer (van der Velden et al. 2012; Bao et al. 2012; reviewed by Micalizzi et al. 2010).

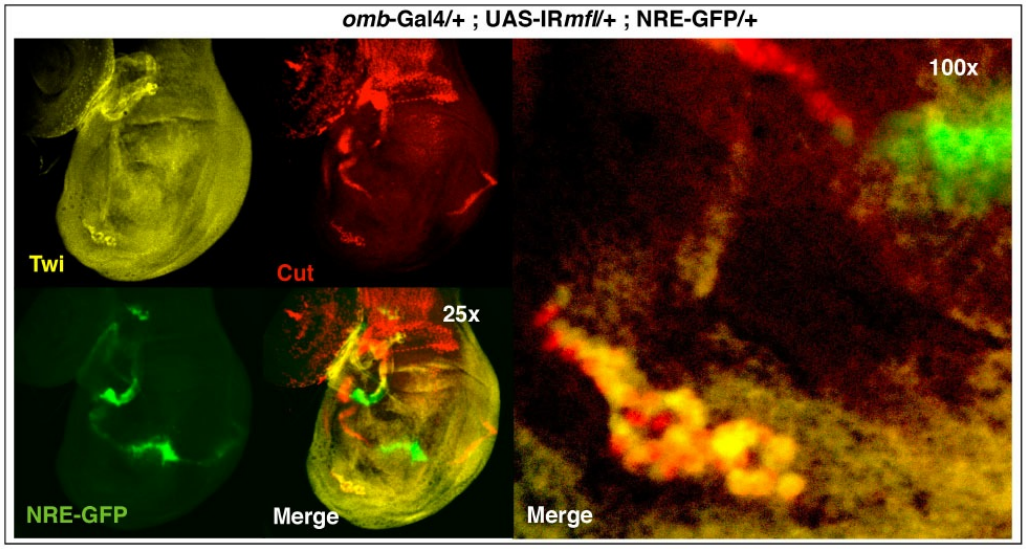

Figure 35. *mfl* RNAi driven by the *omb*-Gal4 driver causes epithelial-mesenchimal transition in same peripodial cells. Wing discs of the *omb*-Gal4/+, UAS-IRmfl/+; NRE-GFP/+ genotype were stained with anti-Cut and anti-Twist antibodies. The peripodial cells ectopically expressing Cut (in red), also express the mesodermal marker Twist (in yellow), revealing the occurrence of EMT.

4.6 Notch dysregulation is independent from cell death

Based on the above data, I wished to define whether the massive apoptosis induced by *mfl* silencing could be responsible for both Wg ectopic secretion and dysregulation of Notch signaling at the D/V boundary. In this case, both

phenomena could be part of a regenerative response of the surrounding tissues. To assess this point, I over-expressed the baculovirus p35 protein, known to inhibits the function of Cas3 but not its activation (Hay et al. 1994; Callus and Vaux 2007), into *mfl* silenced discs. In these experiments, the *omb*-Gal4 driver line directed simultaneous expression of UAS-IR*mfl* and UAS-p35 transgenes, and the morphology of the epithelium was monitored by following the formation of F-actin with phalloidin staining. In all discs analyzed (n = 10), at both 96h AED and 120h AED, the block of apoptosis allowed to recover the overall morphology of the epithelium (Figure 36C) and to reduce Wg up-regulation at the inner ring. However, at the D/V boundary, Wg expression remains up-regulated, indicating that dysregulation of Notch signaling is not

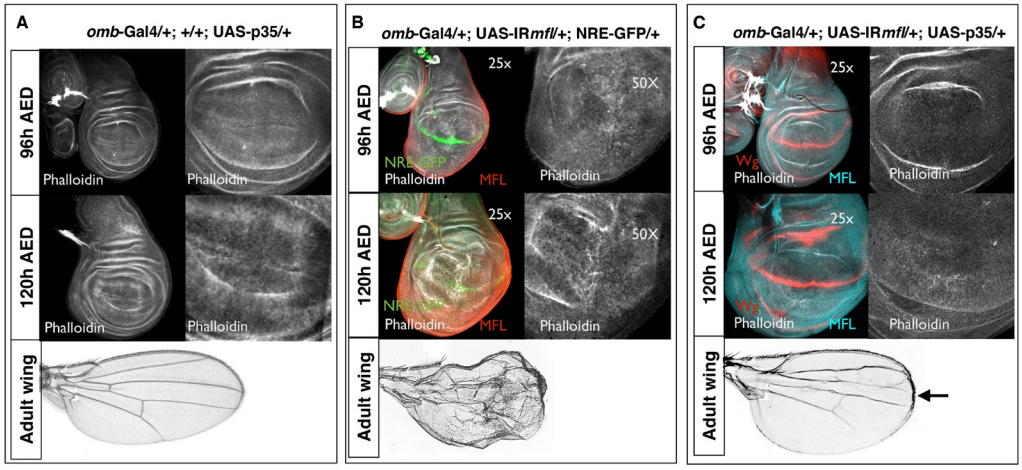

Figure 36. The blocking of apoptosis by baculovirus p35 leads to a rescue phenotype. **(A)** *omb*-Gal4>UAS-p35 control discs (stained with phalloidin) and control adult wings. **(B)** *omb*-Gal4>IR*mfl* silenced discs (stained with phalloidin) and adult wings. Both at 96h and 120h AED, the staining with phalloidin detects a strong degeneration of the epithelium in the central part of the wing pouch. This degeneration is compatible with the degeneration that is observed in the most distal part of the adult wing. **(C)** The contemporaneous expression of UAS-IR*mfl* and UAS-p35 constructs directed by *omb*-Gal4, blocking the apoptosis, leads to a significant rescue of the morphology of the epithelium and to a reduction of over-production of Wg in the dorsal and ventral regions. Adult wings present a Notch gain of function phenotype (with loss of stretches of veins and crossveins) and an altered cell differentiation at D/V margin (loss of bristles; black arrow).

rescued by p35 over-expression. According with this view, I observed that upon apoptosis blockage the silenced adult wings still exhibited the typical Notch gain-of-function phenotype, characterized by loss of veins and crossveins. However, these abnormalities coesist with defects of the D/V margin, (see Figure 36C, 37B) typical of loss of Cut expression. In fact, Cut protein was still undetectable at the D/V boundary in *omb*>IRmfl+p35 discs (Figure 37A), although its ectopic expression into peripodal cells was not more observed. Taken together, these data indicate that *mfl* silencing triggers Notch

dysregulation at the D/V margin independently from cell death. In contrast, ectopic Wg expression is likely to represent a compensatory/regenerative signal sended by the non apoptotic-cells that surround the apoptotic foci; this regenerative response can be activated only after the completion of the apoptotic program. Hence, loss of function of the pseudouridine synthase component of H/ACA snoRNPs may induce some cells to apoptosis, while surrounding cells can be stimulated to secrete pro-proliferative factors and become capable to hyper-proliferate, as it occurs in typical regeneration phenomena.

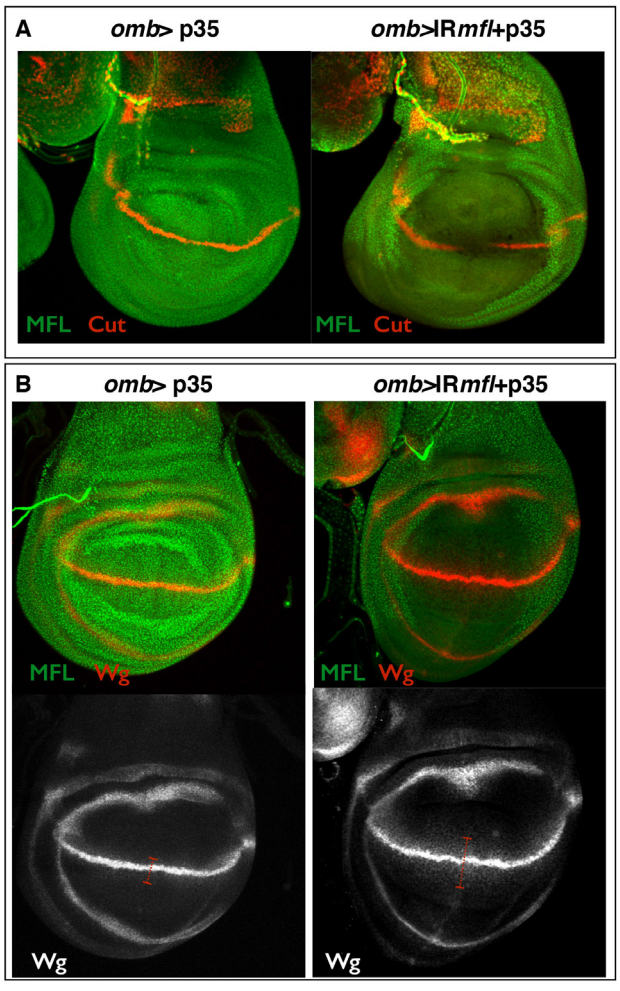

Figure 37. p35 does not recover the dysregulation of the Notch signaling at the D/V boundary but retrieves cell non-autonomous phenomena. (A) *omb*-Gal4/+;+/+;UAS-p35/+ control discs and *omb*-Gal4/+;UAS-IR*mfl*/+;UAS-p35/+ discs stained with anti-MFL and anti-Cut. The blockade of apoptosis by p35 does not restore the expression of Cut at the D/V boundary caused by *mfl* RNAi. In all samples (n=7) was not observed ectopic Cut into peripodial cells. **(B)** *omb*-Gal4/+;+/+;UAS-p35/+ control discs and *omb*-Gal4/+;UAS-IR*mfl*/+;UAS-p35/+ discs stained with anti-MFL and anti-Wg. In all samples (n=10), p35 does not reduce the WG up regulation at the D/V boundary upon *mfl* RNAi, suggesting that after inhibition of the Caspase3 activity, the up-regulation of some Notch targets is still maintained. The increased secretion of Wg at the D/V boundary in the silenced discs, compared to those overexpressing p35 alone, is indicated by the greater length of the gradient (red segment).

4.7 Notch activation induced by *mfl* silencing is not coaused by defective IRES-dependent translation of the antagonist Hairless protein.

Given the variety of biological roles currently attributed to H/ACA pseudouridine synthases, the dysregulation of Notch signaling observed upon *mfl* silencing might be related to a multiplicity of putative effects, such as

alterations of splicing, snoRNA stability or miRNAs biogenesis, as well as translation deficiency, or specific defects in IRES-dependent translation, etc. Since *Dkc1* loss of function mice, as cells from X-DC patients, exhibit specific defects in IRES-dependent translation (Yoon et al. 2006; Montanaro et al. 2010; Bellodi et al. 2010), and this effect is currently considered one of the most relevant telomerase-independent effect triggered by *Dkc1* hypomorphic mutations, I decided to investigate this aspect. In *Drosophila*, the Notch antagonist Hairless protein (for the biological role, see the background section) presents two isoforms: a long one is produced in cap-dependent manner (Hp150), while a short one (Hp120) is produced in IRES-dependent manner (Maier et al. 2002). I reasoned that a possible explanation accounting for the observed Notch dysregulation could depend on an impaired synthesis of Hp120, which is known to be required for efficient Notch repression (Maier et al. 2002). According to this view, *mfl* RNAi would cause production of under pseudouridylated ribosomes that could no longer be able to efficiently synthesize Hp120 in IRES-dependent manner. Indeed, reduced Hp120 synthesis could account for the observed increase of Nintra activity on NRE-GFP, *vg*BE and *wg* targets. To test this hypothesis, I performed a set of collaborative experiments in the laboratory of Professor Annette Preiss (Universität Hohenheim, Institut für Genetik, Stuttgart, Germany), where a large set of molecular tools were already available. The rationale of this set of experiments is outlined in Figure 38. The Hairless (H) gene has a single large ORF, able to encode a protein of 1077 aa; however, the first start codon (M1) does not conform well with the translation initiation consensus site for *Drosophila* genes; in contrast, a second start codon (M2, at position 19) fits well, and is therefore that predicted for the synthesis of a 1059 aa protein (the Hp150 produced in cap-dependent manner; Maier et al. 2002; Maier 2006). A short isoform, Hp120, is produced from codon 148 (M3), and the M2-M3 interval (about 400 nt) has been shown to act as IRES; importantly, both Hp150 and Hp120 are needed for normal Hairless antagonist activity (Maier et al. 2002; Maier 2006). In order to determine whether MFL depletion could specifically affect the IRES-dependent synthesis of the Hp120 isoform, I used an anti-Hairless antibody produced by Maier et al. (1999) that recognizes the central portion of H protein, and thus is able to detect both distinct isoforms (150 and 120 kDa respectively) on western blot analysis (Figure 38A'). I also took advantage of the UAS-*HAflII* transgenic line produced in the laboratory of Anette Preiss (see Figure 38B; Maier et al. 2002). This line carries a UAS-*HAflII* transgene, in which an insertion in the *HAflII* site produces a frame shifting that originates premature stop codons before M3. As consequence, the construct drives Hp120 expression from the M3 site in IRES-dependent manner; moreover, in the transgene the M3 site was placed under the control of

the UAS sequence. The UAS-*HAflII* transgenic line is thus able to over-express specifically the Hp120 isoform under both IRES and UAS control (Figure 38B'), and could be particularly useful for rescue experiments. When I performed anti-Hairless staining of wild type wing discs, an uniform distribution of Hairless proteins (Hp150 + Hp120; Figure 39A) was observed. The staining remained uniform in both A/P compartments also upon *mfl* silencing directed by the *en*-Gal4 driver, (Figure 39B,B') even upon addition

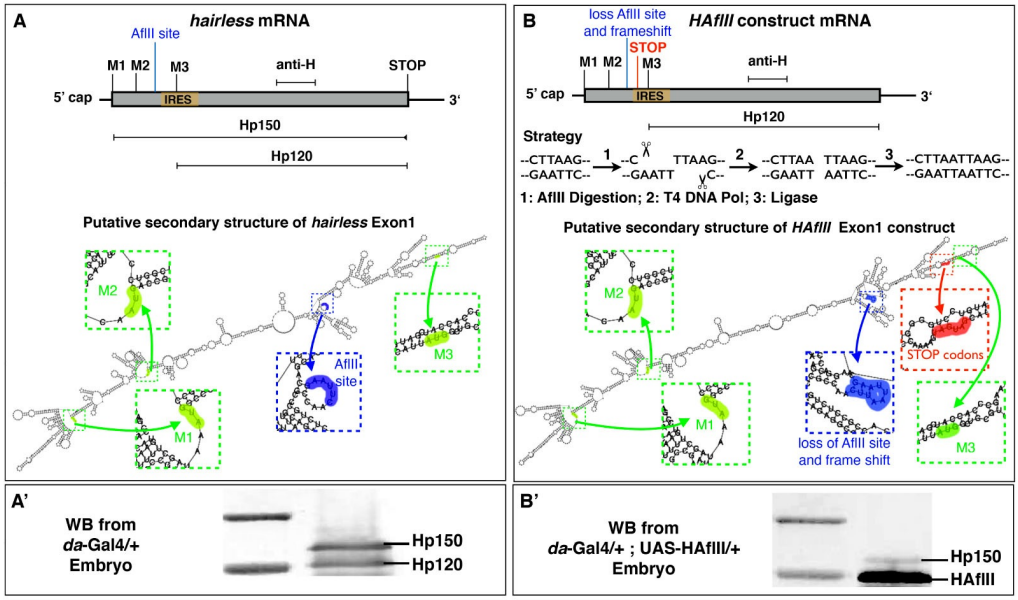

Figure 38. Structure of *hairless* mRNA and *HAflII* construct mRNA. (A) *hairless* mRNA presents three AUG start codon: M1, M2 and M3. M1 does not conform well with the translation initiation consensus site for *Drosophila* genes. M2 is the start codon for the cap-dependent translation of Hp150. M3 is the start codon for the IRES-dependent translation of Hp120. The sequence between M2 and M3 functions as IRES. M3 and M2 AUG codons are in frame, therefore Hp150 has a N-terminal portion longer than Hp120. The putative secondary structure of *hairless* mRNA Exon1 was obtained using RNAfold software (at the http://rna.tbi.univie.ac.at/cgi-bin/RNAfold.cgi site). On the secondary structure, is indicated (in blue) a site recognized by AflII restriction enzyme. **(A')** Western Blot on extracts derived from *da*-Gal4/+ embryos using anti-Hairless against central domain (common to both Hairless isoforms) can detect both Hp150 that Hp120. **(B)** UAS-*HAflII* construct presents an insertion that causes a frame shift with formation of premature stop codons before M3. Therefore *HAflII* mRNA produces only Hp120 in IRES-dependent manner from M3 site. The frame-shift mutation was introduced by digestions with AflII at codon 113, polishing with T4-polymerase and religation. **(B')** Western Blot on extracts derived from *da*-Gal4/+; UAS-*HAflII*/+ embryos using anti-Hairless against central domain shows the over-expression of Hp120.

of the UAS-DCR2 transgene (Figure 39C,C',C''). These findings pointed out that *mfl* silencing do not significantly affect the total accumulation levels of both Hairless proteins (Hp150+Hp120). Then I followed the effects triggered

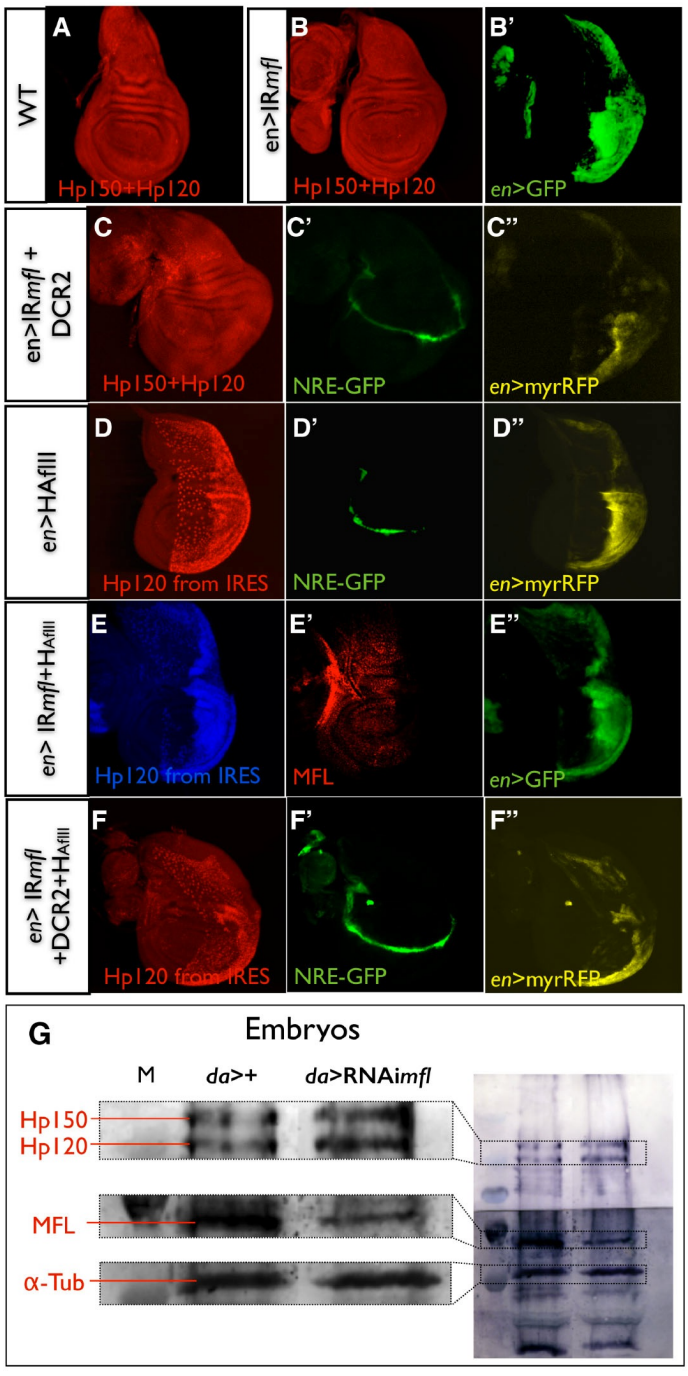

Figure 39. *mfl* RNAi does not alter the production of Hp120 in IRES-dependent manner. (A-F'') Third instar wing discs with different genotypes stained with anti-H against central domain of Hairless proteins. All discs are oriented with posterior to the right and ventral at the bottom. (A) Under Wt conditions the staining with anti-H that reveals Hp150+Hp120 appears uniform. (B,B') Upon *mfl* silencing directed by *engrailed* the staining appears still uniform. (C, C', C'') Increasing RNAi efficiency in UAS-DCR2 background, the staining is still uniform. (D, D', D'') *HAflII* over-expression driven by *en*-Gal4 is capable of strongly repress the Nintra activity at the D/V boundary evaluated by NRE-GFP expression. (E, E', E'') After *mfl* silencing, the UAS-*HAflII* construct can still produce high levels of Hp120 in IRES-dependent manner, but this proteins is not able to cause complete suppression of Nintra acticity (evaluated by NRE-GFP expression) (F, F',F''). (G) Western Blot analysis on extracts derived from da-Gal4/+ (used as control) and da-Gal4/UAS-IR*mfl* embryos collected after over-night deposition, revels that after *mfl* RNAi the levels of Hp120 are not reduced.

by over-expression of the UAS-*HAflII* transgene. As expected, in wild-type wing discs its over-expression driven by the *en*-Gal4 driver was capable of strongly repress Nintra activity at the D/V boundary, as assessed by the strong reduction of the expression of the NRE-GFP reporter (Figure 39D,D',D'').

I observed that upon *mfl* silencing the UAS-*HAflII* construct still produces high levels of Hp120 in IRES-dependent manner, indicating that MFL depletion does not significantly affect its IRES-dependent translation (Figure 39E,E', E''). However, I noticed that, although Hp120 overexpression reduces the NRE-GFP up-regulation induced by *mfl* RNAi, in these conditions is not able to fully suppress Nintra activity (followed by NRE-GFP luminance; Figure 39F,F',F''), as it occurs in the wild-type background (Figure 39D,D',D''). Moreover, the concomitant expression of UAS-IR*mfl* and UAS-*HAflII* in the posterior compartment do not rescue the growth defects, but instead triggers a phenotypic enhancement, characterized by a more extreme reduction of the area of the silenced compartment (Figure 39C'',39F''). Finally, western blot analysis performed on extracts derived from embryos over-expressing the UAS-*HAflII* transgene under the control of the ubiquitous *dautherless*-Gal4 driver (*da*-Gal4) further confirmed that the levels of Hp120 accumulation are unaffected by *mfl* silencing (Figure 39G). Hence, I concluded that depletion of MFL protein does not reduce the IRES-dependent expression of the Hp120 Notch antagonist. Nonetheless, over-expression of this protein in the *mfl* silenced wing cells fails to fully suppress Nintra activity, thus reinforcing the view that *mfl* acts as a subtle modifier able to influence Notch activity.

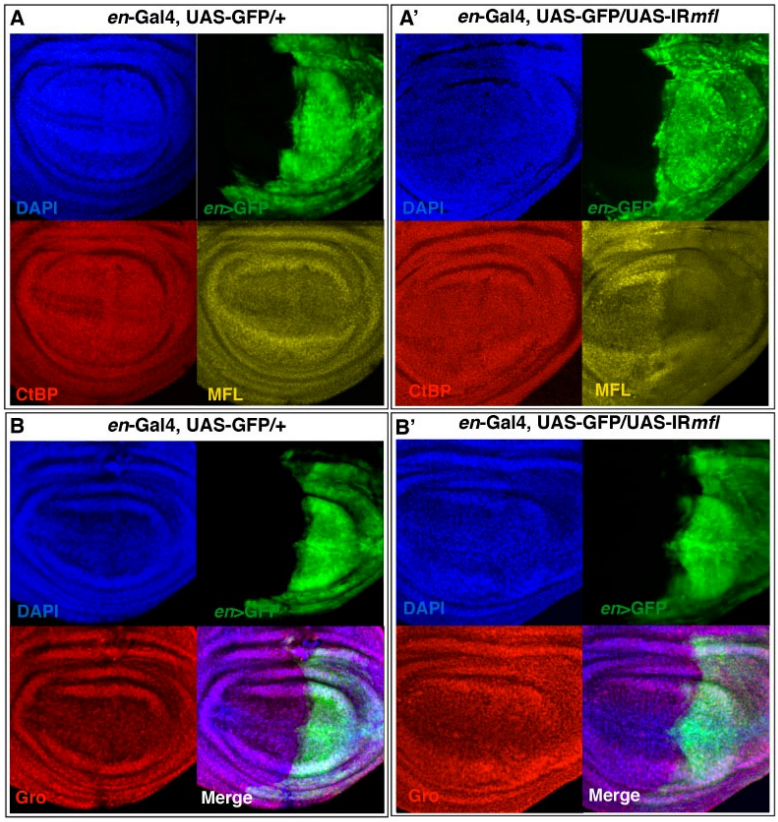

Figure 40. *mfl* RNAi does not alter Gro and CtBP levels. In the control discs **(A, B)**, CtBP **(A)** and Gro **(B)** levels appear uniforms. The levels of this two co-repressors remain almost unchanged after *mfl* RNAi driven by *en*-GAl4 **(A',B')**.

Finally, I checked whether Notch up-regulation could be due to a reduction in the levels of Groucho (Gro) and/or CtBP co-repressor proteins by performing immunostaining of wing imaginal discs with the specific antibodies. However, no significant difference was observed upon MFL depletion (Figure 40), leading to the conclusion that a reduced accumulation of neither H, Gro and CtBP could be invoked as the cause of Notch up-regulation. Thus, alternative mechanisms, such as post-translational modifications of the Notch receptor (or Nintra), alterations of cell-sorting, etc., or activation of non-canonical Notch signaling, need to be further investigated to clarify this aspect. Indeed, a non-canonical Notch function has been described to buffer the activity of Armadillo, a component of the Wg pathway (Sanders et al. 2009). Given that Notch and Wg act together during D/V boundary formation, activation of this non-canonical pathway could possibly be responsible for most of the observed effects. Finally, on the light of the results obtained, the exact cause-effect relationship between JNK and Notch activation represents an additional aspects that attracts further attention.

5 CONCLUSIONS

In vivo silencing of the *Drosophila* pseudouridine synthase component of H/ACA snoRNPs gives rise to complex context-dependent activation of highly conserved key pathways involved in homeostasis, development and differentiation. The results shown here demonstrate in fact that *mfl* gene silencing triggers a concerted activation of Notch, Wg and JNK signaling, revealing for the first time the close link that connects eukaryotic pseudouridine synthases with developmental events.

A first intriguing observation was that, upon MFL depletion, Notch activity was dysregulated in the way that expression of some target genes was highly induced (as the case of *wg*), while that of others was abolished (as the case of *cut*). This finding was unexpected, since Notch activity at the wing disc D/V boundary was always found to trigger parallel activation of these two targets. The opposite response elicited by Notch activation in pseudouridine synthase depleted cells revealed instead that *cut* expression requires a specific additional coactivator that is missing, or scarsely produced, upon *mfl* silencing. Indeed, loss of *cut* expression accounts nicely for the developmental defects observed in the adult silenced wings at the D/V margin, while Wg overexpression is likely to be responsible for the reduction of cell adhesion testified by the lowered levels of Arm and F-actin. In fact, the Wg protein not only acts as morphogen and triggers proliferation, but also plays a role in cell adhesion (Wodarz et al. 2006), through a non canonical pathway involved in the regulation of cytoskeleton remodeling, actin polymerization and cell migration

(reviewed by Rao et Kul. 2010). Moreover, the Notch receptor itself, through a non-canonical but evolutionarily conserved pathway (Andersen et al. 2012), is able to bind the Arm protein and direct it to endosomal degradation (Sanders et al. 2009). Whatever the mechanism, the reduced levels of apical Arm and F-actin observed in the silenced discs disrupted the apical adherens junctions, causing a loss of cell adhesion. This loss is critical to allow the tissue remodeling that occurs in the silenced discs, where the induction of cell death along the A/P axis triggers active proliferation of the surrounding areas. The response of wing cells to gene silencing was in fact found to be clearly context-dependent, underscoring that a wide range of potential functions can be exerted in a developing tissue. In fact, some silenced cells along the A/P boundary are pushed to undergo apoptosis, while others localized at ventral and dorsal tracts of the Wg inner ring are stimulated to strongly over-express this morphogen and to proliferate. Worth noting, this coupling between apoptosis and proliferation do not conform to the process of compensatory proliferation that is described to be mediated by high-level Wg secretion from the so called "undead-cells" that, even if committed to die, are unable to complete the apoptotic program (Martin et al. 2009). Conversely, I observed that Wg is secreted by the MFL-depleted *non*-apoptotic cells; moreover, the p35-mediated apoptotic block did not increase, but instead substantially reduced Wg secretion from the silenced cells. Thus, *mfl* silencing triggers a process of "apoptosis-induced proliferation" that is typical of regenerative phenomena. The activation of the JNK pathway and the induction of Mmp1 further support this view, pointing out a so far unpredicted role of pseudouridine synthases in tissue regeneration. Worth noting, when epithelial cells reduce their intercellular adhesion and increase motility, they can acquire a migratory behaviour and eventually undergo EMT. EMT plays important roles in many physiological developmental events, but when is stress-induced it may favor tumorigenesis, endowing the cells with invasive properties. The finding that pseudouridine synthase depletion pushes patches of peripodial cells to undergo EMT thus adds an unforeseen information that can be of valuable help to understanding the puzzling relationship that links pseudouridine synthases loss-of-function to cancer predisposition. Finally, further experiments are needed to clarify the exact relationship linking JNK induction to Notch activation. The JNK-triggered cell death is not responsible for this effect, since Notch hyper-activation was not rescued by p35-mediated apoptotic blockage.

However, it is possible that JNK signaling may be responsible for the Notch dysregulation by different ways. Indeed, given that the JNK targets are both transcriptional factors and cytoplasmic proteins, the pathway could repress the transcription of *cut* and/or modulate the activity of the Notch signaling by

phosphorylations. Alternative mechanisms based on possible effects triggered by cytoskeletal reorganization on membrane trafficking could also account for Notch activation. Whatever the mechanism, activation of Notch, Wg and JNK pathways has never been linked up to now to the loss of function of pseudouridine synthase of H/ACA snoRNP complexes. Moreover, considering the conserved functions played by these protein in ribosome biogenesis, their deficiency was expected to limit the proliferative capacity of cells, thus making the hyperproliferative phenomena (as tumour predisposition observed in X-DC patients) difficult to understand. On the basis of the results obtained, I speculate that alteration of cell polarity and dysregulation of the JNK signaling could be related to many of the symptoms shown by X-DC patients. Finally, I observed that Notch hyperactivation is not due to IRES-dependent defective translation of the short isoform of its Hairless antagonist. Indeed, when these experiments were performed, IRES-dependent translation was thought to be generally defective in pseudouridine synthase depleted cells (Montanaro et al. 2010; Bellodi et al. 2010). However, further information was added by Rocchi et al. (2013) in the course of this work. These authors assayed the translation efficiency of a pool of viral and cellular IRESs in *DKC1* silenced breast cancer cell lines and concluded that the level of ribosome pseudouridylation can differently modulate IRES-dependent translation: expression of some specific mRNAs could be repressed, while that of others be either unaffected or upregulated. In keeping with these data, it seems likely that pseudouridine synthase depletion can trigger different effects on IRES-dependent translation of specific mRNAs also in *Drosophila* cells.

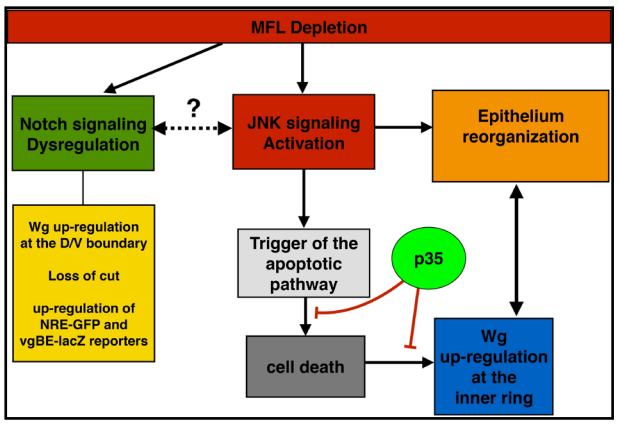

Figure 41. A graphical scheme resuming the main results. *mfl* silencing causes the dysregulation of Notch signaling (expression of NRE-GFP, *vg*Be-lacz and wg target genes highly induced; cut expression abolished) at the D/V boundary of the wing disc. The JNK pathway was also induced, and causes apoptosis. In response to cell death, cells of the inner ring secrete high-level of Wg, that in turn triggers a regenerative proliferation. Concomitant activation of the Mmp1 metalloproteinase further testified the occurrence of active epithelium reorganization. Further studies are required to define the exact relationships between activation of JNK and Notch pathways.

Figure 41 summarizes the main results obtained during this study.

6 AKNOWLEGMENTS

I am grateful to my guide Prof. Maria Furia for her valuable guidance, support and encouragement.

A very special thanks to Prof. Anette Preiss, Dr. Dieter Maier and Dr. Anja Christina Nagel of the University of Hohenheim for their wonderful hospitality and especially for constructive discussions.

A special thanks to Dr. Daniela Sarnataro (Dynamic Imaging facility-CEINGE) for her support in confocal microscopy and to Dr. Gianluca Polese for his help in the realization of laser microdissection.

I also want to thank, Dr. Mimmo Turano, Annamaria Di Giovanni, Arianna Petrizzo, Liliana Felicia Iannucci and Angela Pascarella for the wonderful work days spent together.

DEDICATION

This work is dedicated to my wife, Francesca Vita Palladino, without whose caring support it would not have been possible, and to my parents, Salvatore Vicidomini and Raffaela Pollio, for their sacrifices.

7 REFERENCES

Adachi-Yamada T, Fujimura-Kamada K, Nishida Y, Matsumoto K. Distortion of proximodistal information causes JNK-dependent apoptosis in Drosophila wing. Nature. 1999;400(6740):166-9

Agnès F, Suzanne M, Noselli S. The Drosophila JNK pathway controls the morphogenesis of imaginal discs during metamorphosis. Development. 1999;126(23):5453-62

Agnès F, Noselli S. [Dorsal closure in Drosophila. A genetic model for wound healing?]. C R Acad Sci III. 1999;322(1):5-13

Alawi F and Lin P. Loss of dyskerin reduces the accumulation of a subset of H/ACA snoRNA-derived miRNA. Cell Cycle 2010;9:2467-69

Alawi F, Lin P. Dyskerin is required for tumor cell growth through mechanisms that are independent of its role in telomerase and only partially related to its function in precursor rRNA processing. Mol Carcinog. 2011;50(5):334-45

Alawi F, Lin P. Dyskerin localizes to the mitotic apparatus and is required for orderly mitosis in human cells. PLoS One. 2013;8(11):e80805

Alter BP, Giri N, Savage SA, Rosenberg PS. Cancer in dyskeratosis congenita. Blood. 2009;113(26):6549-57

Andersen P, Uosaki H, Shenje LT, Kwon C. Non-canonical Notch signaling: emerging role and mechanism. Trends Cell Biol. 2012;22(5):257-65

Angrisani A, Vicidomini R, Turano M, Furia M. Human dyskerin: beyond telomeres. Biol Chem. 2014 Jan 28. pii:/j/bchm.just-accepted/hsz-2013-0287/hsz-2013-0287.xml. doi:10.1515/hsz-2013-0287

Baker NE. Transcription of the segment-polarity gene wingless in the imaginal discs of Drosophila, and the phenotype of a pupal-lethal wg mutation. Development. 1988;102(3):489-97

Bao XL, Song H, Chen Z, Tang X. Wnt3a promotes epithelial-mesenchymal transition, migration, and proliferation of lens epithelial cells. Mol Vis. 2012;18:1983-90

Barolo S, Stone T, Bang AG, Posakony JW. Default repression and Notch signaling: Hairless acts as an adaptor to recruit the corepressors Groucho and dCtBP to Suppressor of Hairless. Genes Dev. 2002;16(15):1964-76

Belacortu Y, Paricio N. Drosophila as a model of wound healing and tissue regeneration in vertebrates. Dev Dyn. 2011;240(11):2379-404

Bellodi C, Kopmar N, Ruggero D. Deregulation of oncogene-induced senescence and p53 translational control in X-linked dyskeratosis congenita. EMBO Journal 2010;29:1865–76

Bellodi C, McMahon M, Contreras A, Juliano D, Kopmar N, Nakamura T, Maltby D, Burlingame A, Savage SA, Shimamura A, Ruggero D. H/ACA small RNA dysfunctions in disease reveal key roles for noncoding RNA modifications in hematopoietic stem cell differentiation. Cell Rep. 2013;3(5):1493-502

Bernard F, Krejci A, Housden B, Adryan B, Bray SJ. Specificity of Notch pathway activation: twist controls the transcriptional output in adult muscle progenitors. Development. 2010;137(16):2633-42

Bikkavilli RK, Malbon CC. Mitogen-activated protein kinases and Wnt/beta-catenin signaling: Molecular conversations among signaling pathways.
Commun Integr Biol. 2009;2(1):46-9

Blair SS. Mechanisms of compartment formation: evidence that non-proliferating cells do not play a critical role in defining the D/V lineage restriction in the developing wing of Drosophila. Development. 1993;119(2): 339-51

Borggrefe T, Oswald F. The Notch signaling pathway: transcriptional regulation at Notch target genes. Cell Mol Life Sci. 2009;66(10):1631-46
Bosch M, Serras F, Martín-Blanco E, Baguñà J. JNK signaling pathway required for wound healing in regenerating Drosophila wing imaginal discs. Dev Biol. 2005;280(1):73-86

Bosch M, Baguñà J, Serras F. Origin and proliferation of blastema cells during regeneration of Drosophila wing imaginal discs. Int J Dev Biol. 2008;52(8): 1043-50

Bray SJ. Notch signalling: a simple pathway becomes complex. Nat Rev Mol Cell Biol. 2006;7(9):678-89

Bray S, Bernard F. Notch targets and their regulation. Curr Top Dev Biol. 2010;92:253-75

Bray S, Furriols M. Notch pathway: making sense of suppressor of hairless. Curr Biol. 2001;11(6):R217-21

Brou C, Logeat F, Lecourtois M, Vandekerckhove J, Kourilsky P, Schweisguth F, Israël A. Inhibition of the DNA-binding activity of Drosophila suppressor of hairless and of its human homolog, KBF2/RBP-J kappa, by direct protein-protein interaction with Drosophila hairless. Genes Dev. 1994;8(20):2491-503

Cadwell C, Yoon HJ, Zebarjadian Y, Carbon J. The yeast nucleolar protein Cbf5p is involved in rRNA biosynthesis and interacts genetically with the RNA polymerase I transcription factor RRN3. Mol Cell Biol. 1997;17(10):6175-83

Callus BA, Vaux DL. Caspase inhibitors: viral, cellular and chemical. Cell Death Differ. 2007;14(1):73-8

Carrillo J, González A, Manguán-García C, Pintado-Berninches L, Perona R. p53 pathway activation by telomere attrition in X-DC primary fibroblasts occurs in the absence of ribosome biogenesis failure and as a consequence of DNA damage. Clin Transl Oncol. 2013;[Epub ahead of print]

Cohen SB, Graham ME, Lovrecz GO, Bache N, Robinson PJ, Reddel RR. Protein composition of catalytically active human telomerase from immortal cells. Science 2007;315:1850-53

Cossu F, Vulliamy TJ, Marrone A, Badiali M, Cao A, Dokal I. A novel DKC1 mutation, severe combined immunodeficiency (T+B-NK- SCID) and bone marrow transplantation in an infant with Hoyeraal-Hreidarsson syndrome. Br J Haematol. 2002;119(3):765-8

Couso JP, Bishop SA, Martinez Arias A. The wingless signalling pathway and the patterning of the wing margin in Drosophila. Development. 1994;120(3): 621-36

Davis DR. Stabilization of RNA stacking by pseudouridine. Nucleic Acids Res. 1995;23(24):5020-6

de Celis JF, Garcia-Bellido A, Bray SJ. Activation and function of Notch at the dorsal-ventral boundary of the wing imaginal disc. Development. 1996;122(1): 359-69

Diaz-Benjumea FJ, Cohen SM. Interaction between dorsal and ventral cells in the imaginal disc directs wing development in Drosophila. Cell. 1993;75(4): 741-52

Ding YG, Zhu TS, Jiang W, Yang Y, Bu DF, Tu P, Zhu XJ, Wang BX. Identification of a novel mutation and a de novo mutation in DKC1 in two Chinese pedigrees with Dyskeratosis congenita. J Invest Dermatol. 2004;123(3):470-3

Dobens LL, Martín-Blanco E, Martínez-Arias A, Kafatos FC, Raftery LA. Drosophila puckered regulates Fos/Jun levels during follicle cell morphogenesis. Development. 200;128(10):1845-56

Dokal I, Bungey J, Williamson P, Oscier D, Hows J, Luzzatto L. Dyskeratosis congenita fibroblasts are abnormal and have unbalanced chromosomal rearrangements. Blood. 1992;80(12):3090-6

Dokal I. Dyskeratosis congenita in all its forms. Br J Haematol. 2000;110(4): 768-79

Dokal I. Dyskeratosis congenita. Hematology Am Soc Hematol Educ Program. 2011;2011:480-6

Dorsett D. Distance-independent inactivation of an enhancer by the suppressor of Hairy-wing DNA-binding protein of Drosophila. Genetics. 1993;134(4): 1135-44

Egan ED, Collins K. Specificity and stoichiometry of subunit interactions in the human telomerase holoenzyme assembled in vivo. Mol Cell Biol. 2010;30(11):2775-86

Ender C, Krek A, Friedländer MR, Beitzinger M, Weinmann L, Chen W, Pfeffer S, Rajewsky N, Meister G. A Human snoRNA with MicroRNA-Like Functions. Molecular Cell 2008;32:519-28

Gao B. Wnt regulation of planar cell polarity (PCP). Curr Top Dev Biol. 2012;101:263-95

Garcia-Bellido A, Ripoll P, Morata G. Developmental compartmentalisation of the wing disc of Drosophila. Nat New Biol. 1973;245(147):251-3

Ge J, Rudnick DA, He J, Crimmins DL, Ladenson JH, Bessler M, Mason PJ. Dyskerin ablation in mouse liver inhibits rRNA processing and cell division. Mol. Cell. Biol. 2010;30,413–422

Ge J, Yu YT. RNA pseudouridylation: new insights into an old modification. Trends Biochem Sci. 2013;38(4):210-8

Ghazi A, Anant S, VijayRaghavan K. Apterous mediates development of direct flight muscles autonomously and indirect flight muscles through epidermal cues. Development. 2000;127(24):5309-18

Giordano E, Peluso I, Senger S, Furia M. minifly, a Drosophila gene required for ribosome biogenesis. J Cell Biol. 1999;144(6):1123-33

Gonsalves FC, DasGupta R. Function of the wingless signaling pathway in Drosophila. Methods Mol Biol. 2008;469:115-25

Gorfinkiel N, Schamberg S, Blanchard GB. Integrative approaches to morphogenesis: lessons from dorsal closure. Genesis. 2011;49(7):522-33

Gu BW, Ge J, Fan JM, Bessler M, Mason PJ. Slow growth and unstable ribosomal RNA lacking pseudouridine in mouse embryonic fibroblast cells expressing catalytically inactive dyskerin. FEBS Lett. 2013;587(14):2112-7

Hamma T, Reichow SL, Varani G, Ferré-D'Amaré AR. The Cbf5-Nop10 complex is a molecular bracket that organizes box H/ACA RNPs. Nat Struct Mol Biol. 2005;12(12):1101-7

Hassock S, Vetrie D, Giannelli F. Mapping and characterization of the X-linked dyskeratosis congenita (DKC) gene. Genomics. 1999;55(1):21-7

Hay BA, Wolff T, Rubin GM. Expression of baculovirus P35 prevents cell death in Drosophila. Development. 1994;120(8):2121-9

Heiss NS, Knight SW, Vulliamy TJ, Klauck SM, Wiemann S, Mason PJ, Poustka A, Dokal I. X-linked dyskeratosis congenita is caused by mutations in a highly conserved gene with putative nucleolar functions. Nat Genet. 1998;19(1):32-8

Heiss NS, Mégarbané A, Klauck SM, Kreuz FR, Makhoul E, Majewski F, Poustka A. One novel and two recurrent missense DKC1 mutations in patients with dyskeratosis congenita (DKC). Genet Couns. 2001;12(2):129-36

Hiramatsu H, Fujii T, Kitoh T, Sawada M, Osaka M, Koami K, Irino T, Miyajima T, Ito M, Sugiyama T, Okuno T. A novel missense mutation in the DKC1 gene in a Japanese family with X-linked dyskeratosis congenita. Pediatr Hematol Oncol. 2002;19(6):413-9

Igaki T. Correcting developmental errors by apoptosis: lessons from Drosophila JNK signaling. Apoptosis. 2009;14(8):1021-8

Irvine KD, Wieschaus E. fringe, a Boundary-specific signaling molecule, mediates interactions between dorsal and ventral cells during Drosophila wing development. Cell. 1994;79(4):595-606

Jack J, Dorsett D, Delotto Y, Liu S. Expression of the cut locus in the Drosophila wing margin is required for cell type specification and is regulated by a distant enhancer. Development. 1991;113(3):735-47

Jack K, Bellodi C, Landry DM, Niederer RO, Meskauskas A, Musalgaonkar S, Kopmar N, Krasnykh O, Dean AM, Thompson SR, Ruggero D, Dinman JD. rRNA pseudouridylation defects affect ribosomal ligand binding and translational fidelity from yeast to human cells. Mol Cell. 2011;44(4):660-6

Janody F, Treisman JE. Requirements for mediator complex subunits distinguish three classes of notch target genes at the Drosophila wing margin. Dev Dyn. 2011;240(9):2051-9

Jasper H, Benes V, Schwager C, Sauer S, Clauder-Münster S, Ansorge W, Bohmann D. The genomic response of the Drosophila embryo to JNK signaling. Dev Cell. 2001;1(4):579-86

Jiang W, Middleton K, Yoon H-J, Fouquet C, Carbon J. An Essential Yeast Protein, CBF5p, Binds In Vitro to Centromeres and Microtubules. Molecular and Cellular Biology 1993;13:4884-93

Johnson GL, Nakamura K. The c-jun kinase/stress-activated pathway: regulation, function and role in human disease. Biochim Biophys Acta. 2007;1773(8):1341-8

Jung C-H, Hansen MA, Makunin IV, Korbie DJ, Mattick1 JS. Identification of novel non-coding RNAs using profiles of short sequence reads from next generation sequencing data. BMC genomics 2010;11:77

Khanna A, Stamm S. Regulation of alternative splicing by short non-coding nuclear RNAs. RNA Biol. 2010;7(4):480-5

Kim J, Irvine KD, Carroll SB. Cell recognition, signal induction, and symmetrical gene activation at the dorsal-ventral boundary of the developing Drosophila wing. Cell. 1995 Sep 8;82(5):795-802

Kim J, Sebring A, Esch JJ, Kraus ME, Vorwerk K, Magee J, Carroll SB. Integration of positional signals and regulation of wing formation and identity by Drosophila vestigial gene. Nature. 1996;382(6587):133-8

Kiss T, Fayet E, Jády BE, Richard P, Weber M. Biogenesis and intranuclear trafficking of human box C/D and H/ACA RNPs.
Cold Spring Harb Symp Quant Biol. 2006;71:407-17

Klein T. Wing disc development in the fly: the early stages. Curr Opin Genet Dev. 2001;11(4):470-5

Knight SW, Heiss NS, Vulliamy TJ, Greschner S, Stavrides G, Pai GS, Lestringant G, Varma N, Mason PJ, Dokal I, Poustka A. X-linked dyskeratosis congenita is predominantly caused by missense mutations in the DKC1 gene.
Am J Hum Genet. 1999;65(1):50-8

Knight SW, Heiss NS, Vulliamy TJ, Aalfs CM, McMahon C, Richmond P, Jones A, Hennekam RC, Poustka A, Mason PJ, Dokal I. Unexplained aplastic anaemia, immunodeficiency, and cerebellar hypoplasia (Hoyeraal-Hreidarsson syndrome) due to mutations in the dyskeratosis congenita gene, DKC1. Br J Haematol. 1999;107(2):335-9

Knight SW, Vulliamy TJ, Morgan B, Devriendt K, Mason PJ, Dokal I. Identification of novel DKC1 mutations in patients with dyskeratosis congenita: implications for pathophysiology and diagnosis.
Hum Genet. 2001;108(4):299-303

Komiya Y, Habas R. Wnt signal transduction pathways. Organogenesis. 2008;4(2):68-75

Kovall RA, Blacklow SC. Mechanistic insights into Notch receptor signaling from structural and biochemical studies. Curr Top Dev Biol. 2010;92:31-71

Lafontaine DL, Tollervey D. Birth of the snoRNPs: the evolution of the modification-guide snoRNAs. Trends Biochem Sci. 1998;23(10):383-8

Lee N, Maurange C, Ringrose L, Paro R. Suppression of Polycomb group proteins by JNK signalling induces transdetermination in Drosophila imaginal discs. Nature. 2005;438(7065):234-7

Lestrade L, Weber MJ. snoRNA-LBME-db, a comprehensive database of human H/ACA and C/D box snoRNAs. Nucleic Acids Res. 2006;34(Database issue):D158-62

Lin X, Momany M. The Aspergillus nidulans swoC1 mutant shows defects in growth and development. Genetics. 2003;165(2):543-54

Liu ZG, Hsu H, Goeddel DV, Karin M. Dissection of TNF receptor 1 effector functions: JNK activation is not linked to apoptosis while NF-kappaB activation prevents cell death. Cell. 1996;87(3):565-76

Luzzatto L, Karadimitris A. Dyskeratosis and ribosomal rebellion. Nat Genet. 1998;19(1):6-7

Maceluch J, Kmieciak M, Szweykowska-Kulińska Z, Jarmołowski A. Cloning and characterization of Arabidopsis thaliana AtNAP57--a homologue of yeast pseudouridine synthase Cbf5p. Acta Biochim Pol. 2001;48(3):699-709

Macías A, Romero NM, Martín F, Suárez L, Rosa AL, Morata G. PVF1/PVR signaling and apoptosis promotes the rotation and dorsal closure of the Drosophila male terminalia. Int J Dev Biol. 2004;48(10):1087-94

Maden BE. The numerous modified nucleotides in eukaryotic ribosomal RNA. Prog Nucleic Acid Res Mol Biol.1990;39:241-303

Maier D, Nagel AC, Johannes B, Preiss A. Subcellular localization of Hairless protein shows a major focus of activity within the nucleus. Mech Dev 1999;89(1-2):195-9

Maier D, Nagel AC, Preiss A. Two isoforms of the Notch antagonist Hairless are produced by differential translation initiation. Proc Natl Acad Sci U S A. 2002;99(24):15480-5

Maier D. Hairless: the ignored antagonist of the Notch signalling pathway. Hereditas. 2006;143(2006):212-21

Major RJ, Irvine KD. Influence of Notch on dorsoventral compartmentalization and actin organization in the Drosophila wing. Development. 2005;132(17): 3823-33

Marrone A, Mason PJ. Dyskeratosis congenita. Cell Mol Life Sci. 2003;60(3): 507-17

Martín FA, Peréz-Garijo A, Morata G. Apoptosis in Drosophila: compensatory proliferation and undead cells. Int J Dev Biol. 2009;53(8-10):1341-7

Martin P, Parkhurst SM. Parallels between tissue repair and embryo morphogenesis. Development. 2004;131(13):3021-34

Martin-Blanco E, Gampel A, Ring J, Virdee K, Kirov N, Tolkovsky AM, Martinez-Arias A. puckered encodes a phosphatase that mediates a feedback loop regulating JNK activity during dorsal closure in Drosophila. Genes Dev. 1998;12(4):557-70

Martin-Blanco E, Pastor-Pareja JC, Garcia-Bellido A. JNK and decapentaplegic signaling control adhesiveness and cytoskeleton dynamics during thorax closure in Drosophila. Proc Natl Acad Sci U S A. 2000 Jul 5;97(14):7888-93

Mason PJ, Bessler M. The genetics of dyskeratosis congenita. Cancer Genet. 2011;204(12):635-45

Mattila J, Omelyanchuk L, Kyttälä S, Turunen H, Nokkala S. Role of Jun N-terminal Kinase (JNK) signaling in the wound healing and regeneration of a Drosophila melanogaster wing imaginal disc. Int J Dev Biol. 2005;49(4):391-9

McEwen DG, Peifer M. Puckered, a Drosophila MAPK phosphatase, ensures cell viability by antagonizing JNK-induced apoptosis. Development. 2005;132(17):3935-46

Meier UT, Blobel G. NAP57, a mammalian nucleolar protein with a putative homolog in yeast and bacteria. J Cell Biol. 1994;127(6 Pt 1):1505-14

Micalizzi DS, Farabaugh SM, Ford HL. Epithelial-mesenchymal transition in cancer: parallels between normal development and tumor progression. J Mammary Gland Biol Neoplasia. 2010;15(2):117-34

Micchelli CA, Rulifson EJ, Blair SS. The function and regulation of cut expression on the wing margin of Drosophila: Notch, Wingless and a dominant negative role for Delta and Serrate. Development. 1997;124(8):1485-95

Milán M, Cohen SM. Temporal regulation of apterous activity during developmentof the Drosophila wing. Development. 2000;127(14):3069-78

Mitchell JR, Wood E, Collins K. A telomerase component is defective in the human disease dyskeratosis congenita. Nature. 1999;402(6761):551-5

Mochizuki Y, He J, Kulkarni S, Bessler M, Mason PJ. Mouse dyskerin mutations affect accumulation of telomerase RNA and small nucleolar RNA, telomerase activity, and ribosomal RNA processing. Proc Natl Acad Sci U S A. 2004;101(29):10756-61

Montanaro L, Calienni M, Bertoni S, Rocchi L, Sansone P, Storci G, Santini D, Ceccarelli C, Taffurelli M, Carnicelli D, Brigotti M, Bonafè M, Treré D, Derenzini M. Novel dyskerin-mediated mechanism of p53 inactivation through defective mRNA translation. Cancer Res. 2010;70(11):4767-77

Morel V, Lecourtois M, Massiani O, Maier D, Preiss A, Schweisguth F. Transcriptional repression by suppressor of hairless involves the binding of a hairless-dCtBP complex in Drosophila. Curr Biol. 2001;11(10):789-92

Moreno E, Yan M, Basler K. Evolution of TNF signaling mechanisms: JNK-dependent apoptosis triggered by Eiger, the Drosophila homolog of the TNF superfamily. Curr Biol. 2002 Jul 23;12(14):1263-8

Nam Y, Sliz P, Song L, Aster JC, Blacklow SC. Structural basis for cooperativity in recruitment of MAML coactivators to Notch transcription complexes. Cell. 2006;124(5):973-83

Nepveu A. Role of the multifunctional CDP/Cut/Cux homeodomain transcription factor in regulating differentiation, cell growth and development. Gene. 2001;270(1-2):1-15

Neto-Silva RM, Wells BS, Johnston LA. Mechanisms of growth and homeostasis in the Drosophila wing. Annu Rev Cell Dev Biol. 2009;25:197-220

Neumann CJ, Cohen SM. A hierarchy of cross-regulation involving Notch, wingless, vestigial and cut organizes the dorsal/ventral axis of the Drosophila wing. Development. 1996;122(11):3477-85

Oswald F, Winkler M, Cao Y, Astrahantseff K, Bourteele S, Knöchel W, Borggrefe T. RBP-Jkappa/SHARP recruits CtIP/CtBP corepressors to silence Notch target genes. Mol Cell Biol. 2005;25(23):10379-90

Pardue ML, Rashkova S, Casacuberta E, DeBaryshe PG, George JA, Traverse KL. Two retrotransposons maintain telomeres in Drosophila. Chromosome Res. 2005;13(5):443-53

Parry EM, Alder JK, Lee SS, Phillips JA 3rd, Loyd JE, Duggal P, Armanios M. Decreased dyskerin levels as a mechanism of telomere shortening in X-linked dyskeratosis congenita. J Med Genet. 2011;48(5):327-33

Phillips B, Billin AN, Cadwell C, Buchholz R, Erickson C, Merriam JR, Carbon J, Poole SJ. The Nop60B gene of Drosophila encodes an essential nucleolar protein that functions in yeast. Mol Gen Genet. 1998;260(1):20-9

Radisky ES, Radisky DC. Matrix metalloproteinase-induced epithelial-mesenchymal transition in breast cancer. J Mammary Gland Biol Neoplasia. 2010;15(2):201-12

Rafel N, Milán M. Notch signalling coordinates tissue growth and wing fate specification in Drosophila. Development. 2008;135(24):3995-4001

Rao TP, Kühl M. An updated overview on Wnt signaling pathways: a prelude for more. Circ Res. 2010 Jun;106(12):1798-806

Rebay I, Fleming RJ, Fehon RG, Cherbas L, Cherbas P, Artavanis-Tsakonas S. Specific EGF repeats of Notch mediate interactions with Delta and Serrate: implications for Notch as a multifunctional receptor. Cell. 1991;67(4):687-99

Reuben PM, Cheung HS. Regulation of matrix metalloproteinase (MMP) gene expression by protein kinases. Front Biosci. 2006;11:1199-215

Richard P, Darzacq X, Bertrand E, Jády BE, Verheggen C, Kiss T. A common sequence motif determines the Cajal body-specific localization of box H/ACA scaRNAs. EMBO J. 2003 Aug;22(16):4283-93

Ring JM, Martinez Arias A. puckered, a gene involved in position-specific cell differentiation in the dorsal epidermis of the Drosophila larva. Dev Suppl. 1993:251-9

Rocchi L, Pacilli A, Sethi R, Penzo M, Schneider RJ, Treré D, Brigotti M, Montanaro L. Dyskerin depletion increases VEGF mRNA internal ribosome entry site-mediated translation. Nucleic Acids Res. 2013;41(17):8308-18

Rousset R, Bono-Lauriol S, Gettings M, Suzanne M, Spéder P, Noselli S. The Drosophila serine protease homologue Scarface regulates JNK signalling in a negative-feedback loop during epithelial morphogenesis. Development. 2010;137(13):2177-86

Ruggero D, Grisendi S, Piazza F, Rego E, Mari F, Rao PH, Cordon-Cardo C, Pandolfi PP. Dyskeratosis Congenita and Cancer in Mice Deficient in Ribosomal RNA Modification. Science 2003;299:259-62

Ryoo HD, Gorenc T, Steller H. Apoptotic cells can induce compensatory cell proliferation through the JNK and the Wingless signaling pathways. Dev Cell. 2004;7(4):491-501

Saj A, Arziman Z, Stempfle D, van Belle W, Sauder U, Horn T, Dürrenberger M, Paro R, Boutros M, Merdes G. A combined ex vivo and in vivo RNAi screen for notch regulators in Drosophila reveals an extensive notch interaction network. Dev Cell. 2010;18(5):862-76

Salowsky R, Heiss NS, Benner A, Wittig R, Poustka A. Basal transcription activity of the dyskeratosis congenita gene is mediated by Sp1 and Sp3 and a patient mutation in a Sp1 binding site is associated with decreased promoter activity. Gene. 2002;293(1-2):9-19

Sanders PG, Muñoz-Descalzo S, Balayo T, Wirtz-Peitz F, Hayward P, Arias AM. Ligand-independent traffic of Notch buffers activated Armadillo in Drosophila. PLoS Biol. 2009;7(8):e1000169

Saraiya AA and Wang CC. snoRNA, a Novel Precursor of microRNA in Giardia lamblia. Plos Pathogens 2008;4:e1000224

Savage SA, Giri N, Baerlocher GM, Orr N, Lansdorp PM, Alter BP. TINF2, a component of the shelterin telomere protection complex, is mutated in dyskeratosis congenita. Am J Hum Genet. 2008;82(2):501-9

Savage SA, Bertuch AA. The genetics and clinical manifestations of telomere biology disorders. Genet Med. 2010;12(12):753-64

Schubiger M, Sustar A, Schubiger G. Regeneration and transdetermination: the role of wingless and its regulation. Dev Biol. 2010;347(2):315-24

Stevens LJ, Page-McCaw A. A secreted MMP is required for reepithelialization during wound healing. Mol Biol Cell. 2012;23(6):1068-79

Sudarsan V, Anant S, Guptan P, VijayRaghavan K, Skaer H. Myoblast diversification and ectodermal signaling in Drosophila. Dev Cell. 2001;1(6): 829-39

Tabata T, Kornberg TB. Hedgehog is a signaling protein with a key role in patterning Drosophila imaginal discs. Cell. 1994;76(1):89-102

Taft RJ, Glazov EA, Lassmann T, Hayashizaki Y, Carninci P, Mattick JS. Small RNAs derived from snoRNAs. RNA 2009;15:1233-40

Taulli R, Pandolfi PP. "Snorkeling" for missing players in cancer. J Clin Invest. 2012;122(8): 2765–2768
Tien AC, Rajan A, Bellen HJ. A Notch updated. J Cell Biol. 2009;184(5):621-9

Tortoriello G, de Celis JF, Furia M. Linking pseudouridine synthases to growth, development and cell competition. The FEBS Journal 2010;277:3249- 63

van der Velden JL, Guala AS, Leggett SE, Sluimer J, Badura EC, Janssen-Heininger YM. Induction of a mesenchymal expression program in lung epithelial cells by wingless protein (Wnt)/β-catenin requires the presence of c-Jun N-terminal kinase-1 (JNK1). Am J Respir Cell Mol Biol. 2012;47(3): 306-14

Vicidomini R, Tortoriello G, Furia M, Polese G. Laser microdissection applied to gene expression profiling of subset of cells from the Drosophila wing disc. J Vis Exp. 2010 Apr 30;(38)

Vulliamy TJ, Knight SW, Heiss NS, Smith OP, Poustka A, Dokal I, Mason PJ. Dyskeratosis congenita caused by a 3' deletion: germline and somatic mosaicism in a female carrier. Blood. 1999;94(4):1254-60

Vulliamy TJ, Marrone A, Knight SW, Walne A, Mason PJ, Dokal I. Mutations in dyskeratosis congenita: their impact on telomere length and the diversity of clinical presentation. Blood. 2006;107(7):2680-5

Vulliamy T, Beswick R, Kirwan M, Marrone A, Digweed M, Walne A, Dokal I. Mutations in the telomerase component NHP2 cause the premature ageing

syndrome dyskeratosis congenita. Proceedings of the National Academy of Sciences of the United States of America 2008;105:8073-78

Walne AJ, Vulliamy T, Marrone A, Beswick R, Kirwan M, Masunari Y, Al-Qurashi F-h, Aljurf M, Dokal I. Genetic heterogeneity in autosomal recessive dyskeratosis congenita with one subtype due to mutations in the telomerase-associated protein NOP10. Human Molecular Genetics 2007;16:1619-29

Walne AJ, Vulliamy T, Beswick R, Kirwan M, Dokal I. TINF2 mutations result in very short telomeres: analysis of a large cohort of patients with dyskeratosis congenita and related bone marrow failure syndromes. Blood 2008;112:3594-600

Watanabe Y, Gray MW. Evolutionary appearance of genes encoding proteins associated with box H/ACA snoRNAs: cbf5p in Euglena gracilis, an early diverging eukaryote, and candidate Gar1p and Nop10p homologs in archaebacteria. Nucleic Acids Res. 2000 Jun;28(12):2342-52

Weston CR, Davis RJ. The JNK signal transduction pathway. Curr Opin Cell Biol. 2007;19(2):142-9

Williams JA, Paddock SW, Carroll SB. Pattern formation in a secondary field: a hierarchy of regulatory genes subdivides the developing Drosophila wing disc into discrete subregions. Development. 1993;117(2):571-84

Williams JA, Paddock SW, Vorwerk K, Carroll SB. Organization of wing formation and induction of a wing-patterning gene at the dorsal/ventral compartment boundary. Nature. 1994;368(6469):299-305

Wilson JJ, Kovall RA. Crystal structure of the CSL-Notch-Mastermind ternary complex bound to DNA. Cell. 2006;124(5):985-96

Wodarz A, Stewart DB, Nelson WJ, Nusse R. Wingless signaling modulates cadherin-mediated cell adhesion in Drosophila imaginal disc cells. J Cell Sci. 2006;119(Pt 12):2425-34

Wong JM, Kyasa MJ, Hutchins L, Collins K. Telomerase RNA deficiency in peripheral blood mononuclear cells in X-linked dyskeratosis congenita.
Hum Genet. 2004;115(5):448-55

Wu G, Yu AT, Kantartzis A, Yu YT. Functions and mechanisms of spliceosomal small nuclear RNA pseudouridylation. Wiley Interdiscip Rev RNA. 2011;2(4): 571-81

Wu J, Cohen SM. Repression of Teashirt marks the initiation of wing development. Development. 2002;129(10):2411-8

Xia Z, Dickens M, Raingeaud J, Davis RJ, Greenberg ME. Opposing effects of ERK and JNK-p38 MAP kinases on apoptosis. Science. 1995;270(5240): 1326-31

Yang Y, Isaac C, Wang C, Dragon F, Pogacic V, Meier UT. Conserved composition of mammalian box H/ACA and box C/D small nucleolar ribonucleoprotein particles and their interaction with the common factor Nopp140. Mol Biol Cell. 2000;11(2):567-77

Yoon A, Peng G, Brandenburg Y, Zollo O, Xu W, Rego E, Ruggero D. Impaired Control of IRES-Mediated Translation in X-Linked Dyskeratosis Congenita. Science 2006;312:902-06

Yu AT, Ge J, Yu YT. Pseudouridines in spliceosomal snRNAs. Protein Cell. 2011;2(9):712-25

Zebarjadian Y, King T, Fournier MJ, Clarke L, Carbon J. Point mutations in yeast CBF5 can abolish in vivo pseudouridylation of rRNA. Molecular and Cellular Biology 1999;19:7461-72

Zecca M, Basler K, Struhl G. Sequential organizing activities of engrailed, hedgehog and decapentaplegic in the Drosophila wing. Development. 1995;121(8):2265-78

Zecca M, Basler K, Struhl G. Direct and long-range action of a wingless morphogen gradient. Cell. 1996;87(5):833-44

Zeng XL, Thumati NR, Fleisig HB, Hukezalie KR, Savage SA, Giri N, Alter BP, Wong JM. The accumulation and not the specific activity of telomerase ribonucleoprotein determines telomere maintenance deficiency in X-linked dyskeratosis congenita. Hum Mol Genet. 2012 Feb 15;21(4):721-9

Zhang Y, Morimoto K, Danilova N, Zhang B, Lin S. Zebrafish models for dyskeratosis congenita reveal critical roles of p53 activation contributing to hematopoietic defects through RNA processing. PLoS One. 2012;7(1):e30188

8 ORIGINAL PAPERS

Video Article

Laser Microdissection Applied to Gene Expression Profiling of Subset of Cells from the *Drosophila* Wing Disc

Rosario Vicidomini, Giuseppe Tortoriello, Maria Furia, Gianluca Polese
Dipartimento di Biologia Strutturale e Funzionale, University of Naples

Correspondence to: Maria Furia at mfuria@unina.it

URL: http://www.jove.com/details.php?id=1895
DOI: 10.3791/1895
Citation: Vicidomini R., Tortoriello G., Furia M., Polese G. (2010). Laser Microdissection Applied to Gene Expression Profiling of Subset of Cells from the Drosophila Wing Disc. JoVE. 38. http://www.jove.com/details.php?id=1895, doi: 10.3791/1895

Abstract

Heterogeneous nature of tissues has proven to be a limiting factor in the amount of information that can be generated from biological samples, compromising downstream analyses. Considering the complex and dynamic cellular associations existing within many tissues, in order to recapitulate the *in vivo* interactions thorough molecular analysis one must be able to analyze specific cell populations within their native context. Laser-mediated microdissection can achieve this goal, allowing unambiguous identification and successful harvest of cells of interest under direct microscopic visualization while maintaining molecular integrity. We have applied this technology to analyse gene expression within defined areas of the developing *Drosophila* wing disc, which represents an advantageous model system to study growth control, cell differentiation and organogenesis. Larval imaginal discs are precociously subdivided into anterior and posterior, dorsal and ventral compartments by lineage restriction boundaries. Making use of the inducible GAL4-UAS binary expression system, each of these compartments can be specifically labelled in transgenic flies expressing an UAS-GFP transgene under the control of the appropriate GAL4-driver construct. In the transgenic discs, gene expression profiling of discrete subsets of cells can precisely be determined after laser-mediated microdissection, using the fluorescent GFP signal to guide laser cut.

Among the variety of downstream applications, we focused on RNA transcript profiling after localised RNA interference (RNAi). With the advent of RNAi technology, GFP labelling can be coupled with localised knockdown of a given gene, allowing to determinate the transcriptional response of a discrete cell population to the specific gene silencing. To validate this approach, we dissected equivalent areas of the disc from the posterior (labelled by GFP expression), and the anterior (unlabelled) compartment upon regional silencing in the P compartment of an otherwise ubiquitously expressed gene. RNA was extracted from microdissected silenced and unsilenced areas and comparative gene expression profiling determined by quantitative real-time RT-PCR. We show that this method can effectively be applied for accurate transcriptomics of subsets of cells within the *Drosophila* imaginal discs. Indeed, while massive disc preparation as source of RNA generally assumes cell homogeneity, it is well known that transcriptional expression can vary greatly within these structures in consequence of positional information. Using localized fluorescent GFP signal to guide laser cut, more accurate transcriptional analyses can be performed and profitably applied to disparate applications, including transcript profiling of distinct cell lineages within their native context.

Protocol

Part 1. Preparation of *Drosophila* Imaginal Wing Discs Subjected to Specific and Localized RNAi.

As biological material, we used *Drosophila* imaginal wing discs obtained from transgenic larvae subjected to the localized and specific gene silencing by means of the GAL4/UAS system [1]. This larval progeny orginates from a genetic cross involving two parental lines: one carrying the GAL4 driver, the second the UAS responder. In addition to express GAL4 in a specific temporal and/or spatial pattern, the driver line carries an UAS-GFP reporter that allows to visualize the GAL4 expression domain. The UAS responder line expresses, under the control of the UAS sequence, an hairpin silencing RNA (hpRNA) able to specifically target the selected gene of interest (call it gene X) [2]. Once expressed in the cell, the hpRNA X is cleaved to generate small interfering RNA (siRNA) able to specifically silence the selected gene. In the larval progeny, that carries both driver and responder transgenes, the UAS-silencing construct is only transcribed in those cells expressing the GAL4 protein, and thus is able to induce a spatially restricted silencing of the selected gene X.

Among the variety of possible applications, we applied this approach to silence a selected gene of our interest (gene X) under the control of the *engrailed*-GAL4 (*en*) driver, which can trigger specific silencing in the posterior compartment of the wing disc [3], whose territory was marked by the expression of the UAS-GFP transgene.

The silenced imaginal wing discs were hand-dissected, taking care to eliminate surrounding contaminating tissues, especially the adhering tracheas. Each isolated wing disc was then quickly and gently transferred to a previously treated, RNase free dissection frame for immediate laser microdissection of selected areas.

Part 2. Laser microdissection of selected areas from the silenced (posterior) and unsilenced (anterior) compartments of the wing disc.

Once the wing disc was on the membrane, laser microdissection of specific areas from silenced (posterior; GFP-labelled) and unsilenced (anterior; GFP-unlabelled) compartments was achieved. This was performed by drawing an area that could easily fit in both, the GFP-positive and GFP-negative sides of the disc. Under the microdissector, we first focused the laser beam on the GFP-positive tissue, making a cut along the selected perimeter. The microdissector proceeds with cutting at the selected speed and power, but it is possible to refine the cutting manually,

until the selected area of tissue falls in the tube underneath. This tube contains a small volume of the TRI Reagent, so that the GFP-positive tissue is ready for subsequent RNA extraction.

We subsequently moved the cutting area to the opposite, GFP-negative side of the wing disc, in order to dissect an equivalent territory from the unsilenced, GFP-negative tissue. Once again, after the automatic cut, we proceeded to refining the cut manually. Once the cut was done, also the GFP-negative tissue was recovered in the TRI Reagent, ready for RNA extraction.

Part 3. RNA Extraction and Transcription Profiling from Microdissected Tissue Areas.

We spun the tubes to detach the liquid from the cap and added TRI Reagent up to 1 ml, then performed RNA extraction following the standard TRI Reagent protocol. To collect enough material, we repeated the cutting procedure on 100 imaginal wing discs. Starting from 100 areas of about 5000 μm^2 each, our yield was of 1.5 µg of RNA. Accuracy of the manual dissection was then controlled by checking GFP expression in the silenced and unsilenced samples by RT-PCR, using Super Script III (Invitrogen) to synthesize cDNA with Random Hexamers. Subsequent quantitative analyses focused to determine the expression levels of the silenced gene X, together with those of putative targets of its regulatory pathway, were performed by Real Time RT-PCR using Master Mix (Invitrogen).

Discussion

With respect to their basal expression levels achieved in the anterior/posterior compartments of unsilenced wing discs, the activity of the selected gene X was found reduced to 40% upon silencing. In contrast, one of its putative targets (genes Y) was found significantly up-regulated (7 fold-increase), leading us to validate the hypothesis that it was negatively regulated by gene X.

We conclude that the above described experimental approach can successfully be applied to the validation of putative targets of diverse regulatory pathways.

In addition, we surmise that improvement in the yield of RNA extraction could rapidly allow characterization of localized transcription profiling by microarray analysis. This will open the possibility to achieve a more detailed view of important biological processes. For examples, the localized formation of morphogenetic gradients [4, 5] or the transcriptional switch underlining the process of cell competition [6], where loosing and winner cell clones can be visualized by differential GFP expression, could be more specifically addressed. Whatever the application, this approach can help to define the transcriptional response of different cellular territories in their native tissue context.

Acknowledgements

The authors thank prof. Chiara Campanella and AMRA Center of Competence, University of Naples Federico II, Naples, Italy, for providing them with the use of the laser microdissector, and Mr Vincenzo Vicidomini for generous help in the 3D animation.

References

1. Elliott, D. A., Brand., A. H. The GAL4 System A Versatile System for the Expression of Gene. (ed. Dahmann, C.) (Humana Press Inc., Totowa, NJ, 2008).
2. Klein, T. Wing disc development in the fly: the early stages. Current Opinion In Genetics & Development 11, 470-475 (2001).
3. Dietzl, G. *et al*. A genome-wide transgenic RNAi library for conditional gene inactivation in *Drosophila*. Nature 448, 151-U1 (2007).
4. Martin, F. A. & Morata, G. Compartments and the control of growth in the *Drosophila* wing imaginal disc. Development 133, 4421-4426 (2006).
5. Tabata, T. Genetics of morphogen gradients. Nature Reviews Genetics 2, 620-630 (2001).
6. Moreno, E. & Basler, K. dMyc transforms cells into super-competitors. Cell 117, 117-129 (2004).

Review

Alberto Angrisani[a], Rosario Vicidomini[a], Mimmo Turano and Maria Furia*

Human dyskerin: beyond telomeres

Abstract: Human dyskerin is an evolutively conserved protein that participates in diverse nuclear complexes: the H/ACA snoRNPs, that control ribosome biogenesis, RNA pseudouridylation, and stability of H/ACA snoRNAs; the scaRNPs, that control pseudouridylation of snRNAs; and the telomerase active holoenzyme, which safeguards telomere integrity. The biological importance of dyskerin is further outlined by the fact that its deficiency causes the X-linked dyskeratosis congenita disease, while its over-expression characterizes several types of cancers and has been proposed as prognostic marker. The role of dyskerin on telomere maintenance has widely been discussed, while its functions as H/ACA sno/scaRNP component has been so far mostly overlooked and represent the main goal of this review. Here we summarize how increasing evidence indicates that the snoRNA/microRNA pathways can be interlaced, and that dyskerin-dependent RNA pseudouridylation represents a flexible mechanism able to modulate RNA function in different ways, including modulation of splicing, change of mRNA coding properties, and selective regulation of IRES-dependent translation. We also propose a speculative model that suggests that the dynamics of pre-assembly and nuclear import of H/ACA RNPs are crucial regulatory steps that can be finely controlled in the cytoplasm in response to developmental, differentiative and stress stimuli.

Keywords: *DKC1;* dyskeratosis; H/ACA snoRNPs; NAF1; pseudouridylation; SHQ1.

[a]These authors contributed equally to this work.
***Corresponding author: Maria Furia,** Dipartimento di Biologia, Università di Napoli 'Federico II', via Cinthia, I-80126 Naples, Italy, e-mail: mfuria@unina.it
Alberto Angrisani, Rosario Vicidomini and Mimmo Turano: Dipartimento di Biologia, Università di Napoli 'Federico II', via Cinthia, I-80126 Naples, Italy

Introduction

Clinical presentation of the X-linked dyskeratosis congenita disease (X-DC) embraces a variety of symptoms that includes a classical triad of mucocutaneous features, such as skin pigmentation, nail dystrophy and mucosal leukoplakia, coupled with a plethora of additional symptoms, as bone marrow failure, stem cell defects, mental retardation, premature aging and increased tumour susceptibility. The causative gene, *DKC1*, was identified on 1998, when a screening of candidate cDNAs from unrelated patients revealed that some of them shared mutations in its coding region (Heiss et al., 1998). Later on, *DKC1* mutations were shown to cause also the Hoyeraal-Hreidarsson syndrome (Knight et al., 1999; Yaghmai et al., 2000), characterized by developmental delay, immunodeficiency, aplastic anaemia and precocious mortality, and currently considered as a severe X-DC variant.

Q1: Please insert some paragraph breaks if possible, to aid readability

DKC1 encodes a 58 kDa nucleolar protein, named dyskerin, whose sequence is characterized by a high degree of phylogenetic conservation that testifies a great biological importance. Indeed, the *Cbf5* yeast gene, originally described to encode a centromere and microtubule binding protein (Jiang et al., 1993), was the first member of this gene family to be identified. Immediately after, a mammalian orthologue named *Nap57* was recognized in rats, and postulated to be involved in nucleo-cytoplasmic shuttling of pre-ribosomal structures (Meier and Blobel, 1994). Later, yeast *Cbf5* inactivation was shown to be lethal, and the lethality was attributed to defective processing and pseudouridylation of rRNAs precursors (Cadwell et al., 1997; Zebarjadian et al., 1999). In the same period, a Drosophila orthologue, named *Nop60B/minifly*, was recognized (Phillips et al., 1998) and shown to be necessary for proper maturation and pseudouridylation of rRNAs precursors (Giordano et al., 1999). Identification of *DKC1* as causative of X-DC attracted further attention on members of its gene family, so that related orthologues were then rapidly described in plant, fungal, protist and even archaebacterial genomes (Watanabe and Gray, 2000; Maceluch et al., 2001; Lin and Momany, 2003). In each species where genetic analysis has been performed, functionality of members of this gene family proved to be indispensable for survival, while hypomorphic mutations or gene silencing cause a plethora of disparate phenotypic abnormalities (see for example Giordano et al., 1999; Ruggero et al., 2003; Tortoriello et al., 2010; Zhang et al., 2012). Members of the

DKC1 gene family from different organisms have often been named differently, so that for the sake of simplicity hereafter we shall refer to them mostly as *DKC1* orthologues, and to their encoded proteins as dyskerins. All eukaryal dyskerins described so far have a prevalent nuclear localization. Within the nucleus, dyskerins participate in three essential complexes (see Figure 1): the H/ACA small nucleolar ribonucleoparticles (snoRNPs; Kiss et al., 2006), the active telomerase holoenzyme (Cohen et al., 2007), and the specific Cajal body ribonucleoparticles (scaRNPs). H/ACA snoRNPs are hetero-pentameric complexes in which dyskerin associates with one molecule of a small nucleolar RNA (snoRNA) of the H/ACA class and three highly conserved proteins: NOP10, NHP2 and GAR1 (Kiss et al., 2006). Functional conservation of these H/ACA snoRNP 'core' protein components is so notable that archaeal Cbf5p can

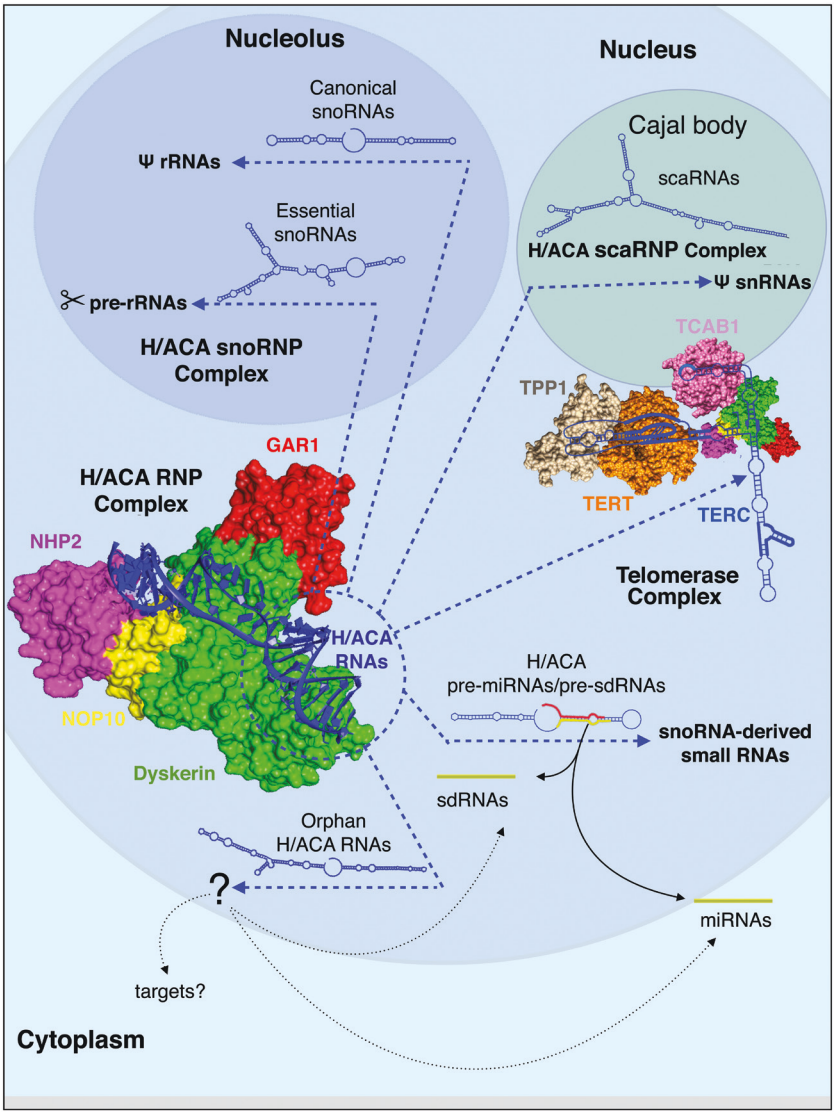

Figure 1 The diverse dyskerin-containing nuclear complexes.
Mature H/ACA snoRNPs are composed by a dyskerin-NOP10-NHP2-GAR1 tetramer assembled with a molecule of H/ACA RNA. These complexes localize in the nucleus where – depending on the specific recruited RNAs – they play different functions. While RNPs assembled with essential snoRNAs direct pre-rRNA processing, those assembled with canonical snoRNAs direct RNA pseudouridylation. When associated with orphan H/ACA RNAs, that do not have recognized target, these complexes might either guide modification of cellular RNAs or act as precursors of smaller regulatory RNAs (miRNAs/sdRNAs). H/ACA snoRNAs already identified as miRNA/sdRNA precursors are referred to as H/ACA pre-miRNAs or pre-sdRNAs. If assembled with a scaRNA, the dyskerin-NOP10-NHP2-GAR1 tetramer composes the scaRNPs, which localize in the Cajal bodies and direct pseudouridylation of snRNAs. The whole tetramer also participates in the formation of the telomerase active complex, together with the reverse transcriptase TERT, the TCAB1 protein, which directs the complex to the Cajal bodies, and the TPP1 protein, that binds the DNA template. Within the telomerase holoenzyme, dyskerin binds the TERC 3′ H/ACA domain.

assemble efficiently with yeast Nop10p protein, consistent with the high sequence conservation observed between archaea and eukarya (Hamma et al., 2005). The specific snoRNA that is recruited by the complex determines both the target recognition and the biological role of snoRNP complexes (see Figure 1). By acting as guide, each assembled snoRNA selects by base complementarity the target RNA and the specific site to be pseudouridylated (Lafontaine and Tollervey, 1998). Most common targets are rRNAs, while snRNAs of the U1 spliceosome are modified by a specific subgroup of specimens that do not localize in the nucleoli but in the Cajal bodies, and have thus been named Cajal body-specific RNAs (scaRNAs; Richard et al., 2003). In the pseudouridylation process, dyskerin acts as catalytic pseudouridine synthase, directing the isomerisation of specific uridines to pseudouridines. Furthermore, although the exact molecular mechanism still awaits to be fully elucidated, H/ACA snoRNPs also direct the endonucleolytic cleavages required for rRNA processing, under the guide of U17, E2 and E3 H/ACA snoRNAs, all essential for cell growth. Maturation of the 5′ end of the 18S rRNA requires the activity, most probably as chaperone, of the U17 snoRNA (also called E1), that in human cells is present in two isoforms, called U17a and U17b. In turn, the snoRNA E2 is needed for the maturation of the 3′ end of 18S rRNA, whereas the snoRNA E3 drives the maturation of the 5′ end of the 5.8S rRNA (for a comprehensive review of snoRNAs see http://www-snorna.biotoul.fr; Lestrade and Weber, 2006). Finally, a large number of 'orphan' snoRNAs, which lack a known target, has been identified and their functions remain to be defined. Dyskerin-H/ACA snoRNAs association attracted further attention after the discovery that, beside acting in RNA modification processes, snoRNAs can be maturated to produce short regulatory RNAs able to modulate alternative splicing (reviewed by Khanna and Stamm, 2010), or microRNAs (miRNAs). This last feature is largely widespread in eukaryotes, since snoRNA-derived miRNAs have been described in protozoa (Saraiya and Wang, 2008), humans (Ender et al., 2008), mouse, Arabidopsis, yeast, chicken (Taft et al., 2009) and Drosophila (Jung et al., 2010). Intriguingly, the percentage of snoRNAs that is able to be processed into miRNAs has been estimated to range from 60% in humans and mouse to more than 90% in Arabidopsis (Taft et al., 2009). Although the snoRNA-miRNA processing mechanism is mostly unclear, it appears to be Dicer1-dependent but Drosha/DCGR8-independent (Ender et al., 2008; Taft et al., 2009). Given the fundamental role played by miRNAs in post-transcriptional gene regulation, it is expected that dyskerin deficiency might affect a large set of biological processes through the snoRNA-derived miRNA regulatory pathway. Consistent with these expectations, a large variety of developmental defects has been described in Drosophila as a consequence of dyskerin depletion (Tortoriello et al., 2010). Lastly, through its ability to bind the telomerase RNA component (TERC), which harbours a 3′ H/ACA domain, dyskerin participates in the telomerase holoenzyme that is assembled in the Cajal bodies, and thus plays a well-established role in the maintenance of telomere integrity. This additional function was firstly revealed by Mitchell and co-workers (1999), who found that primary fibroblasts and lymphoblasts from X-DC-affected males had lower levels of telomerase RNA and telomerase activity, and shorter telomeres than matched normal cells, casting doubt on the initial view of X-DC as a ribosome deficiency disorder. Subsequently, telomerase RNA deficiency was also reported in the circulating lymphocytes of X-DC patients, indicating that this defect was not caused by cell culture (Wong et al., 2004). The involvement of dyskerin in maintenance of the telomere ends was definitively established by Cohen et al. (2007), which identified dyskerin as a component of the telomerase active holoenzyme. Subsequently, mutations in NOP10 and NHP2 that, similarly to dyskerin, participate in both H/ACA snoRNPs and active telomerase complex, were also shown to cause autosomal forms of DC (Savage and Bertuch, 2010). Mutations in other genes involved in telomerase activity, as *TERC*, *TERT*, *TINF2* (which encodes a member of the shelterin complex that protects telomere ends), and *TCAB1* (also named WDR79 or WRAP53), which is required for scaRNAs and TERC transit in the Cajal bodies, were also shown to cause DC (reviewed by Dokal, 2011; Mason and Bessler, 2011). Successive works indicated that each TERC molecule associates to two full sets of all four core H/ACA RNP components, i.e., dyskerin, NOP10, NHP2, and GAR1 (Egan and Collins, 2010). Overall, this picture led many researchers to conclude that X-DC was mainly caused by compromised telomerase function. However, pathogenic *DKC1* mutations affect not only telomere maintenance, but also rRNA processing and pseudouridylation of cellular RNAs, thus provoking a long-standing question: is X-DC mainly a telomerase disorder, or telomere deficiency is just one of the consequences of perturbed H/ACA snoRNP functions? While the role of dyskerin in telomeric stability has also extensively been reviewed by several authors in recent years (see for example Dokal, 2011; Mason and Bessler, 2011), this review intends to focus on the increasing list of diverse functions that are currently attributed to H/ACA RNPs, with the attempt to outline their general impact on a wide range of basic cellular processes. On the basis of a detailed view of more recently published data, we also propose a working model in which regulatory

events occurring in the cytoplasm would determine the rate of nuclear import of pre-assembling H/ACA RNPs, this way modulating both cell growth and telomerase activity.

Dyskerin: information from sequence conservation, post-transcriptional modifications and mutational hot spots

Sequence alignment of dyskerins from various organisms reveals presence of highly conserved regions that mirrors their functional conservation. This aspect was directly attested by swapping experiments, which showed that Drosophila and rat dyskerin were both able to rescue yeast *Cbf5* mutations (Phillips et al., 1998; Yang et al., 2000).

Sequence analysis in the Pfam databank (http://pfam.sanger.ac.uk/ accession O60832) identifies at least three well-preserved functional domains: the Dyskerin-like domain (DKLD; 48-106 aa) so far with an unknown function, but typical of this protein family; the TruB_N pseudouridine synthase catalytic domain, that includes the active site (110-226 aa) directly involved in the pseudouridylation process, and the PUA RNA binding domain (297-370 aa), involved in recognition of RNAs of the H/ACA family (Figure 2A). In addition, most metazoan homolog proteins exhibit two nuclear localization signals (NLSs, identified as lysine rich sequences), localized respectively at the N- and C- termini, that are thought to ensure the typical nucleolar localization. Looking at protein sequences, the main points of divergence observed between eukaryal and archaeal dyskerins lie at N- and C-termini, where eukaryal proteins exhibit typical extensions (Figure 2B, and C). Intriguingly, we noticed that the length of the N-terminal extension is significantly increased in metazoans, in which a conserved block of about 30 aa (2–34 in humans), absent from the yeast protein, is clearly recognizable (Figure 2B). The possibility that this tract might play a regulative, although still undefined, function is reinforced by the observation that it is subjected to two post-transcriptional modifications, i.e., K16 sumoylation and S21 phosphorylation (Figure 2B). The uneven distribution of X-DC pathogenic mutations also argues for the functional relevance of dyskerin N-terminus. In fact, most mutations found in patients do not cluster at the catalytic domain, but instead concentrate at the PUA RNA binding domain and at the N-extension (Figure 2A) absent in archaeal proteins. Furthermore, archaeal and eukaryal N-termini cannot be unambiguously aligned, and when *Pyrococcus furiosus* (1–19 aa) and *Saccharomyces cerevisiae* (1–32 aa) crystal structures were superimposed, they assumed a different fold, supporting the view that they play different roles (Li et al., 2011). Despite these strong indications, poor functional information is so far available on

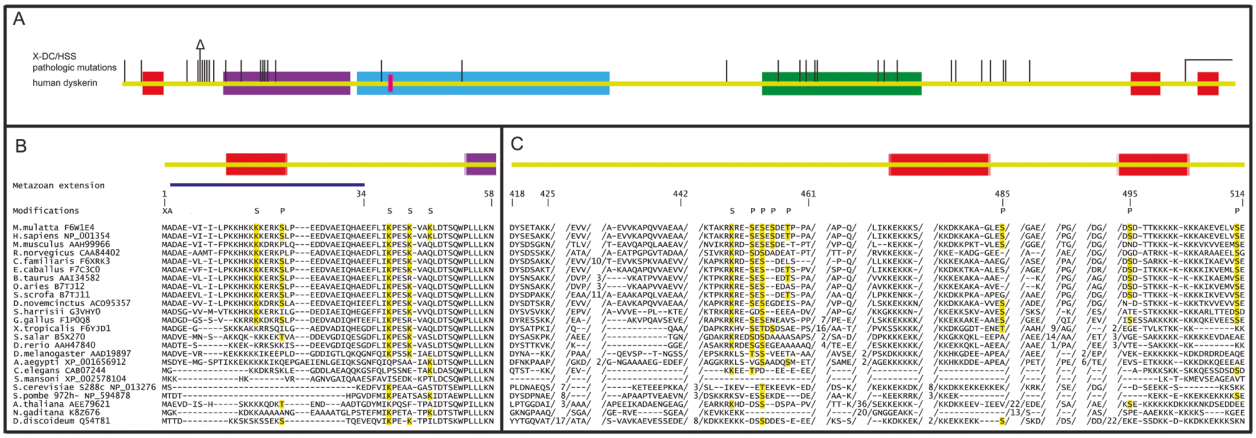

Figure 2 Dyskerin structure and sequence conservation.
(A) Overall organization of dyskerin functional domains. N- and C- terminal red boxes represent lysine-arginine rich NLSs; the DKCLD domain is purple, the TruB_N domain in blue, and the PUA domain in green; the pink rod within the TruB_N domain marks the catalytic aspartic acid residue. Position of currently annotated X-DC and Hoyeraal-Hreidarsson syndrome (HHS) pathological mutations is depicted; vertical lines rising from protein structure (|) correspond to missense mutations, the triangle (Δ) marks the p.Leu37 in-frame deletion, while (Γ) indicates the p.Asp493ValfsX12 deletion. (B,C) Sequence conservation analysis of the N- (B) and C-terminal (C) regions of human dyskerin; the multiple sequence alignments were obtained by a T-Coffee algorithm; residues subjected to post-translational modifications are indicated above the alignments and their position is referred to the human protein. X stands for elimination, A for N-acetylation, S for sumoylation, P for phosphorylation; putatively conserved sites are highlighted in yellow. Archaeal sequences cannot be unambiguously aligned at these two terminal regions.

this basic region, which is generally thought to play the unique role of acting synergically with the C-terminal NLS to ensure the dyskerin nucleolar localization.

The C-terminal extension (390–514 in humans) lacking in archaea is extremely varied in length and sequence among eukaryotes (Figure 2C). Biological relevance of this region is supported by presence of a bipartite NLS and of several potentially modified residues (see Figure 2C), as well as by a large bulk of published data. Firstly, earlier work on yeast indicated that deletion of the Cbf5p C-terminal basic domain lead to a delay at the G2/M phase, suggesting that this region may be linked to cell cycle control (Jiang et al., 1993). Secondly, a deletion of the terminal part of the last exon causes X-DC in some patients (Vulliamy et al., 1999), while a small deletion covering only the last *DKC1* exon proved to be lethal in knock-out mice experiments (He et al., 2002), confirming that this region is biologically relevant also in mammals. Thirdly, alternative truncated dyskerin isoforms lacking variable tracts of the C-terminal region have been identified in Drosophila (Riccardo et al., 2007) and in several human tissues and cell lines (Angrisani et al., 2011; Turano et al., 2013). One of these alternative isoforms (isoform 3) includes the catalytic and the PUA domains, but lacks the C-terminal NLS and shows a prevalent cytoplasmic localization. Based on its structure and localization, we suggested that this variant dyskerin might favour the transport of pre-ribosomal structures from the nucleus to the cytoplasm, and/or possibly influence translation by contacting ribosomes or cytoplasmic mRNAs (Angrisani et al., 2011). Some hints about the possible roles played by this isoform derive from the effects triggered by its over-expression, which included increased growth rate, changes in cell morphology and increase of cell-cell and cell-substratum adhesion (Angrisani et al., 2011). In keeping with these observations, a role for dyskerin in cell morphology and adhesion was already reported in human cells (Sieron et al., 2009; Alawi and Lin, 2011) and in Drosophila (Tortoriello et al., 2010). Other short isoforms devoid not only of the C-terminal region, but also of the PUA domain, have recently been described (Turano et al., 2013), and the possibility that they can play yet undescribed functions remains to be investigated.

An obvious way to finely regulate dyskerin functionality might be based on its post-translational modification. Looking at this aspect, it is worth noting that all modifications annotated so far by high-throughput mass spectrometry (MS) experiments (2013_9 update, The UniProt Consortium 2013; http://www.uniprot.org/ accession O60832) reside at the N-and C-terminal extensions that are absent from archaeal counterparts. These modifications show a different degree of phylogenetic conservation, with the elimination of initiator methionine and N-acetylation of residue 2 (alanine in Euteleostomi) characteristic of eukaryota, with a few exceptions in unicellular organisms, and phosphorylation of serines 21, 451, 453, 455, 485, 494, 513 and of threonine 458, and sumoylation of lysines 16, 39, 46 and 448 evolutively preserved at variable degree (see Table 1). For example, sumoylation at K39 appears to be potentially conserved in all eukaryotes, while that at K46 should be restricted to Catarrhini old world monkeys. Worth noting, conservation analysis of phosphorylated residues (Table 1) is weakened by the absence of known effector kinases and is mainly based on multiple sequence alignment, and remains an aspect that needs to be investigated in more detail. For example, even if no specific function has been attributed so far to any phosphorylation event, it is interesting to note that three of them (at Ser 21, 485 and 494) are reported to occur specifically at mitosis, and might thus be related to cell proliferation. More detailed functional information is presently available for sumoylation, which could be relevant for both localization and assembly of the protein. Modification of dyskerin by SUMO1 and SUMO2/3, firstly revealed by high-throughput MS experiments at four residues (Manza et al., 2004; Blomster et al., 2009; Westman et al., 2010), has

Table 1 Evolutive conservation of modified residues of human dyskerin.

Amino acid[a]	Modification[b]	Phylogenetic conservation
M1	Elimination	Eukaryota
A2	N-acetylation	Eukaryota
K16	Sumoylation	Amniota
S21	Phosphorylation	Amniota
K39	Sumoylation	Eukaryota
K43	Sumoylation	Eutelostomi
K46	Sumoylation	Catarrhini
K448	Sumoylation	Eutelostomi
S451	Phosphorylation	Eutelostomi and Ecdysozoa
S453	Phosphorylation	Eukaryota
S455	Phosphorylation	Euarchontoglires
T458	Phosphorylation	Euarchontoglires
S485	Phosphorylation	Theria
S494	Phosphorylation	Euarchontoglires and Laurasiatheria
S513	Phosphorylation	Theria

[a]Amino acid residues are numbered respect to sequence of human dyskerin.

[b]Sumoylation was considered conserved when the minimal consensus sequence (KXE/D) was detected in the multiple sequence alignment. Phosphorylation was considered conserved when an S/T occupied the same position in the multiple sequence alignment, given that no information about effectors kinases is available and no consensus sequence is applicable.

recently been directly confirmed by Brault et al. (2013). These authors also provided a direct correlation between pathologic mutations and sumoylation defects. It was not only lack of sumoylation on residues mutated in X-DC patients was shown to reduce protein stability, but the K39R mutation could be rescued by a chimeric SUMO3-dyskerin product in which this modification was mimicked, demonstrating its fundamental effect on dyskerin functionality. Overall, the ensemble of potential modifications outlines a complex dyskerin post-translational regulation that has been so far mostly ignored, despite the fact that it could largely contribute to modulate its activity and its interaction properties. Finally, the fact that the C-terminal moiety deleted in dyskerin shorter isoforms is particularly rich in putative phosphorylation sites might furnish them a further distinctive trait, raising the possibility that they can be regulated differently in response to growth conditions, or during the cell cycle. Differential expression during the cell cycle may be biologically significant especially because, despite the ubiquity of dyskerin, X-DC symptoms are essentially restricted to highly proliferative tissues, such as epithelia and bone marrow. Analysis of the expression of dyskerin and its variant isoforms in resting or actively dividing cells, definition of their phosphorylation and sumoylation status, stability, nuclear localization and/or retention in different growth conditions or cell types represent a central issue that would deserve further investigation.

The level of accumulation of unmutated dyskerin is crucial for X-DC manifestation

Several lines of evidence from different organisms or different mammalian cell lines support the existence of a direct relationship between the amount of unmutated dyskerin and the efficiency of rRNA processing, RNA pseudouridylation, and telomere shortening. This direct dose-effect relationship was firstly outlined in both yeast and Drosophila systems (Cadwell et al., 1997; Giordano et al., 1999; Zebarjadian et al., 1999). Subsequently, an X-DC patient carrying a promoter mutation that affected expression of dyskerin rather than its amino acid sequence was identified (Knight et al., 1999; Salowsky et al., 2002). More recently, by analysing an X-linked pedigree presenting familial pulmonary fibrosis, a symptom showed by 20% of X-DC patients, Parry et al. (2011) found that affected males had short telomeres and reduced levels of both TERC and unmutated dyskerin. The authors suggested that a low dyskerin level, in the absence of any coding mutation, can itself be a cause of the disorder. A large number of experiments based on *DKC1* silencing or knock-down, whether in cultured cells or transgenic model organisms, further supports this view. Collectively, these data pose a crucial question: is the loss of the catalytic activity of dyskerin or the dose of the protein the main cause of X-DC typical defects? Are X-DC pathological mutations acting qualitatively or also quantitatively? In the latter case, any parameter affecting protein accumulation and stability may be critical. The answer to these questions might be relevant to understanding the molecular mechanisms underlying X-DC pathogenesis, as despite their apparent diversity the ensemble of affected processes could all be related to a unique dyskerin ability to ensure sufficient synthesis or steady-state levels of H/ACA RNAs, including TERC. According to this view, several dyskerin mutations were found to affect steady-state TERC levels and not the functionality of the telomerase complex (Zeng et al., 2012). In keeping with previous observations, these results outlined a rate-limiting role for dyskerin in telomerase activity. In turn, the general role of dyskerin in ensuring biogenesis and stability of H/ACA snoRNAs might mediate a wide range of different outcomes (Figure 3). For example, rRNA processing may be affected by reduced levels of snoRNAs

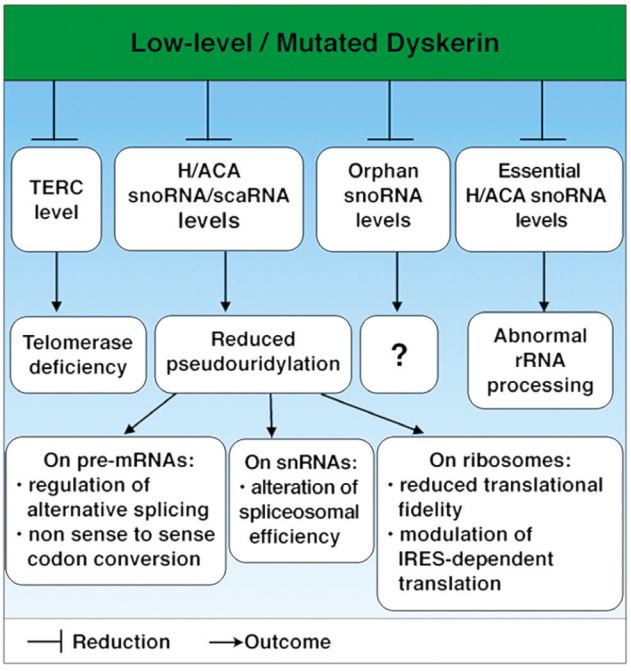

Figure 3 Schematic overview of the variety of effects potentially triggered by dyskerin malfunction.
Loss-of-function mutation and *DKC1* gene silencing both cause reduced levels of TERC and H/ACA sno/scaRNAs, as they are able to trigger the variety of the different outcomes described in recent years.

essential for its maturation, while reduced pseudouridylation can be a consequence not only of loss of dyskerin catalytic activity, but also of low levels of guide snoRNAs, and a variety of different effects could derive from altered levels of snoRNA smaller processed fragments. Intriguingly, a yet unexplained degree of complexity is generated by the observation that the stability of different H/ACA RNAs can be differentially affected by distinct *DKC1* mutations or by *DKC1* silencing (Mochizuki et al., 2004; Alawi and Lin, 2010; Ge et al., 2010; Bellodi et al., 2013); this differential effect extends also to snoRNA-derived miRNA-like molecules (Alawi and Lin, 2010). Although the physiological consequences are presently unknown, it is plausible that some features of X-DC may be related to the functional roles played by these processed molecules.

Finally, *DKC1* harbours two intronic H/ACA snoRNAs (SNORA36A and SNORA56), both of which are involved in rRNA pseudouridylation; moreover, SNORA56 acts as a miRNA precursor (Ender et al., 2008). Although generally overlooked, this coding/non-coding structure, which is shared with its Drosophila orthologue (Riccardo et al., 2007), suggests that the ratio between its proteinaceous or ncRNA products may also play a role on overall gene functionality.

Pseudouridylation: a flexible mechanism to modulate gene expression

Pseudouridylation represents the most abundant type of RNA modification occurring in eukaryotic cells, but its specific roles have only been closely addressed in recent years. Because pseudouridines promote base stacking interactions and acquire chemical properties that make them able to form hydrogen bridges with bases other than adenine, their presence on RNA facilitates base-pairing, influences folding and increases duplex stability (Davis, 1995). All these parameters can logically have a strong impact on both activity and potential interactions of target RNAs. Given that most common targets of pseudouridylation are stable RNAs that play key roles in basic cellular processes such as rRNAs and snRNAs, where pseudouridylated residues are often found at highly conserved functional positions (reviewed by Maden, 1990; Yu et al., 2011; Ge and Yu, 2013), it was predictable that isomerisation of uridines into pseudouridines could modulate gene expression in a variety of ways. As concerning ribosome structure, it was earlier suggested that this modification not only contributed to rRNA folding and ribosomal subunit assembly, but could also influence translation efficiency and codon recognition (Luzzatto and Karadimitris, 1998). Not surprisingly, these predictions have largely been verified in the last decade, as detailed studies on cells in which dyskerin activity was reduced, either by mutations or by specific gene silencing, demonstrated experimentally most of the evoked effects. In 2006, Yoon et al. revealed for the first time that *DKC1* mutations impaired translation from internal ribosome entry sites (IRESs) of specific cellular mRNAs, such as those encoding the apoptotic protein p27 and the antiapoptotic factors XIAP and Bcl-2. The authors suggested that the level of rRNA pseudouridylation could influence the ability of the ribosome to recognize highly structured IRESs, a fundamental step for cap-independent translation. Although active also in physiological conditions, IRES-dependent translation has a key role in the response to apoptotic stimuli and in cell cycle phases, when cap-dependent translation is reduced (i.e., G_0/G_1 phases). Under-pseudouridylated ribosomes were supposed to affect the ratio between antiapoptotic and proapoptotic factors at the translational level, and this could be one of the causes of bone marrow failure and tumour susceptibility in X-DC patients (Yoon et al., 2006). This conclusion was subsequently supported by the findings that reduced ribosome pseudouridylation, attributed to either *DKC1* pathologic mutations or reduced dyskerin level, downregulates IRES-mediated translation of p27 and p53 tumour suppressor genes (Bellodi et al., 2010; Montanaro et al., 2010). Further information was recently provided by Rocchi et al. (2013), who assayed the translation efficiency of a pool of viral and cellular IRESs in *DKC1* silenced breast cancer cell lines. These authors observed that p53 and CrPV IRES-mediated translation were reduced, while c-myc, HCV and EMCV IRES-dependent translation were unaffected. Furthermore, VEGF and HSP70 IRES-mediated translation were upregulated. These results lead to the conclusion that the level of ribosome pseudouridylation can differently modulate IRES-dependent translation: expression of some specific mRNAs could be repressed, while that of others could be either unaffected or upregulated. In addition, to modulate IRES-dependent translation the level of ribosome pseudouridylation can trigger additional and unpredicted effects. In fact, it reduces the binding affinity of aminoacyl-tRNA at both A and P sites, generates translation frameshift, and leads to an increase in the recognition of *in-frame* stop codons. These effects are conserved from yeast to humans, and result in a decrease of translational fidelity (Jack et al., 2011). It is worth noting that effects of reduced pseudouridylation are not limited

to rRNA, as spliceosomal snRNAs also represent common targets. Pseudouridylation of snRNAs, which occurs in the Cajal bodies, proved to be crucial for both spliceosomal assembly and mRNA splicing in different organisms as yeast, Xenopus and mammals (reviewed by Wu et al., 2011). Given the significant impact that snRNA pseudouridylation can exert on splicing, it is particularly intriguing that yeast U2 snRNA was found to be inducibly pseudouridylated at two new sites upon stress conditions (Wu et al., 2011). After this finding, the possibility that pseudouridylation may represent a flexible mechanism able to modulate RNA function in response to cellular signals will be seriously considered. Further relevance to this issue is added by several lines of evidence that revealed the potential effects of this modification on target pre-mRNAs. Pseudouridylation of these molecules has in fact been shown to influence the choice of alternative splice sites or change their coding properties. First evidence of these regulatory effects was reported by Chen et al. (2010), who showed that conversion of specific uridines within the pyrimidine tracts of adenovirus pre-mRNA, or β-globin pre-mRNA, had a negative effect on splicing. Pseudouridylation at specific sites increased the rigidity of the polypyrimidine tract backbone, which in turn reduced the binding of the U2AF essential splicing factor. Subsequently, Karijolich and Yu (2011) reported that pseudouridylation of nonsense codons, either inserted *in vitro* within an artificial mRNA, or modified by artificial H/ACA guide RNAs, converted them into sense codons. Hence, pseudouridylation can change the coding properties of mRNAs, generating protein diversity. Altogether, these data indicate that this widespread RNA modification can regulate gene expression at different levels and in different ways (see Figure 3).

Dyskerin and cancer: an intimate but contradictory connection

In 1992, Dokal et al. observed that primary skin fibroblast cultures derived from DC patients were abnormal both in morphology and growth rate (doubling time about twice the normal) compared to control cells. Since then, many papers have highlighted that dyskerin deficiency perturbs cell cycle progression and proliferation. In particular, a G2/M arrest has been observed in yeast cells with mutated *Cbf5* (Jiang et al., 1993), in transformed dyskerin-depleted cells (Alawi and Lin, 2011, 2013), in fibroblasts from X-DC patients (Carrillo et al., 2013), and in mouse embryonic fibroblasts expressing only catalytically inactive dyskerin (Gu et al., 2013). Nonetheless, cancer susceptibility represents a main characteristic of X-DC, with head and neck squamous cell carcinomas most frequently observed, followed by skin and anorectal cancer. Cumulatively, the incidence of cancer in X-DC patients was reported to be around 40–50% by the age of 50 years (Alter et al., 2009). Considering the functions played by dyskerin as component of H/ACA snoRNPs and telomerase, its deficiency was expected to limit the proliferative capacity of cells, thus making the tumour predisposition observed in the patients difficult to understand. When this aspect was studied in *DKC1* hypomorphic mice (*Dkc1*^{m}), increased susceptibility to tumour formation was observed in first and second generations. Because in these mice rRNA pseudouridylation was significantly reduced, while defects in telomere length were not yet evident (Ruggero et al., 2003), this observation firstly suggested the existence of a link between deregulated rRNA modification and tumour formation. This view was further supported by the subsequent finding that, as reported above, under-pseudouridylated ribosomes affect translation of a subset of IRES-containing mRNAs that have a key role in cancer (Yoon et al., 2006; Bellodi et al., 2010; Montanaro et al., 2010; Rocchi et al., 2013). By altering the balance between pro- and anti-apoptotic factors, the degree of rRNA pseudouridylation can thus promote neoplastic susceptibility in X-DC cells. Worth noting is that dyskerin deficiency may contribute to tumorigenesis also by altering the splicing of specific mRNAs, or by modulating the level of certain snoRNAs. Indeed, fluctuations in the levels of several snoRNAs have been recently observed in various types of cancers, establishing an unexpected link between deregulated expression of these molecules and both cell proliferation and stress response (reviewed by Taulli and Pandolfi, 2012).

Looking at sporadic cancers, we noted that 38 additional *DKC1* mutations (25 missense, 5 nonsense, 1 in-frame deletion and 7 synonymous) have been identified (complete list on the COSMIC database, Forbes et al., 2011). It is noteworthy that none of these mutations corresponds to those found in X-DC patients (reference list was taken from the NCBI Gene Review), but a few of them fall just beside (see Table 2). However, due to the complex background of cancer cells, it is not easy to predict if and how these mutations can affect gene functions. It is also worth noting that dyskerin over-expression has been observed in several cancers, including colorectal cancer (Turano et al., 2008; Witkowska et al., 2010), breast cancer (Montanaro et al., 2006, 2008) prostate cancer (Sieron et al., 2009), ovarian carcinoma (Schaner et al., 2003), melanoma (McDonald et al., 2004), neuroblastoma (Westermann et al., 2007; von Stedingk et al., 2013), lymphoma

Q2: "Alter 2009" has been changed to "Alter et al. 2009" to match with reference list. Please check and confirm

Table 2 List of *DKC1* somatic mutations detected in sporadic cancers lying beside X-DC pathologic mutations.

X-DC mutations		Cancer mutations	
Nucleotide	**Amino acid**	**Nucleotide**	**Amino acid**
c.29C→T	p.Pro10Leu	c.39T→G	p.H13Q
c.91C→G	p.Gln31Glu	c.90A→G	p.I30M
c.91C→A	p.Gln31Lys		
c.214_215CT→TA	p.Leu72Tyr	c.217G→T	p.A73S
c.361A→G	p.Ser121Gly	c.358C→A	p.H120N
c.965G→A	p.Arg322Gln	c.971A→G	p.E324G

(Piva et al., 2006), and hepatocellular carcinoma (Liu et al., 2012), suggesting that it may be an important signature of the increased rate of growth and proliferation typical of cancer cells. In effect, several reports pointed out a significant correlation between increased dyskerin level and high clinical stage (Montanaro et al., 2006; Sieron et al., 2009; Witkowska et al., 2010; Liu et al., 2012), suggesting that the amount of the protein could be used as a prognostic marker, at least in some tumours. For example, high levels of dyskerin, GAR1 and NHP2 have independently been identified as top predictors of poor prognosis in neuroblastoma, and concerted high-level expression of these three proteins composes a 'SnoRNP signature' with a high prognostic value for progression of this tumour (von Stedingk et al., 2013). By analogy with the model recently proposed for telomerase loss and reactivation during progression of prostate cancer and T cell lymphoma (Ding et al., 2012; Hu et al., 2012), von Stedingk et al. (2013) suggested that cells having a low-level expression of these three H/ACA RNP components may undergo genetic alterations and instability, accompanied by telomere dysfunction. These conditions would characterize early pre-clinical stages of tumour development. In keeping with this model, dyskerin co-purifies with spindle extracts (Sauer et al., 2005; Dephoure et al., 2008), and its loss leads to genetic instability (Kirwan and Dokal, 2008) accompanied by accumulation of atypical mitoses with multipolar spindles (Alawi and Lin, 2011; Alawi and Lin, 2013). At subsequent stages of tumour development, over-expression of H/ACA RNP components, coupled with telomerase reactivation, would overcome the block of cell proliferation due to apoptosis or abortive mitosis, thus favouring tumour progression. In this prospect, high-level expression of dyskerin, GAR1 and NHP2 would sustain telomerase activity and reduce genetic instability, stabilizing advanced tumours and favouring their aggressiveness. Although the precise mechanisms underlying dyskerin over-expression in tumour progression remains to be fully defined, this model could nicely explain the puzzling predisposition to cancer typical of X-DC patients.

Dyskerin and stemness maintenance

Bone marrow failure and stem cell deficiency are important consequences of X-DC progression, and both features are thought to be caused primarily by telomerase deficiency and reduced TERC levels. While in most somatic cells the telomerase holoenzyme is inactive, in stem cells the complex is functioning, so that it is plausible that these cells are more sensitive to its deficiency. Furthermore, high levels of telomerase activity and ribosome biogenesis are required to sustain growth and proliferation of stem or progenitor cells, making dyskerin loss or malfunction more detrimental. According to this view, tissues characterized by high proliferation rate and constant renewal (e.g., skin, blood, gut) are those preferentially suffering progressive telomere shortening and dyskerin malfunction. Not surprisingly, attempts to induce pluripotent stem cells (iPSCs) from fibroblasts of X-DC patients were characterized by a poor reprogramming efficiency, which increased upon exogenous over-expression of TERC and TERT (Agarwal et al., 2010; Batista et al., 2011; Zeng et al., 2012). Cell reprogramming was also increased by lowering oxygen concentration (Batista et al., 2011), suggesting a link between oxidative stress and dyskerin malfunction. Such a relationship was also described in mice, where X-DC symptoms were found to be attenuated by antioxidant treatment (Gu et al., 2011). Nonetheless, proliferative capacity of *DKC1* mutant iPSCs was also observed in normal oxygen concentration and in the absence of exogenous TERC and TERT over-expression. In a first study, self-renewal was observed until passage 26, and correlated with robust endogenous induction of TERC and TERT (Agarwal et al., 2010). In a second approach, TERT and TERC induction was low compared with wild type iPSCs, and telomerase activity remained weak. Nonetheless, one of these iPSC clones reached passage 36, but subsequent culture was impeded by the inability of cells to retain the undifferentiated state (Batista et al., 2011). Although these disparities may depend on several aspects that can include clonal variability, different levels of induction of telomerase complex endogenous components, or heterogeneity of iPSC culture, more efforts remain to be made to define the standardized growth conditions that allow indefinite propagation of *DKC1* mutant iPSCs. Tuning these conditions would permit to investigate the effects

triggered by *DKC1* mutations on rRNA maturation, RNA modification, and IRES-mediated translation specifically in the stem cell compartment. These aspects, not yet investigated in these cell types, can provide new insights on X-DC pathogenesis. Indeed, relevant information coming from iPSCs studies concerns the identification of a direct link between stemness factors and *DKC1* regulation. In fact, *DKC1* was found upregulated in iPSCs respect to parental fibroblasts, and the Nanog and Oct4 stemness factors were found to bind its promoter. The finding that both *DKC1* and telomerase upregulation are typical of the pluripotent state of ES cells (Agarwal et al., 2010) raises the possibility that both dyskerin and telomerase expression levels can be rate-limiting for stemness maintenance.

The hidden side of multifaced H/ACA RNP biogenesis

Structure of H/ACA snoRNPs has firstly been delineated by X-ray analysis of archaeal crystallized complexes, whose results lead to propose a three-dimensional structural model in which the snoRNA is directly bound not only by dyskerin, but also by NHP2 and NOP10 proteins (Li and Ye, 2006; Rashid et al., 2006). By adapting this model to human dyskerin, it was noticed that most pathologic mutations mapped at N- and C-terminal extensions, despite being remote in the primary sequence, were predicted to fold in proximity of the PUA domain. This observation suggested that these residues, all missing in the archaeal proteins, might influence the PUA binding properties (Rashid et al., 2006). The crystal structure of reconstituted yeast H/ACA RNPs confirmed a three-dimensional model in which a composite surface formed by a dyskerin-NHP2-NOP10 heterotrimer participates in snoRNA binding, with the fourth core component, GAR1, contacting only dyskerin (Li et al., 2011). These structural data, in keeping with a variety of molecular approaches, lead to draw a clearer picture on the organization, assembly and functional properties of H/ACA RNPs. It is now ascertained that, although these mature complexes localize at nucleoli or Cajal bodies, their assembly is a multistep process that includes events occurring at the sites of RNA transcription (Darzacq et al., 2006; Richard et al., 2006). Nascent H/ACA sno/scaRNAs are mainly intronic, and associate with the dyskerin-NOP10-NHP2 trimer cotranscriptionally, before the host intron is spliced out from the primary transcript. Although each component of the trimer contacts directly the snoRNA, the only association with dyskerin is precocious and irreversible, and probably requires *de novo* synthesis of the recruited RNA (Richard et al., 2006). Association of other core components occurs later and appears to be weaker, as, differently from dyskerin, they can be interchanged among different snoRNPs (Kittur et al., 2006). Not surprisingly, assembly of eukaryotic H/ACA RNPs is emerging as an intricate and presumably finely regulated process. Crucial regulatory functions are played by two essential factors, NAF1 and SHQ1 (Fatica et al., 2002; Yang et al., 2002), which are conserved from yeast to mammals but absent in archaea. These factors regulate the efficiency of H/ACA RNP biogenesis, but do not associate to the mature active complexes (Yang et al., 2005; Darzacq et al., 2006; Hoareau-Aveilla et al., 2006; Rashid et al., 2006; Leulliot et al., 2007; Grozdanov et al., 2009a). NAF1 depletion has been associated to defective rRNA processing and reduced accumulation of H/ACA RNP components, including dyskerin and snoRNAs, in both yeast (Dez et al., 2002; Fatica et al., 2002; Yang et al., 2002) and human cells, where accumulation of TERC was also found affected (Hoareau-Aveilla et al., 2006). Through a homologous domain, NAF1 contacts directly dyskerin at the same GAR1 site (Leulliot et al., 2007) and it is thought to act as a chaperone, by safeguarding dyskerin until it associates to mature snoRNPs (Yang et al., 2002; Hoareau-Aveilla et al., 2006). NAF1 localizes at snoRNA/scaRNA transcription sites and participates in the early steps of RNPs assembling, but it is absent from the fully mature complexes localized in nucleoli and Cajal bodies. Its participation in snoRNPs is thus transient, and during snoRNP maturation NAF1 is displaced by GAR1 that, vice versa, is absent from snoRNA transcription sites and associates to the assembled complexes only at later stages (Ballarino et al., 2005; Yang et al., 2005; Darzacq et al., 2006; Leulliot et al., 2007). It is worth noting that NAF1 presents a canonical NLS and shuttles between the nucleus and the cytoplasm but, when over-expressed, it accumulates mostly in the cytoplasm (Kittur et al., 2006). This dynamics suggests a possible role not only in the assembly, but also in the nuclear import of H/ACA RNPs.

The specific function of the other regulatory factor, SHQ1, is presently unclear. In yeast cells, this protein associates to Naf1p and dyskerin, either alone or bound to Nop10p, and its depletion lead to defects in RNA processing, snoRNA accumulation and cell growth (Yang et al., 2002). Purified yeast Shq1p retains the ability to bind directly dyskerin, and this interaction is unaffected by addition of either Naf1p or snoRNP core proteins (Li et al., 2011). Identification of critical regions required for Shq1p binding has been approached by structural studies of Shq1p-dyskerin (Walbott et al., 2011) and Shq1p-dyskerin-Nop10p-Gar1p yeast crystallized

complexes (Li et al., 2011). In both cases, the contact region was found to overlap with the PUA domain, indicating that Shq1p can interfere with association of dyskerin with snoRNAs or other promiscuous cellular RNAs. It is worth noting that the dyskerin-Shq1p interface also includes part of the catalytic domain and the C-terminal extension, whose role appears relevant, since deletion of the C-terminal residues after Pro354 causes a 4-fold decrease of Shq1 binding affinity (Li et al., 2011). Moreover, many dyskerin pathogenic mutations map within this interaction surface (Grozdanov et al., 2009b; Li et al., 2011). Recently, SHQ1 has been independently isolated as an IFN-inducible gene associated with retinoid-interferon-induced mortality-1 (GRIM-1; Nallar et al., 2011), revealing an unexpected link between IFN/RA-induced growth repression and snoRNP biogenesis. Remarkably, unpredicted results were obtained by over-expressing different GRIM1/SHQ1 isoforms in HeLa cells. In contrast with results obtained in an *in vitro* reconstitution assay (Grozdanov et al., 2009a), SHQ1 was found able to associate to endogenous NAF1, as it was observed in yeast. However, this association displaced NAF1 from the nucleus, pushing this factor to accumulate in the cytoplasmic perinuclear region (Nallar et al., 2011). Consistent with this outcome, GRIM1/SHQ1 over-expression caused downregulation of some tested H/ACA snoRNAs, including TERC, and repressed rRNA processing. In keeping with these results, GRIM1/SHQ1 silencing reversed these effects, and both snoRNA accumulation and rRNA processing were favoured. These results were opposite to those obtained in yeast, as the level of GRIM1/SHQ1 expression correlated directly with detrimental effects on ribosome biogenesis, telomere stability and cell growth. Consequently, a negative regulatory role on H/ACA snoRNP biogenesis emerged for this factor. In keeping with this picture, GRIM1/SHQ1 expression is lost or reduced in 75% of prostate tumours, indicating that this gene may act as tumour suppressor (Nallar et al., 2011). After these results, a crucial question arose: is the GRIM1/SHQ1 regulatory role conserved between yeast and higher eukaryotes? Looking at the intricate picture of H/ACA snoRNP biogenesis, we find it particularly interesting that NAF1 and GRIM1/SHQ1 do not show a strict nuclear localization and, if over-expressed, both accumulate mostly in the cytoplasm (Kittur et al., 2006; Grozdanov et al., 2009a; Nallar et al., 2011). Further indications that key regulatory events on snoRNP biogenesis might occur in the cytoplasm derived from identification of dyskerin isoform 3, which lacks a C-terminal tract of dyskerin (94 aa) that includes the NLS, and localizes in the cytosol (Angrisani et al., 2011).

Q3: "Grodzanov et al., 2009a" has been changed to "Grozdanov et al., 2009a" to match with reference list. Please check and confirm

A new regulatory model for H/ACA RNP assembly

Based on the bulk of presently available data, we propose a hypothetical 'cytoplasmic assembly regulation' (CAR) model for H/ACA snoRNP biogenesis, with the aim of conciliating the contrast emerging from the different role played by SHQ1 in yeast and human cells. According to this model, the nuclear import of H/ACA RNP complexes is identified as a key regulatory step of their biogenesis, and its dynamics are predicted to be finely controlled in the cytoplasm. The model, depicted in Figure 4, predicts that two types of cytosolic tetrameric complex are assembled in human cells: in the first type (type 1), dyskerin-NOP10-NHP2 are assembled with a yet unidentified mammalian-specific factor (MSF), present in these cells but absent in yeast, whose function would be binding and blocking the PUA domain; in a second type (type 2), dyskerin-NOP10-NHP2- are assembled with SHQ1. At the perinuclear region, NAF1 would join transiently to both types of complexes to promote, synergistically with dyskerin, their nuclear import. A crucial point of the model is that, considering the lack of NLS and its prevalent cytoplasmic localization, SHQ1 would act as a 'dead weight', hindering and making more energy-consuming the nuclear translocation of type 2 complexes. Conversely, nuclear import of type 1 complexes is assumed to be facilitated, being more efficient and/or less energy-consuming. The key point of the regulation would be the balance between the two types of assembled complexes: if formation of type 1 is favoured, cell growth is promoted. To this regard, we noted that NAF1 is abundant and expressed at significantly higher levels than SHQ1 in human cells (http://www.proteinatlas.org/, NAF1 ENSG00000145414 and SHQ1 ENSG00000144736, Uhlen et al., 2010). This observation is consistent with the view that, in the absence of inductive signals, SHQ1 expression is maintained low. In the same database, we also noticed that in squamous epithelia (e.g., oesophagus, vagina, oral mucosa) NAF1 nuclear accumulation inversely correlates with SHQ1 expression, with the latter excluded from the basal proliferating layer. Moreover, SHQ1 is undetectable in bone marrow hematopoietic cells. These data testified a low-level SHQ1 expression in proliferating progenitor cells, and fully support a negative regulatory role on cell proliferation, as proposed by Nallar et al. (2011). Finally, it is worth noting that nuclear import of the dyskerin-NOP10-NHP2 trimer, which is also part of the telomerase holoenzyme, should have a similar impact on snoRNP biogenesis and telomerase activity, and would thus represent a common step in the regulation of these two nuclear

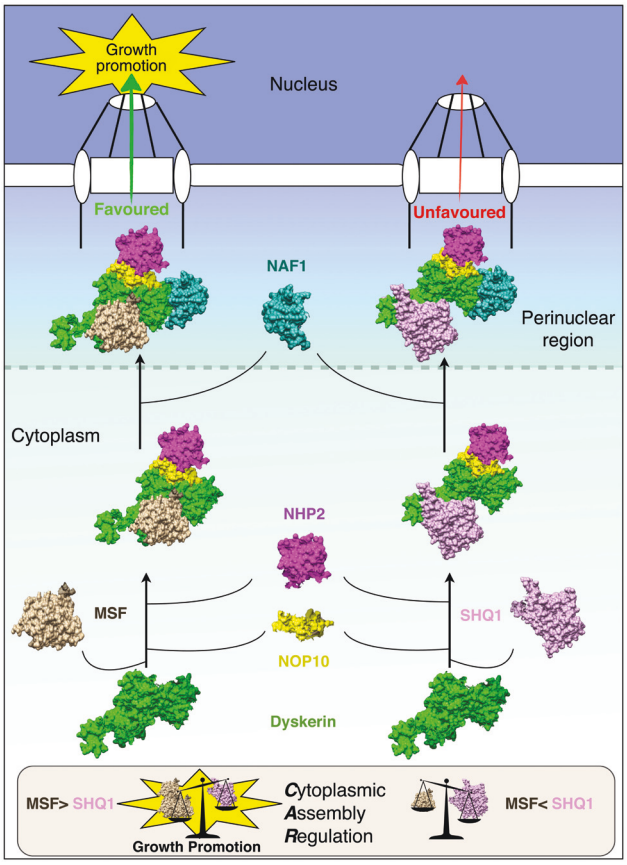

Figure 4 The Cytoplasmic assembly regulatory (CAR) model for H/ACA RNP assembly and nuclear import.
In this speculative model, newly synthesized dyskerin, the PUA domain is supposed to be quickly bound by either the SHQ1assembly factor (right), or by a still unidentified mammalian-specific factor (MSF), that might also correspond to mammalian-specific dyskerin extensions able to encircle and mask it. When NOP10 and NHP2 proteins are added, two types of tetrameric complexes are formed and move to the perinuclear region, where they are both bound by the NAF1 shuttling factor. However, the two complexes are predicted to be imported at different efficiencies, with nuclear translocation of MSF-containing complexes expected to be favoured respect to SHQ1-containing complexes. A key regulatory point would then be the ratio of cellular MSF/SHQ1-containing complexes, with the first complex acting in growth-promotion and the second in growth suppression.

complexes. As concerning yeast cells, the model predicts that, in the absence of MSF, only type 2 complexes would be formed; consequently, H/ACA snoRNP biogenesis would be directly dependent on the amount of SHQ1, thus explaining the opposite role played by this factor in unicellular eukaryotes. In this view, the evolution in mammalian cells of a competing factor able to bind the PUA domain would have reversed the growth-promoting role originally played by SHQ1 in yeast. Notably, it is plausible that the role attributed to the MSF factor could be played by dyskerin terminal regions, whose length and sequence are significantly different between mammalian and yeast proteins (see Figure 2B and C), and whose structures are not yet fully defined. It is also to note that, with respect to yeast, a further degree of complexity to the regulation of H/ACA RNP biogenesis might be added in higher eukaryotes by increased recurrence of alternative splicing. For example, a critical regulatory role might be played in human cells by the dyskerin alternative isoform 3, whose structure prediction, obtained by using Modeler 9.12 (Sali and Blundell, 1993) and the yeast Cbf5p structure (PDB::3UAI) as template, proves to be very similar to that of the yeast protein, except for the presence of the N-terminal extension and part of the C-terminal extension (Figure 5). Although this isoform retains all sequences required for both NAF1 and SHQ1 binding, its cytoplasmic localization might mostly favour its association to SHQ1. By sequestering this factor, isoform 3 could promote cell growth, an effect that has readily been observed upon its over-expression (Angrisani et al., 2011).

According to the model, the two crucial parameters for H/ACA RNPs biogenesis would thus be: 1) the balance between the cytoplasmic levels of type1/2 complexes; 2) the levels of full-length dyskerin and its truncated alternative isoform(s). Both these parameters are expected to be dynamically and finely regulated in each cell type in response to different developmental, differentiative and stress stimuli, with all these inputs converging in the cytoplasm to be transmitted to the nucleus. Although the model fits well with all published data, focused experiments are needed to directly test its validity.

Concluding remarks

While it is ascertained that X-DC causes reduction of TERC levels and its progression correlates with telomere shortening, it is clear nowadays that the disease is also typically accompanied by defective rRNA processing, destabilization of a subset of H/ACA snoRNAs and defective RNA pseudouridylation. Collectively, these data make plausible that loss of telomere integrity can be only one of the consequences triggered by defective metabolism of H/ACA snoRNPs. As X-DC tackles hot topics in cellular biology, as functionality of the ribosome, RNA pseudouridylation, snoRNA functions and telomerase activity, all of which intimately connected with basic processes regulating cell growth and proliferation, its study could help to understand how these basic processes are coordinated and integrated with metabolic and external stimuli. A relevant issue is that dyskerin, the protein encoded by the X-DC

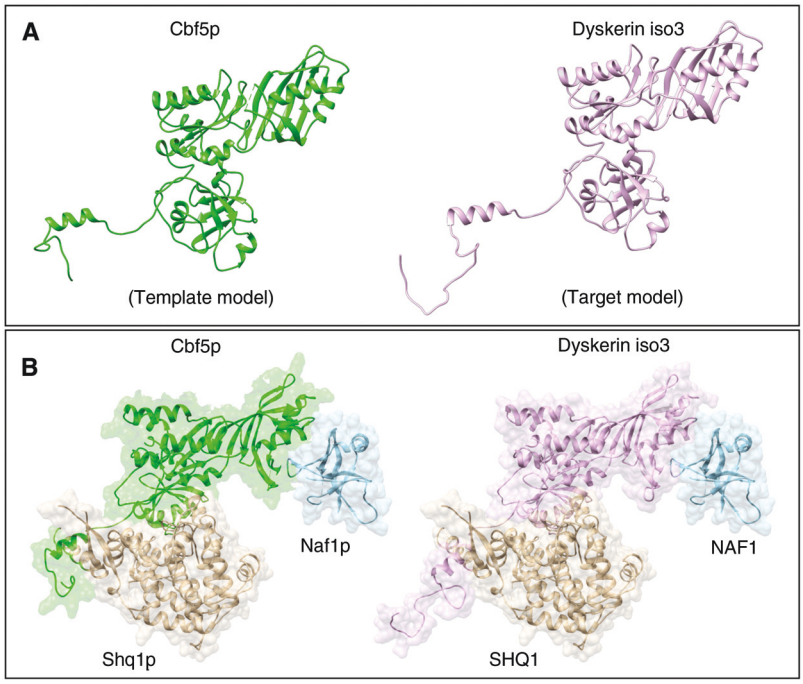

Figure 5 Structure and properties of dyskerin isoform 3.
(A) Yeast Cbf5p structure (left; accession PDB::3UAI) was utilized as a template to model human dyskerin isoform 3 (right). According to the MODELLER software, the two proteins assume a very similar structure. (B) Despite its cytoplasmic localization, isoform 3 retains the sequences known to be involved in SHQ1 and NAF1/GAR1 binding.

causal gene, exhibits ubiquitous expression, has a well-established role of tumour suppressor and is an essential component of both H/ACA snoRNPs and telomerase active holoenzyme. Nonetheless, only poor functional information is available so far on its post- translational modifications, despite the fact that they might be dynamically regulated and play a major role in modulating protein stability and activity, or influencing its participation in the different nuclear complexes. By this view, attempts to reconstitute protein interaction using *in vitro* translated proteins could give limited or biased information. Finally, emerging evidence indicates that cytoplasmic assembly and nuclear import of H/ACA pre-RNPs can be common important steps for both H/ACA sno/scaRNPs and telomerase activity, leading us to propose a model of 'cytoplasmic assembly regulation' for their biogenesis.

Acknowledgments: This work was supported by University Federico II of Naples and by P.O.R. Campania FSE 2007–2013 Project CREMe, which supported Alberto Angrisani's postdoctoral fellowship.

Received November 29, 2013; accepted January 24, 2014

References

Agarwal, S., Loh, Y.H., McLoughlin, E.M., Huang, J., Park, I.H., Miller, J.D., Huo, H., Okuka, M., Dos Reis, R.M., Loewer, S., et al. (2010). Telomere elongation in induced pluripotent stem cells from dyskeratosis congenita patients. Nature *464*, 292–296.

Alawi, F. and Lin, P. (2010). Loss of dyskerin reduces the accumulation of a subset of H/ACA snoRNA-derived miRNA. Cell Cycle *9*, 2467–2469.

Alawi, F. and Lin, P. (2011). Dyskerin is required for tumor cell growth through mechanisms that are independent of its role in telomerase and only partially related to its function in precursor rRNA processing. Mol. Carcinog. *50*, 334–345.

Alawi, F. and Lin, P. (2013). Dyskerin localizes to the mitotic apparatus and is required for orderly mitosis in human cells. PLoS One *8*, e80805.

Alter, B.P., Giri, N., Savage, S.A., and Rosenberg, P.S. (2009). Cancer in dyskeratosis congenita. Blood *113*, 6549–6557.

Angrisani, A., Turano, M., Paparo, L., Di Mauro, C., and Furia, M. (2011). A new human dyskerin isoform with cytoplasmic localization. Biochim. Biophys. Acta *1810*, 1361–1368.

Ballarino, M., Morlando, M., Pagano, F., Fatica, A., and Bozzoni, I. (2005). The cotranscriptional assembly of snoRNPs controls the biosynthesis of H/ACA snoRNAs in *Saccharomyces cerevisiae*. Mol. Cell Biol. *25*, 5396–5403.

Batista, L.F., Pech, M.F., Zhong, F.L., Nguyen, H.N., Xie, K.T., Zaug, A.J., Crary, S.M., Choi, J., Sebastiano, V., Cherry, A., et al. (2011). Telomere shortening and loss of self-renewal in dyskeratosis congenita induced pluripotent stem cells. Nature *474*, 399–402.

Bellodi, C., Krasnykh, O., Haynes, N., Theodoropoulou, M., Peng, G., Montanaro, L., and Ruggero, D. (2010). Loss of function of the tumor suppressor DKC1 perturbs p27 translation control and contributes to pituitary tumorigenesis. Cancer Res. *70*, 6026–6035.

Bellodi, C., McMahon, M., Contreras, A., Juliano, D., Kopmar, N., Nakamura, T., Maltby, D., Burlingame, A., Savage, S.A., Shimamura, A., et al. (2013). H/ACA small RNA dysfunctions in disease reveal key roles for noncoding RNA modifications in hematopoietic stem cell differentiation. Cell. Rep. *3*, 1493–1502.

Q4: Please update the references "Brault et al. 2013, Carrillo et al. 2013"

Blomster, H.A., Hietakangas, V., Wu, J., Kouvonen, P., Hautaniemi, S., and Sistonen, L. (2009). Novel proteomics strategy brings insight into the prevalence of SUMO-2 target sites. Mol. Cell. Proteomics *8*, 1382–1390.

Brault, M.E., Lauzon, C., and Autexier, C. (2013). Dyskeratosis congenita mutations in dyskerin SUMOylation consensus sites lead to impaired telomerase RNA accumulation and telomere defects. Hum. Mol. Genet. [Epub ahead of print].

Cadwell, C., Yoon, H.J., Zebarjadian, Y., and Carbon, J. (1997). The yeast nucleolar protein Cbf5p is involved in rRNA biosynthesis and interacts genetically with the RNA polymerase I transcription factor RRN3. Mol. Cell Biol. *17*, 6175–6183.

Carrillo, J., Gonzalez, A., Manguan-Garcıa, C., Pintado-Berninches, L., and Perona, R. (2013). p53 pathway activation by telomere attrition in X-DC primary fibroblasts occurs in the absence of ribosome biogenesis failure and as a consequence of DNA damage. Clin. Transl. Oncol. [Epub ahead of print].

Chen, C., Zhao, X., Kierzek, R., and Yu, Y.T. (2010). A flexible RNA backbone within the polypyrimidine tract is required for U2AF65 binding and pre-mRNA splicing *in vivo*. Mol. Cell. Biol. *30*, 4108–4119.

Cohen, S.B., Graham, M.E., Lovrecz, G.O., Bache, N., Robinson, P.J., and Reddel, R.R. (2007). Protein composition of catalytically active human telomerase from immortal cells. Science *315*, 1850–1853.

Darzacq, X., Kittur, N., Roy, S., Shav-Tal, Y., Singer, R.H., and Meier, U.T. (2006). Stepwise RNP assembly at the site of H/ACA RNA transcription in human cells. J. Cell. Biol. *173*, 207–218.

Davis, D.R. (1995). Stabilization of RNA stacking by pseudouridine. Nucleic Acids Res. *23*, 5020–5026.

Dephoure, N., Zhou, C., Villen, J., Beausoleil, S.A., Bakalarski, C.E., Elledge, S.J., and Gygi, S.P. (2008). A quantitative atlas of mitotic phosphorylation. Proc. Natl. Acad. Sci. USA *105*, 10762–10767.

Dez, C., Noaillac-Depeyre, J., Caizergues-Ferrer, M., and Henry, Y. (2002). Naf1p, an essential nucleoplasmic factor specifically required for accumulation of box H/ACA small nucleolar RNPs. Mol. Cell Biol. *22*, 7053–7065.

Ding, Z., Wu, C.J., Jaskelioff, M., Ivanova, E., Kost-Alimova, M., Protopopov, A., Chu, G.C., Wang, G., Lu, X., Labrot, E.S., et al. (2012). Telomerase reactivation following telomere dysfunction yields murine prostate tumors with bone metastases. Cell *148*, 896–907.

Dokal, I. (2011). Dyskeratosis congenita. Hematology Am. Soc. Hematol. Educ. Program. *2011*, 480–486.

Dokal, I., Bungey, J., Williamson, P., Oscier, D., Hows, J., and Luzzatto, L. (1992). Dyskeratosis congenita fibroblasts are abnormal and have unbalanced chromosomal rearrangements. Blood *80*, 3090–3096.

Egan, E.D. and Collins, K. (2010). Specificity and stoichiometry of subunit interactions in the human telomerase holoenzyme assembled *in vivo*. Mol. Cell. Biol. *30*, 2775–2786.

Ender, C., Krek, A., Friedländer, M.R., Beitzinger M., Weinmann, L., Chen, W., Pfeffer, S,. Rajewsky, N., and Meister, G. (2008). A human snoRNA with microRNA-like functions. Mol. Cell *32*, 519–528.

Fatica, A., Dlakic, M., and Tollervey, D. (2002). Naf1p is a box H/ACA snoRNP assembly factor. RNA *8*, 1502–1514.

Forbes, S.A., Bindal, N., Bamford, S., Cole, C., Kok, C.Y., Beare, D., Jia, M., Shepherd, R., Leung, K., Menzies, A., et al. (2011). COSMIC: mining complete cancer genomes in the Catalogue of Somatic Mutations in Cancer. Nucleic Acids Res. *39* (Database issue), D945–950.

Ge, J. and Yu, Y.T. (2013). RNA pseudouridylation: new insights into an old modification. Trends Biochem. Sci. *38*, 210–218.

Ge, J., Rudnick, D.A., He, J., Crimmins, D.L., Ladenson, J.H., Bessler, M., and Mason, P.J. (2010). Dyskerin ablation in mouse liver inhibits rRNA processing and cell division. Mol. Cell. Biol. *30*, 413–422.

Giordano, E., Peluso, I., Senger, S., and Furia M. (1999). Minifly, a *Drosophila* gene required for ribosome biogenesis. J. Cell. Biol. *144*, 1123–1133.

Grozdanov, P.N., Roy, S., Kittur, N., and Meier, U.T. (2009a). SHQ1 is required prior to NAF1 for assembly of H/ACA small nucleolar and telomerase RNPs. RNA *15*, 1188–1197.

Grozdanov, P.N., Fernandez-Fuentes, N., Fiser, A., and Meier, U.T. (2009b). Pathogenic NAP57 mutations decrease ribonucleoprotein assembly in dyskeratosis congenita. Hum. Mol. Genet. *18*, 4546–4551.

Gu, B.W., Fan, J.M., Bessler, M., and Mason, P.J. (2011). Accelerated hematopoietic stem cell aging in a mouse model of dyskeratosis congenita responds to antioxidant treatment. Aging Cell *10*, 338–348.

Gu, B.W., Ge, J., Fan, J.M., Bessler, M., and Mason, P.J. (2013). Slow growth and unstable ribosomal RNA lacking pseudouridine in mouse embryonic fibroblast cells expressing catalytically inactive dyskerin. FEBS Lett. *58*, 2112–2117.

Hamma, T., Reichow, S.L., Varani, G., and Ferré-D'Amaré, A.R. (2005). The Cbf5-Nop10 complex is a molecular bracket that organizes box H/ACA RNPs. Nat. Struct. Mol. Biol. *12*, 1101–1107.

He, J., Navarrete, S., Jasinski, M., Vulliamy, T., Dokal, I., Bessler, M., and Mason, P.J. (2002). Targeted disruption of Dkc1, the gene mutated in X-linked dyskeratosis congenita, causes embryonic lethality in mice. Oncogene *21*, 7740–7744.

Heiss, N.S., Knight, S.W., Vulliamy, T.J., Klauck, S.M., Wiemann, S., Mason, P.J., Poustka, A., and Dokal, I. (1998). X-linked dyskeratosis congenita is caused by mutations in a highly conserved gene with putative nucleolar functions. Nat. Genet. *19*, 32–38.

Hoareau-Aveilla, C., Bonoli, M., Caizergues-Ferrer, M., and Henry, Y. (2006). hNaf1 is required for accumulation of human box H/ACA snoRNPs, scaRNPs, and telomerase. RNA *12*, 832–840.

Hu, J., Hwang, S.S., Liesa, M., Gan, B., Sahin, E., Jaskelioff, M., Ding, Z., Ying, H., Boutin, A.T., Zhang, H., et al. (2012). Antitelomerase therapy provokes ALT and mitochondrial adaptive mechanisms in cancer. Cell *148*, 651–663.

Jack, K., Bellodi, C., Landry, D.M., Niederer, R.O., Meskauskas, A., Musalgaonkar, S., Kopmar, N., Krasnykh, O., Dean, A.M., Thompson, S.R., et al. (2011). rRNA pseudouridylation defects affect ribosomal ligand binding and translational fidelity from yeast to human cells. Mol. Cell *44*, 660–666.

Jiang, W., Middleton, K., Yoon, H.J., Fouquet, C., and Carbon, J. (1993). An essential yeast protein, CBF5p, binds *in vitro* to centromeres and microtubules. Mol. Cell. Biol. *13*, 4884–4893.

Jung, C.H., Hansen, M.A., Makunin, I.V., Korbie, D.J., and Mattick, J.S. (2010). Identification of novel non-coding RNAs using profiles of short sequence reads from next generation sequencing data. BMC Genomics 11:77.

Karijolich, J. and Yu, Y.T. (2011). Converting nonsense codons into sense codons by targeted pseudouridylation. Nature *474*, 395–398.

Khanna, A. and Stamm, S. (2010). Regulation of alternative splicing by short non-coding nuclear RNAs. RNA Biol. *7*, 480–485.

Kirwan, M. and Dokal, I. (2008). Dyskeratosis congenita: a genetic disorder of many faces. Clin. Genet. *73*, 103–112.

Kiss, T., Fayet, E., Jády, B.E., Richard, P. and Weber, M. (2006). Biogenesis and intranuclear trafficking of human box C/D and H/ACA RNPs. Cold Spring Harb. Symp. Quant. Biol. *71*, 407–417.

Kittur, N., Darzacq, X., Roy, S., Singer, R.H., and Meier, U.T. (2006). Dynamic association and localization of human H/ACA RNP proteins. RNA *12*, 2057–2062.

Knight, S.W., Heiss, N.S., Vulliamy, T.J., Aalfs, C.M., McMahon, C., Richmond, P., Jones, A., Hennekam, R.C., Poustka, A., Mason, P.J., et al. (1999). Unexplained aplastic anaemia, immunodeficiency, and cerebellar hypoplasia (Hoyeraal-Hreidarsson syndrome). due to mutations in the dyskeratosis congenita gene, DKC1. Br. J. Haematol. *107*, 335–339.

Lafontaine, D.L. and Tollervey, D. (1998). Birth of the snoRNPs: the evolution of the modification-guide snoRNAs. Trends Biochem. Sci. *23*, 383–388.

Lestrade, L. and Weber, M.J. (2006). snoRNA-LBME-db, a comprehensive database of human H/ACA and C/D box snoRNAs. Nucleic Acids Res. *34* (Database issue), D158–D162.

Leulliot, N., Godin, K.S., Hoareau-Aveilla, C., Quevillon-Cheruel, S., Varani, G., Henry, Y., and Van Tilbeurgh, H. (2007). The box H/ACA RNP assembly factor Naf1p contains a domain homologousto Gar1p mediating its interaction with Cbf5p. J. Mol. Biol. *371*, 1338–1353.

Li, L. and Ye, K. (2006). Crystal structure of an H/ACA box ribonucleoprotein particle. Nature *443*, 302–307.

Li, S., Duan, J., Li, D., Yang, B., Dong, M. and Ye, K. (2011). Reconstitution and structural analysis of the yeast box H/ACA RNA-guided pseudouridine synthase. Genes Dev. *25*, 2409–2421.

Lin, X. and Momany, M. (2003). The Aspergillus nidulans swoC1 mutant shows defects in growth and development. Genetics *165*, 543–554.

Liu, B., Zhang, J., Huang, C., and Liu, H. (2012). Dyskerin overexpression in human hepatocellular carcinoma is associated with advanced clinical stage and poor patient prognosis. PLoS One *7*, e43147.

Luzzatto, L. and Karadimitris, A. (1998). Dyskeratosis and ribosomal rebellion. Nat. Genet. *19*, 6–7.

Maceluch, J., Kmieciak, M., Szweykowska-Kulińska, Z., and Jarmołowski, A. (2001). Cloning and characterization of Arabidopsis thaliana AtNAP57 – a homologue of yeast pseudouridine synthase Cbf5p. Acta Biochim. Pol. *48*, 699–709.

Maden, B.E. (1990). The numerous modified nucleotides in eukaryotic ribosomal RNA. Prog. Nucleic Acid. Res. Mol. Biol. *39*, 241–303.

Manza, L. L, Codreanu, S.G., Stamer, S.L., Smith, D.L., Wells, K.S., Roberts, R.L., and Liebler, D.C. (2004). Global shifts in protein sumoylation in response to electrophile and oxidative stress. Chem. Res. Toxicol. *17*, 1706–1715.

Mason, P.J. and Bessler, M. (2011). The genetics of dyskeratosis congenita. Cancer Genet. *204*, 635–645.

McDonald, S.L., Edington, H.D., Kirkwood, J.M., and Becker, D. (2004). Expression analysis of genes identified by molecular profiling of VGP melanomas and MGP melanoma-positive lymph nodes. Cancer. Biol. Ther. *3*, 110–120.

Meier, U.T. and Blobel, G. (1994). NAP57, a mammalian nucleolar protein with a putative homolog in yeast and bacteria. J. Cell Biol. *127*, 1505–1514.

Mitchell, J.R., Wood, E., and Collins, K. (1999). A telomerase component is defective in the human disease dyskeratosis congenital. Nature *402*, 551–555.

Mochizuki, Y., He, J., Kulkarni, S., Bessler, M., and Mason, P.J. (2004). Mouse dyskerin mutations affect accumulation of telomerase RNA and small nucleolar RNA, telomerase activity, and ribosomal RNA processing. Proc. Natl. Acad. Sci. USA *101*, 10756–10761.

Montanaro, L., Brigotti, M., Clohess, J., Barbieri, S., Ceccarelli, C., Santini, D., Taffurelli, M., Calienni, M., Teruya-Feldstein, J., Trerè, D., et al. (2006). Dyskerin expression influences the level of ribosomal RNA pseudo-uridylation and telomerase RNA component in human breast cancer. J. Pathol. *210*, 10–18.

Montanaro, L., Calienni, M., Ceccarelli, C., Santini, D., Taffurelli, M., Pileri, S., Treré, D., and Derenzini, M. (2008). Relationship between dyskerin expression and telomerase activity in human breast cancer. Cell Oncol. *30*, 483–490.

Montanaro, L., Calienni, M., Bertoni, S., Rocchi, L., Sansone, P., Storci, G., Santini, D., Ceccarelli, C., Taffurelli, M., Carnicelli, D., et al. (2010). Novel dyskerin mediated mechanism of p53 inactivation through defective mRNA translation. Cancer Res. *70*, 4767–4777.

Nallar, S.C., Lin, L., Srivastava,V., Gade, P., Hofmann, E.R., Ahmed, H., Reddy, S.P., and Kalvakolanu, D.V. (2011). GRIM-1, a novel growth suppressor, inhibits rRNA maturation by suppressing small nucleolar RNAs. PLoS One *6*, e24082.

Parry, E.M., Alder, J.K., Lee, S.S., Phillips J.A.3rd, Loyd, J.E., Duggal, P., and Armanios, M. (2011). Decreased dyskerin levels as a mechanism of telomere shortening in X-linked dyskeratosis congenita. J. Med. Genet. *48*, 327–333.

Phillips, B., Billin, A.N., Cadwell, C., Buchholz, R., Erickson, C., Merriam, J.R., Carbon, J., and Poole, S.J. (1998). The Nop60B gene of *Drosophila* encodes an essential nucleolar protein that functions in yeast. Mol. Gen. Genet. *260*, 20–29.

Piva, R., Pellegrino, E., Mattioli, M., Agnelli, L., Lombardi, L., Boccalatte, F., Costa, G., Ruggeri, B.A., Cheng, M., Chiarle, R., et al. (2006). Functional validation of the anaplastic lymphoma kinase signature identifies CEBPB and BCL2A1 as critical target genes. J. Clin. Invest. *116*, 3171–3182.

Rashid, R, Liang, B., Baker, D.L., Youssef, O.A., He, Y., Phipps, K., Terns, R.M., Terns, M.P., and Li, H. (2006). Crystal structure of a Cbf5-Nop10-Gar1 complex and implications in RNA-guided pseudouridylation and dyskeratosis congenita. Mol. Cell *21*, 249–260.

Riccardo, S., Tortoriello, G., Giordano, E., Turano, M., and Furia, M. (2007). The coding/non-coding overlapping architecture of the gene encoding the *Drosophila* pseudouridine synthase. BMC Mol. Biol. *8*, 1–17.

Richard, P., Darzacq, X., Bertrand, E., Jády, B.E., Verheggen, C., and Kiss, T (2003). A common sequence motif determines the Cajal body-specific localization of box H/ACA scaRNAs. Embo. J. *22*, 4283–4293.

Richard, P., Kiss, A.M., Darzacq, X., and Kiss, T. (2006). Cotranscriptional recognition of human intronic box H/ACA snoRNAs occurs in a splicing-independent manner. Mol. Cell Biol. *26*, 2540–2549.

Rocchi, L., Pacilli, A., Sethi, R., Penzo, M., Schneider, R.J., Treré, D., Bigotti, M., and Montanaro, L. (2013). Dyskerin depletion increases VEGF mRNA internal ribosome entry site-mediated translation. Nucleic Acids Res. *41*, 8308–8318.

Ruggero, D., Grisendi, S., Piazza, F., Rego, E., Mari, F., Rao, P.H., Cordon-Cardo, C., and Pandolci, P.P. (2003). Dyskeratosis congenita and cancer in mice deficient in ribosomal RNA modification. Science *299*, 259–262.

Sali, A. and Blundell, T.L. (1993). Comparative protein modelling by satisfaction of spatial restraints. J. Mol. Biol. *234*, 779–815.

Salowsky, R., Heiss, N.S., Benner, A., Wittig, R., and Poustka, A. (2002). Basal transcription activity of the dyskeratosis congenita gene is mediated by Sp1 and Sp3 and a patient mutation in a Sp1 binding site is associated with decreased promoter activity. Gene *293*, 9–19.

Saraiya, A.A. and Wang, C.C. (2008). snoRNA, a novel precursor of microRNA in *Giardia lamblia*. PLoS Pathog. *4*, e1000224.

Sauer, G., Korner, R., Hanisch, A., Ries, A., Nigg, E.A. and Sillje, H.H. (2005). Proteome analysis of the human mitotic spindle. Mol. Cell. Proteomics *4*, 35–43.

Savage, S.A. and Bertuch, A.A. (2010). The genetics and clinical manifestations of telomere biology disorders. Genet. Med. *12*, 753–764.

Schaner, M.E., Ross, D.T., Ciaravino, G., Soglie, T., Troyanskaya, O., Diehn, M., Wang Y.C., Duran, G.E., Sikic, T.L., Caldeira, S., et al. (2003). Gene expression patterns in ovarian carcinomas. Mol. Biol. Cell *14*, 4376–4386.

Sieron, P., Hader, C., Hatina, J., Engers, R., Wlazlinski, A., Müller, M., and Schulz, W.A. (2009). DKC1 overexpression associated with prostate cancer progression. Br. J. Cancer *101*, 1410–1416.

Taft, R.J., Glazov, E.A., Lassmann, T., Hayashizaki, Y., Carninci, P., and Mattick, J.S. (2009). Small RNAs derived from snoRNAs. RNA *15*, 1233–1240.

Taulli, R. and Pandolfi, P.P. (2012). 'Snorkeling' for missing players in cancer. J. Clin. Invest. *122*, 2765–2768.

Tortoriello, G., de Celis, J.F., and Furia, M. (2010). Linking pseudouridine synthases to growth, development and cell competition. FEBS J. *277*, 3249–3263.

Turano, M., Angrisani, A., De Rosa, M., Izzo, P., and Furia, M. (2008). Real-time PCR quantification of human DKC1 expression in colorectal cancer. Acta Oncol. *47*, 1598–1599.

Turano, M., Angrisani, A., Di Maio, N., and Furia, M. (2013). Intron retention: a human DKC1 gene common splicing event. Biochem. Cell Biol. *91*, 506–512.

Uhlen, M., Oksvold, P., Fagerberg, L., Lundberg, E., Jonasson, K., Forsberg, M., Zwahlen, M., Kampf, C., Wester, K., Hober, S., et al. (2010). Towards a knowledge-based Human Protein Atlas. Nat. Biotechnol. *28*, 1248–1250.

von Stedingk, K., Koster, J., Piqueras, M., Noguera, R., Navarro, S., Påhlman, S., Versteeg, R., Ora, I., Gisselsson, D., Lindgren, D., et al. (2013). snoRNPs regulate telomerase activity in neuroblastoma and are associated with poor prognosis. Transl. Oncol. *6*, 447–457.

Vulliamy,T.J., Knight, S.W., Heiss, N.S., Smith, O.P., Poustka, A., Dokal, I., and Mason, P.J. (1999). Dyskeratosis congenita caused by a 3' deletion: germline and somatic mosaicism in a female carrier. Blood *94*, 1254–1260.

Walbott, H., Machado-Pinilla, R., Liger, D., Blaud, M., Réty, S., Grozdanov, P.N., Godin, K., van Tilbeurgh, H., Varani, G., Meier, U.T., et al. (2011). The H/ACA RNP assembly factor SHQ1 functions as an RNA mimic. Genes Dev. *25*, 2398–2408.

Watanabe, Y. and Gray, M.W. (2000). Evolutionary appearance of genes encoding proteins associated with box H/ACA snoRNAs: cbf5p in *Euglena gracilis*, an early diverging eukaryote, and candidate Gar1p and Nop10p homologs in archaebacteria. Nucleic Acids Res. *28*, 2342–2352.

Westermann, F., Henrich, K.O., Wei, J.S., Lutz, W., Fischer, M., König, R., Wiedemeyer, R., Ehemann, V., Brors, B., Ernestus, K., et al. (2007). High Skp2 expression characterizes high-risk neuroblastomas independent of MYCN status. Clin. Cancer Res. *13*, 4695–4703.

Westman, B.J., Verheggen, C., Hutten, S., Lam, Y.W., Bertrand, E., and Lamond, A.I. (2010). A proteomic screen for nucleolar SUMO targets shows SUMOylation modulates the function of Nop5/Nop58. Mol. Cell *39*, 618–631.

Witkowska, A., Gumprecht, J., Glogowska-Ligus, J., Wystrychowski, G., Owczarek, A., Stachowicz, M., Bocianowska, A., Nowakowska-Zajdel, E., and Mazurek, U. (2010). Expression profile of significant immortalization genes in colon cancer. Int. J. Mol. Med. *25*, 321–329.

Wong, J.M., Kyasa, M.J., Hutchins, L., and Collins, K. (2004). Telomerase RNA deficiency in peripheral blood mononuclear cells in X-linked dyskeratosis congenita. Hum. Genet. *115*, 448–455.

Wu, G., Yu, A.T., Kantartzis, A., and Yu, Y.T. (2011). Functions and mechanisms of spliceosomal small nuclear RNA pseudouridylation. Wiley Interdiscip. Rev. RNA *2*, 571–581.

Yaghmai, R., Kimyai-Asadi, A., Rostamiani, K., Heiss, N.S., Poustka, A., Eyaid, W., Bodurtha, J., Nousari, H.C., Hamosh, A., and Metzenberg, A. (2000). Overlap of dyskeratosis congenita with the Hoyeraal-Hreidarsson syndrome. J. Pediatr. *136*, 390–393.

Yang, Y., Isaac, C., Wang, C., Dragon, F., Pogacic, V., and Meier, U.T. (2000). Conserved composition of mammalian box H/ACA and box C/D small nucleolar ribonucleoprotein particles and their interaction with the common factor Nopp140. Mol. Biol. Cell. *11*, 567–577.

Yang, P.K., Rotondo, G., Porras, T., Legrain, P., and Chanfreau, G. (2002). The Shq1pdNaf1p complex is required for box H/ACA small nucleolar ribonucleoprotein particle biogenesis. J. Biol. Chem. *277*, 45235–45242.

Yang, P.K., Hoareau, C., Froment, C., Monsarrat, B., Henry, Y., and Chanfreau, G. (2005). Cotranscriptional recruitment of the

pseudouridylsynthetase Cbf5p and of the RNA binding protein Naf1p during H/ACA snoRNP assembly. Mol. Cell. Biol. *25*, 3295–3304.

Yoon, A., Peng, G., Brandenburger, Y., Zollo, O., Xu, W., Rego, E., and Ruggero, D. (2006). Impaired control of IRES-mediated translation in X-linked dyskeratosis congenital. Science *312*, 902–906.

Yu, A.T., Ge, J., and Yu, Y.T. (2011). Pseudouridines in spliceosomal snRNAs. Protein Cell *2*, 712–725.

Zebarjadian, Y., King, T., Fournier, M.J., Clarke, L., and Carbon, J. (1999). Point mutations in yeast CBF5 can abolish *in vivo* pseudouridylation of rRNA. Mol. Cell Biol. *19*, 7461–7472.

Zeng, X.L., Thumati, N.R., Fleisig, H.B., Hukezalie K.R., Savage, S.A., Giri, N., Alter, B.P., and Wong, J.M. (2012). The accumulation and not the specific activity of telomerase ribonucleoprotein determines telomere maintenance deficiency in X-linked dyskeratosis congenita. Hum. Mol. Genet. *21*, 721–729.

Zhang, Y., Morimoto, K., Danilova, N., Zhang, B., and Lin, S. (2012). Zebrafish models for dyskeratosis congenita reveal critical roles of p53 activation contributing to hematopoietic defects through RNA processing. PLoS One *7*, e30188.

Q5: Please supply the CV and photo for all authors